University of Alberta

Lagrangian-to-Eulerian Conversion Scheme For Aerosol Deposition In Human Respiratory Tract

by

Mohammad Iftekher Rahman 

A thesis submitted to the Faculty of Graduate Studies and Research in partial fulfillment of the requirements for the degree of Master of Science

Department of Mechanical Engineering

Edmonton, Alberta
Spring 2007

Your file Votre référence
ISBN: 978-0-494-30007-7
Our file Notre référence
ISBN: 978-0-494-30007-7

To my family and friends

Abstract

The environment surrounding us is composed of aerosol particles, which can be radioactive, allergic, or therapeutic in nature. Toxic particles when deposited on the respiratory tract may lead to the pathogenesis of lung disease. On the other hand, therapeutic aerosols are used for many respiratory diseases. Moreover, long term space travel and associated risk of inhaling hazardous nonterrestrial aerosol have made it significant to study the impact of gravity on particle deposition. Accurate deposition prediction is prerequisite for both toxicity measurement and drug delivery. Lung deposition of aerosols may be a very sensitive time dependent phenomenon. So to capture the true effect of time-dependency and to predict the transient local deposition, functions based on instantaneous deposition rate are required. An attractive alternative is to develop a numerical scheme that gives a better agreement with experiments using the existing functions. In the present study two such schemes will be described and implemented in an Eulerian deposition model (TECHAero) to predict some practical cases.

Acknowledgements

I would like to express my sincere appreciation and gratitude to Dr. Carlos Frederico Lange for his insight, guidance, leadership and patience throughout the course of this study and completion of the manuscript. Appreciation is also expressed to Anwer-Ul Hasan and Jeff Davis for their ideas and support. I would also like to thank my former colleague and friend Luis Prieto who was a constant source of inspiration and motivation.

I am grateful to my family and friends for their love and support. I would specially state my appreciation to my wife for her kind consideration and constant cooperation.

Finally, i would like to acknowledge the financial support provided by the Mechanical Engineering Department, University of Alberta, NSERC, Alberta Lung Association and Dr. Carlos Lange.

Contents

1 Introduction 1

2 Literature Review 6

2.1 Introduction . . . 6

2.2 Deposition Mechanism . . . 6

2.2.1 Inertial Impaction . . . 7

2.2.2 Sedimentation . . . 9

2.2.3 Diffusion . . . 9

2.3 Extrathoracic Deposition . . . 11

2.4 Factors Affecting Deposition . . . 13

2.5 Deposition Modeling . . . 14

2.5.1 Lagrangian Dynamic Model . . . 14

2.5.2 Eulerian Dynamic Model . . . 16

2.6 Microgravity, Respiratory System and Deposition . . . 20

2.6.1 Effect on Respiratory System . . . 21

2.6.1.1 Lung Volume: . . . 21

2.6.1.2 Chest Wall Configuration: . . . 21

2.6.1.3 Ventilation and Perfusion: . . . 21

2.6.2 Microgravity Lung Deposition . . . 22

2.7 Summary . . . 23

3 Theory and Model 24

3.1 Introduction . . . 24

3.2 Description of the Model . . . 24

3.2.1 New Dimensions . . . 25

3.2.2 Governing Equations . . . 26

3.2.3 Cross-Sectional Averaging and Simplifications . . . 27

3.2.4 Total Particle Deposition 29
3.2.5 Lagrangian to Eulerian Conversion 30
3.2.5.1 Total Deposition Based on Lung Generation Residence Time (GRT) 31
3.2.5.2 Total Deposition Based on Control Volume Residence Time (CVRT) 33
3.2.6 Lung Model 34
3.2.7 Boundary Conditions 35
3.2.8 TECHAero Usage 36
3.3 Scaling Lung Geometry 36
3.3.1 Summary 37

4 Results and Discussion **38**
4.1 Introduction 38
4.2 Validation of the Conversion Schemes 38
4.2.1 Different Sedimentation Functions 39
4.2.2 Validation: CVRT Approach 42
4.2.3 Validation: GRT Approach 48
4.2.4 Comparison Of The Two Approaches 50
4.2.5 Discussion on CVRT Approach 55
4.3 Lung Deposition Model Validation 58
4.4 Highly Transient Deposition 62
4.5 Deposition at Very Low Flow Rate 64
4.6 Microgravity Deposition 65
4.6.1 Effect of Geometry 65
4.6.2 Comparison of Total Deposition 66

5 Conclusions **70**

Bibliography **72**

Appendix **81**

A Derivation **81**

B TECHAero Subroutine **83**
B.1 Original *deposprob.f* 83

B.2 Modified *deposprob.f* 88

C TECHAero Data Files **92**

C.1 Input file: *input.dat* 92

C.2 Grid File: *grid.out* 93

C.3 Local Deposition : *locdep.out* 95

C.4 Generation Deposition : *gendep.out* 97

C.5 Regional Deposition : *regdep.out* 98

List of Tables

2.1 Various impaction functions available in the literature. DR is the daughter to parent airway diameter ratio (from Finlay [25]) 8
2.2 Various sedimentation functions available in the literature. 10

3.1 Deposition functions used in TechAero. 29

List of Figures

2.1 Schematic diagram of human extrathoracic region. 12

3.1 Discretization of the domain 31
3.2 Discretization of the domain 33
3.3 Schematic diagram of symmetrically branching lung model. 35

4.1 Comparison of various sedimentation function in 14th generation for varying particle size. 40
4.2 Comparison of various sedimentation function in 16th generation for varying particle size. 40
4.3 Comparison of various sedimentation function in 14th generation for varying flow rate. 41
4.4 Comparison of various sedimentation function in 16th generation for varying flow rate. 41
4.5 Deposition fraction against the volume flow rate. 43
4.6 Relative error against the volume flow rate. 43
4.7 Relative error as it changes with the increase of CV number. 44
4.8 Relative error as a function of pipe length. 46
4.9 Relative error as a function of pipe diameter. 47
4.10 Relative error as a function of particle diameter. 48
4.11 Deposition fraction against the volume flow rate. 49
4.12 Relative error against the volume flow rate. 49
4.13 Relative error as it changes with the increase of CV number. 50
4.14 Relative error as a function of pipe length. 51
4.15 Relative error as a function of pipe diameter. 52
4.16 Relative error as a function of particle diameter. 52
4.17 Relative error as a function of number of control volumes. 53

4.18 Relative error as it changes with the increase tube length with 100 control volumes. 54
4.19 Relative error as it changes with the increase tube diameter with 100 control volumes. 54
4.20 Relative error as it changes with the increase tube diameter with 100 control volumes. 55
4.21 Relative error as it changes with the increase of flow rate a) between 20 to 100 l/min, b)wider range 56
4.22 Flow rate at minimum relative error (intersection point))as it changes with the increase of tube length with 100 control volumes. 57
4.23 Flow rate at minimum relative error (intersection point) as it changes with the increase particle diameter with 100 control volumes. 57
4.24 An attempt to unify the error curves (L= 100 cm, D = 0.8 cm, d= 3.5 /mum. 59
4.25 Convergence of TECHAero using CVRT approach (d = 3.25 microns, time step = 10e-4 s). 60
4.26 Comparison of extra-thoracic (ET) deposition. 60
4.27 Comparison of tracheo-bronchial (TB) deposition. 61
4.28 Comparison of alveolar deposition. 61
4.29 Comparison of total lung deposition. 62
4.30 Contribution to deposition by different mechanisms. 63
4.31 Simulating time dependent breathing pattern. 63
4.32 Comparison of transient deposition for two different approaches. . . . 64
4.33 Effect of lung geometry on total deposition. 66
4.34 Total deposition in microgravity. 67
4.35 Comparison of Impaction functions in calculating Total Deposition in Microgravity 68
4.36 Comparison of ET functions in calculating Total Deposition in Microgravity. 69

List of Symbols

a = cross-sectional area of individual airway in any lung generation
A = total cross-sectional area of all airways in a lung generation (single straight tube)
c = particle number concentration
C or C_c = Cunnungham slip factor
C_∞ = vapour concentration of the volatile species
d or d_p = particle diameter
D = diameter of airway or tube
D_a = axial or apparent diffusion coefficient
D_d = Brownian diffusion coefficient
D_{mean} = mean diamter of the extra-thoracic region
DR = parent to daughter diameter ration
g = acceleration due to gravity
h = diffusion parameter
H = enthalpy of the particle
H_∞ = enthalpy of air-vapor mixture
K_{rm} = deposition rate coefficient
l = length of control volume
L = length of lung generation or tube
L_{c_i} = cumulative length of i control volumes
L_i = length of i'th control volume
L_{mean} = mean length of the extra-thoracic region
m_1 = mass of solute
n = particle number concentration
N_a = number of alvoli in any lung generation
P = deposition probability
P_i = deposition probability at i'th control volume
P_k = deposition probability of k'th generation
P_m = deposiiton probability of different mechanismss
$\dot{p}$ = deposition probability rate
Q = volume flow rate
$\dot{Q}_{ev,\,co,\,de}$ = combined heat loss by evaporation, conduction and deposition
$\dot{Q}_{\infty\,co,\,ev,\,w}$ = heat transferred by conduction, evaporation and heat exchanged with the boundary walls
R = diameter of lung airways or the tube
Re = Reynolds number

Stk = Stokes number
t_m = generation residence time
U or u = mean airway or tube velocity
v_s = particle settling velocity
V = volume of extra-thoracic region
V_{aT} = total alveolar volume in the lung
w_1 = mass of solvent
$\dot{W}_{ev,\,w}$ = rate of evaporative mass from the particles in the control volume

Greek symbols
α = fraction of airway covered with alveoli
β = average inclination angle of airways in lung
γ = apparent diffusion coefficient
ϵ = sedimentaion parameter
η = deposition probability
$dot\eta_{de}$ = deposition rate
μ = fluid dynamic viscosity
ρ = fluid density
ρ_d = density of solute
τ = particle residence time

System of coordinates
$\vec{\chi} = (x, e, \theta, R, m_1)$ = new and extended hyper-space
$\vec{X} = (x, e, \theta)$ = regular space

Star
* = Non-averaged quantities

Chapter 1

Introduction

The air surrounding us is composed of aerosol particles having a variety of physical, chemical and biological properties. The troposphere contains approximately 10^2 to 10^6 particles per milliliter within the size range of 0.01 to 1.0 μm. These particles may exist in the form of pure liquids or heterogeneous micro-crystals, and may be radioactive, allergic, or therapeutic in nature [55]. Airborne particles, which can cause health hazard, have become a major public concern in the recent years with the growth of industrialization and urbanization. Recent studies suggest that the airborne particulate matter, at concentration levels below present U.S. National Ambient Air Quality Standards and United Kingdom PM-10 workplace regulations, negatively affect human health and worker's productivity [90].

Airborne particles, inhaled during normal respiration, deposit in the respiratory tract when they come into contact with the airway surfaces. There are three main mechanisms that cause the deposition of inhaled particles in the respiratory tract: impaction (due to change of air flow direction), sedimentation (due to gravity), and diffusion (due to Brownian motion) [25]. If the particle is toxic, then its deposition may lead to the pathogenesis of lung disease. Respiratory diseases having etiologies related to the deposition of airborne particles include: silicosis, asbestosis, coal workers pneumoconiosis, bronchogenic carcinoma, allergic rhinitis, and influenza [90]. The deposited particles in the lung constitute the initial dose, and eventually, determine the possi-

bility and severity of a toxic response.

Moreover, the renewed emphasis on human space exploration and the associated risk of long term space travel has brought the issue of the impact of gravity on aerosol inhalation to the fore. As with terrestrial aerosols, lunar and Martian dusts are potential sources for health hazards if inhalation exceeds a safe level. Lunar dust is known to contain silica and is likely to have similar hazardous characteristics as many harmful industrial aerosols. Furthermore, for the case of dust entrainment in near-zero gravity spacecraft environments the situation become even worse, since no sedimentation can occur and the potential for significant air-borne particle concentration is high. Also when inhaled, particles will penetrate deeper into the sensitive gas exchange regions of the lung and may cause severe local damage, as well as, enter the blood causing systemic toxic reactions. Knowledge of the total deposition characteristics of particles is, therefore, an important issue to determine the accurate deposition predictions to implement risk mitigation strategies.

Characterization of particle deposition has clinical applications as well. Therapeutic aerosols are presently being used in the treatment of many respiratory diseases such as asthma, cystic fibrosis and chronic obstructive pulmonary disorder. This method of drug delivery allows effective local concentrations to be achieved without creating high systemic levels that may cause deleterious side effects. Soluble drugs can also be delivered through inhalation, because the lung provides efficient access to the blood stream. Because of its advantages, aerosolized drug delivery is an attractive option for regular systematic treatment, such as morphine as analgesic or for routine insulin delivery for diabetes. Accurate inhalation dosage prediction is also an important parameter in aerosolized drug delivery.

One approach to understanding the deposition of inhaled particles is the use of mathematical models. In mathematical modeling, a set of equations is formulated which represent the physical phenomenon by the use of the physical laws governing the flow. The resulting equations are then usually solved numerically for a given modeled lung

geometry.

Lagrangian deposition models are frequently used for predicting deposition in the respiratory track [23, 79, 80]. In a Lagrangian model, an aerosol bolus is explicitly tracked as it travels through the lung. These models approximate the inhalation and deposition from steady continuous flow (e.g. continuous nebulizers for drug delivery) well. But deposition may become a very sensitive time dependent phenomenon (e.g. from new Smart Nebulizers [47, 74]), because deposition is highly sensitive to the inhalation flow rate and to the aerosol concentration that varies during a breathing cycle. Existing Lagrangian models have difficulty in treating this issue. To meet the demand of determining the most accurate deposition prediction, i.e. drug dosage, a model is needed which takes into account the time dependency in inhalation and particle deposition. The obvious choice is to use an Eulerian deposition model, which can account for the effect of changes in flow rate during inhalation.

From the perspective of inhaled pharmaceutical aerosol, an Eulerian model will allow the development of inhalers or nebulizers with individually optimized therapy, i.e. to estimate deposited dosage and concentration in the lung for individual patient based on breathing patterns. This could eventually lead to the development of smart multiple breath inhalers capable of delivering precise, individually adjusted dosages to the lung[47].

In contrast to the Lagrangian deposition models, the Eulerian deposition models use a fixed frame of reference. Most of the Eulerian models available [17, 20, 83] are designed primarily for monodisperse non-hygroscopic particles. A more recent Eulerian model [46, 65], which can treat hygroscopic effect of polydispersed particles, shows particle size dependency on deposition and no limiting trajectory. This is due to the assumption of homogeneous and well mixed aerosol at any point, which is not rigorously true throughout the entire respiratory tract.

Although designed for time dependent conditions, Eulerian deposition models currently lack properly derived Eulerian deposition functions. All the existing Eulerian

models use deposition functions, which are either empirical or derived from the Lagrangian frame of reference. These functions are used to estimate the probability of deposition over an entire generation of the respiratory tract, and are then converted into deposition probability rate by dividing it by the generation residence time, the time required for a particle to travel a single generation.

A proper Eulerian deposition model can also aid in predicting micro-gravity deposition, because of the inclusion of axial diffusion which is beyond the scope of the typical Lagrangian model. Micro-gravity causes significant change in lung geometry and breathing parameters [60, 64], and causes major changes in transport mechanisms. These changes can result in substantial alteration in the amount and location of particle deposition in lung, and require proper investigation.

In this thesis, two approaches will be investigated to convert the generation deposition probability for the Eulerian frame of reference valid for each cell in the discretized domain. The conversion schemes will be implemented into the program TechAero [46]. The numerical solution will be compared with experimental results. Predicting aerosol behavior in the respiratory system is difficult due to the complex geometry of the lung and of the associated airways. Moreover, there is considerable person to person variation in the respiratory track geometry. All mathematical models need proper match and consistency with experimental data. Most of the models used are validated using simplified lung and airway geometry due to the complexity associated with the modeling of such geometry. But recent development in imaging, designing, and machining make it feasible to obtain the main barometric parameters and to create more sophisticated model of respiratory airways. The Aerosol Research Laboratory of Alberta (ARLA) has very recent and accurate experimental data for respiratory track deposition using the latest airway geometry.

At the same time, the effect of altered lung geometry and breathing conditions on deposition in weightlessness to quantify its impact will be investigated. The investigation will be extended to analyse whether the lung geometry plays a major role

on estimation of aerosol deposition in micro-gravity, or other physical phenomenon such as axial diffusion, non-reversibility of flow impose significant influence on it. TechAero will be used to estimate total aerosol deposition in the absence of gravity, and the result will be compared with the recent microgravity experimental results by Darquenne et al. [12].

Chapter 2

Literature Review

2.1 Introduction

The main objective of this chapter is to provide a brief overview of modeling of aerosol deposition in human respiratory tract. The general mechanisms of aerosol deposition and the factors influencing these are reviewed in the first two sections. Next, a discussion on deposition modeling techniques used for the complete respiratory tract is presented. Finally, a summary of how these mechanisms and factors are influenced by microgravity is given.

2.2 Deposition Mechanism

Particle deposition in the lung is governed mainly by three mechanisms : inertial impaction, sedimentation, and diffusion. The efficiency or probability of deposition by each mechanism depends upon ventilatory parameters, lung morphology and aerosol characteristics. Interception and electrostatic precipitation are two mechanisms that contribute less to deposition, and for aqueous pharmaceutical aerosols their contribution is even less signifcant, and can often be neglected [50].

2.2.1 Inertial Impaction

Inertial impaction takes place when particles with relatively high momentum deviate from curved pathways, such as at the airway bifurcations, and impact at the airway surface. The probability of a particle being deposited by impaction is characterized by the Stokes number which is a ratio of particle stopping distance S to the characteristic dimension of the flow D:

$$\mathrm{Stk} = \frac{S}{D} = \frac{\rho d^2 U C_c}{18 \mu D} \tag{2.1}$$

where ρ is the particle density, d is the particle diameter, U is the fluid velocity scale, C_c is the Cunningham slip factor, μ is fluid dynamic viscosity and D is the tube diameter. Apart from the Stokes number, impaction can also be influenced by the flow Reynolds number and geometric parameters such as the branching angle and the parent-to-daughter diameter ratio (DR). In general, if the Stokes number is very small (Stk $<<$ 1) particles can follow the flow's streamlines. On the other hand, particles with a Stokes number close to or in the order of 1 are not able to follow the fluid's streamlines and will impact onto the airway surface. Inertial impaction, based on the typical values found for therapeutic aerosols applications, is most important in the upper airways [25].

Impaction modeling with reasonable accuracy is not straightforward because particles are unable to follow the curved streamlines when passing through the bifurcations. Modeling with a simple plug or Poiseuille flow is inadequate; instead, more complex flows must be considered. Stapleton and Finlay [78] cite numerous studies which have been carried out to obtain an impaction deposition model with casts of airways (Schlesinger et al. [73]; Chan and Lippmann [8]; Gurman et al. [35]), or with models of bifurcations (Johnston et al. [42]; Kim et al. [43]), or by theoretical analysis of geometry and flow conditions (Gawronski and Szewczyk [30]; Cai and Yu [7]; Balásházy et al. [1]). A summary of the resulting equations as a function of Stokes number in the parent airway and diameter ratio, taken from [25], is presented in Table 2.1.

Table 2.1: Various impaction functions available in the literature. DR is the daughter to parent airway diameter ratio (from Finlay [25])

Formula	Source
$P_i = 0,\ if$ Stk < 0.02, otherwise, $P_i = -0.0394 + 3.417(2 \text{ Stk } DR^3)^{1.16}$ for DR=0.8-1.0	Kim et al. [43]
$P_i = -0.1299 + 1.5714(2 \text{ Stk } DR^3)^{0.62}$ for DR=0.64	Kim et al. [43]
$P_i = a$ Stk where a = $f(\beta,\ DR)$ and a = 1.53473 for Poiseuille flow and brancing angle of $\beta = 35°$, $DR = 0.7853$	Cai and Yu [7]
$P_i = b\,\text{Stk}/(1 + b\,\text{Stk})$ where b =$4\,DR^3 \sin\beta$ and b = 1.1111 for $\beta = 35°$, $DR = 0.7853$	Landahl [44]
$P_i = 1 - \frac{2}{\pi}\arccos(\beta\,\text{Stk}) + \frac{1}{\pi}\sin[2 \arccos(\beta\,\text{Stk})]$ Note : $\beta = 0.568977\ for 32.6°$ average branching angle	Yeh and Schum [92]
$P = 1.606$ Stk $+ 0.0023$	Chan and Lippmann [8]
$P_i = 1.3$ (Stk $- 0.001$)	Taulbee and Yu [83]
$P_i = 6.4\ \text{Stk}^{1.43}$ for generations 1-3 $P_i = 1.78\ \text{Stk}^{1.25}$ for generations 4-5	Smith [75]
$P_i = 0$ if Stk < 0.1 $P_i = 4$ (Stk $- 0.1$) / (Stk $+ 1$)	Ferron et al. [23]

2.2.2 Sedimentation

Sedimentation occurs when particles, traveling in the airflow, are deposited on-to the airway surface due to the force of gravity. Sedimentation can occur in all airways, except those that are vertical. The probability of deposition by sedimentation within a given section of the lung is a function of particle settling velocity, v_s

$$v_s = \frac{\rho g C_c d^2}{18\mu}. \tag{2.2}$$

Other important factors are the length of the airway, the airflow velocity, the diameter of the airway, and the angle of inclination of the airway with respect to the vertical axis. Settling velocity increases with increasing particle diameter, and airflow velocity affects the deposition as it influences the residence time. Considering the typical values of the above mentioned parameters, sedimentation plays a significant role deep into the lung.

In the literature, there are two sets of equations (presented in Table 2.2) used to estimate the deposition probability by sedimentation. Beeckmans [2], Findeisen [24], Landahl [44] used a similar deposition function for sedimentation, which was further modified by Taulbee and Yu [83] for the alveolated airways, and then adopted by Darquenne and Paiva [11] . The last function was established by Fuchs [29] and Thomas [86] independently, and was further generalized by Pich [63] and Wang [89], and finally adopted by Taulbee et al. [84], Nixon and Egan [57], Finlay and Stapleton [26] and Lange and Finlay [46].

2.2.3 Diffusion

Diffusion results from a constant collision of particles with gas molecules. Diffusion is important only for particles smaller than approximately 1 μm. However, it is included in most of the deposition models to improve the deposition estimates of particles in the range of 0.05 to 10 μm (Stapleton and Finlay [78]).

Table 2.2: Various sedimentation functions available in the literature.

Formula	Source
$P_s = 1 - \exp\left\{-\frac{gd^2\rho C\tau}{9\pi\mu R}\right\}$	Beeckmans [2]
$P_s = (1-\alpha)\left\{1 - \exp\left[-2\sqrt{\frac{N(z)}{\pi s}}\frac{v_s l s}{Q}\right]\right\} + \phi\frac{N\!a_g}{l}$	Darquenne and Paiva [11]
$P_s = \frac{2}{\pi}[2\epsilon\sqrt{(1-\epsilon^{2/3})} - \epsilon^{1/3}\sqrt{(1-\epsilon^{2/3})} + \arcsin\epsilon^{1/3}]$	Pich [63]

α = Fraction of alveolated surface of airway
ρ = Particle density
μ = Air viscosity
τ = Particle residence time
g = Gravitational acceleration
l = Airway length
d = Particle diameter
$N\!a_g$ = Number of alveoli contained in one generation
$N(z)$ = Number of airways in generation z
v_s = Settling velocity
s = Total airway cross section
$\epsilon = \frac{3v_s l}{4DU}$ = Sedimentation parameter
D = Airway diameter = $2R$
U = Mean flow velocity in the airway

Existing equations used in the literature (Gormley and Kennedy [32], Beeckmans [2], Ingham [41]) to estimate deposition efficiency by diffusion are derived by solving the Navier-Stokes equations with the standard convection-diffusion equation for aerosol particles (Fuchs [29]) under the assumption of Poiseuille flow. These diffusion probability functions are written in terms of a diffusion parameter, h,

$$h = \frac{D_d t}{4r^2}. \tag{2.3}$$

Flow in the alveolar region is much different from Poiseuille flow, and neither of the previously cited functions fully represent the alveolar deposition. Because of this reason, various researchers (cf. Finlay [25]) have proposed alternative diffusion models based on a non-Poiseuille flow velocity field using geometries which resemble more closely the alveolated airways.

2.3 Extrathoracic Deposition

The extrathoracic region includes nasal passages, oral cavity, pharynx, larynx and upper part of the trachea [76, 87] (see figure 2.1). The geometry within this region is not only complex, but varies also with time, and varies from person-to-person. The fluid flow in this region is normally turbulent [25]. For these reasons, deposition modeling in this region has proceeded mainly in the form of empirical formulas based on experimental data.

DeHaan [14] has summarized extra-thoracic deposition modeling up to 2002. According to his summary, the equations used to predict deposition probability in the nasal passage are based on experimental data proposed by Cheng et al. [10], Martonen and Zhang [52], Stahlhofen et al. [77], Swift et al. [82], Yu et al. [95] and Sarangapani and Wexler [69]. The oral route of drug delivery causes less aerosol deposition than the nasal route (Lippmann [50], Stahlhofen et al. [77], Yu et al. [95]). A number of experiments have been carried out to develop mouth deposition models [4, 8, 28, 49, 50, 75], and based on these results, numerous empirical fits have been

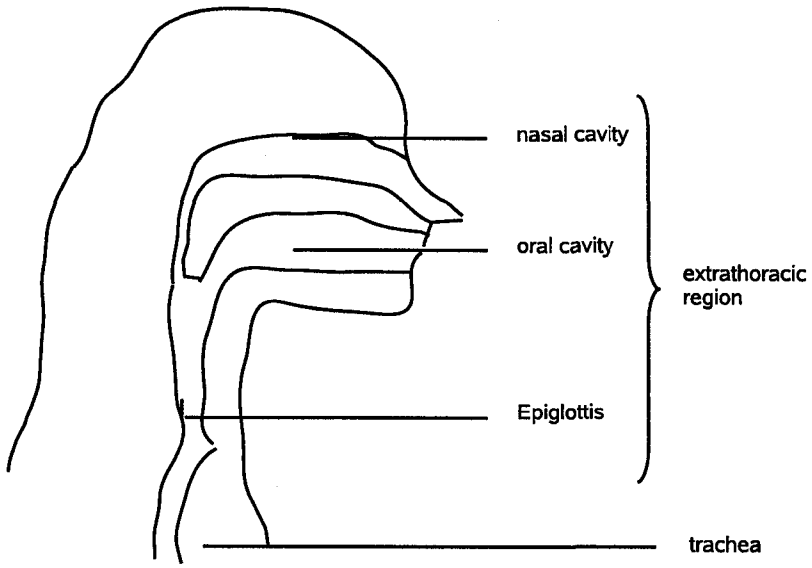

Figure 2.1: Schematic diagram of human extrathoracic region.

proposed [8, 28, 50, 51, 54, 68, 77, 93, 95]. Most of these models predict deposition as a function of an inertial parameter ($d_{ae}^2 Q$ where, d_{ae} is the aerodynamic diameter and Q is fow rate). In a recent study, DeHaan and Finlay [15] have proposed a new model to predict mouth-throat deposition as a function of the Stokes number, taking into account the effect of different geometries and inlet diameter conditions. Grgic et al. [33] have further modified the analysis and proposed a single equation to predict extrathoracic deposition as a function of both Stokes and Reynolds number,

$$\eta = 100 - \frac{100}{11.5\mathrm{Stk}^{1.912}\mathrm{Re}^{0.707} + 1} \tag{2.4}$$

where a mean equivalent diameter $D_{mean} = 2\sqrt{\frac{V}{\pi L}}$ (V is mouth-throat volume, and L is centerline length) and mean velocity $U_{mean} = \frac{4Q}{\pi D_{mean}^2}$ (Q inhalation flow rate) are used to calculate Stokes and Reynolds numbers.

2.4 Factors Affecting Deposition

Aerosol particles, when inhaled, deposit on the surface of the respiratory tract through various mechanisms. The deposition site and the amount deposited depend upon the interaction between the particles and their environment. Factors affecting this process can be physical, mechanical, anatomical, and physiological.

Particle size is the primary factor affecting deposition for spherical particles. Other particle properties, such as shape and density, also affect deposition. For particles that are not spherical, an aerodynamic diameter is often used to characterize the particle size for deposition estimation. Hygroscopicity and electric charge are also important considerations in deposition modeling.

Anatomical features of the lung (airway dimension, branching pattern along the respiratory tract) influence particle deposition. There is considerable intersubject variability in the lung geometry and it is preferable to consider an idealized lung geometry for simulation. Weibel [91] pioneered the first comprehensive morphological study of the human lung. In this model, the lung is represented as a network of cylindrical tubes which branch in a regular dichotomous fashion. Since then modifications to the original lung model have been proposed [27, 37, 38, 58, 92, 94] which include altering the length and diameter of different generations and introduce more realistic asymmetry into the bifurcations.

Particle deposition in the respiratory tract also depends strongly upon breathing parameters, which include tidal volume and breathing frequency. These parameters determine the duration of residence time and the depth of penetration of particles in the lung.

2.5 Deposition Modeling

A mathematical model describing aerosol deposition in the respiratory tract consists of a set of equations which contain a sufficient amount of physical information to simulate the dynamics of aerosol deposition along with information on the lung geometry. A proper mathematical model must be able to match experimental results, and be able to provide information on the aspects of respiratory tract deposition which are inaccessible to direct measurement. There are a number of deposition models available in the literature and they can be categorized into three major classes: empirical models (Davies [13], Rudolf et al. [67], Rudolf et al. [68], Yu et al. [96]), Lagrangian dynamic models and Eulerian deposition models. In the following subsections, discussion will be limited to the last two categories, which are based on the dynamics of fluid flow and particle motion.

2.5.1 Lagrangian Dynamic Model

In the Lagrangian model, the respiratory tract is viewed as a series of segments (lung generations) that work as filters. When air passes through the airways, some of the particles are deposited in each segment, and the rest are passed to the next segment. The amount deposited in each lung generation is estimated based on the deposition probability functions derived on the basis of physics of particle transport through an idealized lung model.

Findeisen [24] was a pioneer in the modeling of aerosol deposition, who studied NaCl aerosol deposition in animal lungs, correlated aerosol deposition in the lungs with the physical laws that govern aerosol dynamics in the atmosphere, and developed the first particle deposition model for the human respiratory tract. There have been many refinements to Findeisen's general model, but it still forms the basis for any Lagrangian dynamic model.

Findeisen's simplified lung model has eight generations of symmetrically branching

cylindrical tubes, with each tube of the final generation terminated by two spherical alveoli. Landahl [44] extended Findeisen's lung model to twelve generation, and included mouth and pharynx in the model. He [44] derived new expressions for deposition probabilities, and proposed a new formula for adding these probabilities. He was the first researcher to consider deposition during breath hold. Beeckmans [2] included the concept of mechanical mixing and dispersion in the flowing aerosol stream, and used the airway morphometric model of Weibel [91]. Gerrity et al. [31] were the first group to address the issue of regional aerosol deposition, distinguishing the thracheobronchial and alveolar regions of the lung.

All models previously mentioned consider stable particles inside the respiratory tract. If the particles are hygroscopic in nature, then the growth of such aerosol particles plays a significant role in the fate of the inhaled particles, i.e. in the deposited amount. Growth of hygroscopic aerosol has been studied theoretically by Langmuir [48], Mason [53], Ferron [22], Wagner [88]. Persons et al. [61], Ferron et al. [23] and Stapleton et al. [80] included the effect of hygroscopicity in their Lagrangian deposition models, where they only consider the effect of surrounding continuous phase on the the particle phase (one-way coupling). Persons et al. [61] followed a slightly different approach. The model started with an Eulerian formulation with logarithmic particle diameter distribution as an independent variable. But the model calculated the total generational deposition at the end of each generation in the respiratory tract. Finlay and Stapleton [26] were the first to extend their Lagrangian model to include the effect of two-way hygroscopic couplings.

The development of *in vivo* imaging techniques and a better understanding of the *in vivo* aerosol data have made recent improvement in aerosol deposition modeling possible. However, these Lagrangian models suffer from a number of limitations. They cannot simulate axial dispersion in aerosol bolus due to the use of only one spatial dimension and the assumed fluid dynamics, and it is difficult to treat a time-dependent flow rate and aerosol concentration [25]. An Eulerian deposition model can be an appropriate solution to these difficulties.

2.5.2 Eulerian Dynamic Model

In the Eulerian dynamic model, a fixed frame of reference is used instead of tracking an aerosol bolus. In the existing Eulerian models, the whole respiratory tract is treated as one-dimensional. The airway tree is approximated by a one-dimensional, variable cross-section channel. The cross-sectional area of all airways at a given distance from the mouth is the same as the total cross-sectional area of all airway units in that corresponding lung generation. An Eulerian dynamic model is based primarily on the concept of solving a convection-diffusion equation with a simplified lung geometry.

Taulbee and Yu [83] developed the first Eulerian model to predict the total and regional aerosol deposition in the human respiratory tract for any breathing condition. By considering the mass balance of particles in a channel of finite length, they developed the following convection-diffusion equation for particle concentration with a loss term to describe particle deposition,

$$(A+v)\frac{\partial c}{\partial t}+Q\frac{\partial c}{\partial x}=\frac{\partial}{\partial t}(AD\frac{\partial c}{\partial t})-L \tag{2.5}$$

where, c is the area averaged particle concentration, A is the total airway cross-sectional area, v is the alveolar volume per unit length of the airway, L is the deposition per unit length per unit time (deposition rate) due to the combined action of impaction, sedimentation and diffusion, and D is the apparent diffusion or axial diffusion coefficient.

Diffusion in the airways can arise from a number of mechanisms. Brownian diffusion is due to intrinsic particle motion. The combined action of radial diffusion and velocity gradient in the radial direction can cause Taylor diffusion, provided that laminar flow exists in the airways. Turbulent diffusion may occur in the upper airways, especially in the trachea. As mentioned by the authors (Taulbee and Yu [83]), there might exist a velocity distribution in the airways at a single generation, because standard deviation exists in the airway length and diameter distribution (between 0.5 and

0.8). They consider this as the primary process for pulmonary air mixing. The geometric model proposed by Scherer et al. [71] was used. The beathing process was simulated as the movement of particles suspended in air into and out of the variable cross-sectional channel as the alveolar volume expands and contracts uniformly. The inlet particle concentration was defined at the mouth during inhalation, and during exhalation only convection is specified in the trachea as boundary condition. Taulbee et al. [84] proposed a number of modifications to the original model, one of which was the replacement of the deposition functions. They also improved the apparent diffusion by including mechanical mixing due to turbulence and disturbance in the upper airways, and alveolar mixing.

Darquenne and Paiva [11] used a similar model for the prediction of deposition. The form of the final transport equation is slightly different with the temporal and axial dimensions being used as independent variables, whereas in the previous model time and the generation number were considered as independent quantities. Another major difference was the factor used in the apparent diffusion term. Apparent or axial diffusion coefficient has the following general form,

$$D_a = \gamma u d \tag{2.6}$$

where γ is a constant factor, u is mean flow velocity and d is the particle diameter. Taulbee et al. [84] used a value of 1.08 for inhalation and 0.37 for exhalation, while a value of 0.167, for both inhalation and exhalation, was used by Darquenne and Paiva [11].

In the 1980's, Nixon and Egan [57] proposed another aerosol deposition model which was an extension of the gas transport model previously developed by Pack et al. [59] and Scherer et al. [71]. Pack et al. [59] proposed a gas transport model assuming that the lung branching structure was symmetric, the airways were compliant, and an instantaneous mixing of gases occured in alveolar duct and alveoli. In the model (Pack et al. [59]), a transfer term was used to characterize the gas exchange between alveolar gas and blood. Egan and Nixon [20] then extended this model to predict

aerosol transport in the human respiratory tract. The resulting model was similar in structure to that developed by Taulbee and Yu [83], however, the effective axial diffusion was treated in a completely different manner. Here, they incorporated the experimental findings of Scherer et al. [72], who suggested that the axial diffusion coefficient is different for inhalation and exhalation. They also suggested that the enhanced mixing (due to convection) is not dependent of molecular diffusivity, but depends only on fluid dynamic effects.

Later the 1990's, Edwards [18] reported a different way to model aerosol deposition based on the macro-transport theory (Brenner [6]). In any convective flow and dispersion of solute dissolved in a solvent in circular tube where the flow can be characterized by Poiseuille flow, the flow is governed by a convection-diffusion equation involving radial, azimuthal and axial transport. Taylor [85] introduced a new way of describing such a system by the mean, axial transport of solute down the tube. This theory was recently named "the macro-transport processes". In the proposed model, after an aerosol tracer is introduced in the system, the scalar probability density can be determined in order to locate the representative aerosol tracer by solving the micro-scale conservation equation for conditional probability density. Then the mean conditional probability density is calculated. But according to the macro-transport theory, the mean probability density itself obeys a conservation equation, which includes mean phenomenological coefficients. The macro-transport equation has a unique solution along with its initial and boundary conditions (Chandrasekhar [9]), which form the basis of predicting aerosol concentration as a function of time.

Edwards [18] used the exponential deposition functions used by Gerrity et al. [31], and added them to obtain the overall deposition rate coefficient after converting them into a deposition probability rate using the following relations,

$$P_m = 1 - \exp\{-K_{rm} t_m\}, \text{ for sedimentation and diffusion} \tag{2.7}$$

$$P_m \approx K_{rm} t_m, \text{ for impaction} \tag{2.8}$$

where, K_{rm} is the deposition rate coefficient, t_m is the generation residence time, and

P_m represents the individual deposition probability. The author estimated the axial dispersion coefficient taking into account that near the peripheries of the airways deposition of particles causes a reduction in axial dispersion.

In these models, the deposition rate is calculated by estimating the particles depositing per unit time throughout a lung generation, and then dividing it by the length of the generation. The main advantage of Eulerian deposition models is treatement of the unsteady deposition. To capture the true effect of the breathing pattern and to predict the transient local deposition, deposition functions based on instantaneous deposition rate are required. But, at present, no such deposition function is available. Existing Eulerian models use deposition functions which are either empirical or derived under steady state conditions.

Development of such analytical expressions involve complex mathematics and require sophisticated experimental facilities for the development of empirical correlations, both of which are time consuming. An attractive alternative is to develop a numerical technique to convert the generational deposition probabilities into an Eulerian frame of reference valid for each control volume within the domain.

Roth [65] and Roth et al. [66] adopted such a technique into the truly Eulerian deposition model, TechAero, developed by Lange and Finlay [46]. The model predicts particle deposition probabilities by taking into account the two-way coupled heat and mass transfer between the carrier gas phase and the particle (or droplet) phase. The droplet phase is characterized by three coordinates: the distance from the beginning of the mouthpiece, the particle radius and mass of solute in the droplet. TechAero possesses an additional advantage over the existing Eulerian models, which are mainly developed for monodispersed particles and treat droplet phase as an additional continuous phase. Although modification can be made to deal with polydisperse particles, these traditional models cannot differentiate particles of the same size with varying solute concentration. This new model is discussed in detail in the following chapter.

2.6 Microgravity, Respiratory System and Deposition

Of the three mechanisms responsible for aerosol deposition in human respiratory tract, only sedimentation is dependent on gravity. In a closed, near-zero gravity environment (e.g. in a spacecraft), no sedimentation occurs and airborne particle concentration remains high. New plans for long term human space exploration, and potential exposure to hazardous lunar and Martian aerosols, make the study of the effect of gravity on aerosol lung deposition of considerable interest. Gravity also plays a very important role on the function of the human lung. An exposure to microgravity brings an imbalance to the physiological equilibrium, some effects of which are instantaneous while others occur over a period of time. Researchers have studied the influence of gravity on the human lung in numerous studies. Parabolic flight and spaceflight are the two practical means of achieving microgravity appropriate for human experimentation.

Before going into microgravity lung deposition, one should examine how the respiratory physiology is affected by microgravity. The respiratory system is very susceptible to microgravity. Alveoli at the base of the lung are relatively compressed compared with the apical ones, since the lung gets distorted under its own weight. Poorly expanded alveoli being more compliant, there is a ventilation gradient from bottom to the top in the lung. Weightlessness tends to alter this gradient and this change in the ventilation distribution is expected to influence the distribution and amount of particle deposition in the lung.

2.6.1 Effect on Respiratory System

2.6.1.1 Lung Volume:

Functional Residual Capacity (FRC) is defined as the airspace volume during tidal breathing at the beginning of inhalation. Short exposure of microgravity in parabolic flight results in a reduction of about 400 ml (Paiva et al. [60]). This is in agreement with the measurement from Spacelab SLS-1, where a 15% reduction in FRC was recorded (Elliott et al. [21]). Vital capacity (VC),the exhaled amount after maximum inhalation, is recorded to go down by 8% during parabolic flight (Paiva et al. [60]) and by 10% during sustained microgravity in spacelab study (Sawin et al. [70]). Residual volume (RV), the volume of airspaces when lung is minimally inflated, is reduced by an amount of about 310 ml (18%) in microgravity (Elliott et al. [21]). Total lung capacity (TLC), defined as the maximum amount a person can inhale, is reported to be reduced by 18% which is mainly due to the reduction in RV (Elliott et al. [21]). Finally, the tidal volume is approximately 15% less in microgravity than that in normal gravity (Elliott et al. [21]).

2.6.1.2 Chest Wall Configuration:

In microgravity, an inward displacement of the abdominal wall elevates the diaphragm and results in a reduction in lung volume without any associated change in the rib cage. Edyvean et al. [19] noted an increase in the abdominal contribution to the tidal volume from 33% in normal gravity to 51% in microgravity.

2.6.1.3 Ventilation and Perfusion:

A non-uniform distribution of ventilation-perfusion exists in the lung under normal gravity. A near zero gravity environment makes the distribution uniform since the lung distorts without its own weight. Apart from gravity, the incomplete diffusion equilibration along the acinus and the convection-diffusion interaction brings inhomo-

geneities into small regions of the lung. Differing lung compliance, airway resistance, chest wall and diaphragm have a greater influence on ventilation distribution (Guy et al. [36]). Guy et al. [36] and Prisk et al. [64], in their recent experiments, found that a small amount of ventilation and perfusion inhomogeneity still persists in prolonged microgravity.

2.6.2 Microgravity Lung Deposition

Hoffman and Billingham [40] did the first experimental study to obtain deposition of 2 μm particle in various gravity levels. Twenty years later Darquenne et al. [12] performed a similar study to measure intrapulmonary deposition of 0.5, 1, 2 and 3 μm particles during the parabolic flights using NASA Microgravity Research Aircraft. Although microgravity data has only recently become available, numerous theoretical studies have been performed in the past to quantify microgravity lung deposition. Back in the 1960s, Muir [56] theoretically examined the influence of gravity on aerosol deposition. Beeckmans [3] used his deposition model (Beeckmans [2]), developed using normal gravity data, to predict deposition with microgravity. Recently Darquenne et al. [12] used their numerical model, also developed for normal gravity, to predict micro- and hyper- gravity deposition.

Although predicting microgravity deposition, neither of these models adopted any change in lung geometry or breathing parameters that are so obvious from the previous experimental studies. So, it is a matter of great interest to examine these effects on microgravity deposition. Axial diffusion can also play a significant role in microgravity, since in the absence of settling effect, more particles are likely to be carried deeper into the lung.

2.7 Summary

Deposition of aerosol in the human respiratory tract is mainly due to impaction, sedimentation and diffusion, and is influenced by physical properties of the particle, the lung geometry and the breathing parameters. An appropriate deposition model should address all the above mentioned mechanisms and parameters. When considering an Eulerian version of the model, a properly derived deposition function is a precondition along with these factors. In a situation when such an Eulerian equation is not available, one should adopt a proper conversion technique. In this thesis, two Lagrangian-to-Eulerian conversion schemes will be introduced and applied into TechAero. Issues of effect of change of lung geometry on total deposition will be addressed. Finally, this model will be used to predict microgravity deposition and what factors, other than lung geometry, can significantly influence aerosol deposition in microgravity will be discussed.

Chapter 3

Theory and Model

3.1 Introduction

In this chapter, the theory behind the lung deposition code TECHAero will be discussed in brief, followed by the introduction of two Lagrangian-to-Eulerian conversion techniques, one based on generation residence time and the other on control volume residence time.

3.2 Description of the Model

Pharmaceutical aerosols are usually a mixture of two components, a non-volatile drug (solute) and water or a volatile solvent. To simulate deposition of such aerosols it is necessary to consider simultaneous heat and mass transport between the solute and the solvent. Information about the solute concentration in the particle is important for a couple of reasons. Although mass transport between the particle and the surrounding involves only the solvent, the amount of solute deposition is the main objective. Mass transport, on the other hand, can be strongly influenced by the solute concentration. Moreover, diffusion can lead to the occurrence of particles with different size and solute concentration originating from the same particle class at inlet.

An appropriate Eulerian deposition model must have the capability to resolve these issues. The model presented in this thesis is an attempt to include these issues.

3.2.1 New Dimensions

This new method introduces two new dimensions in addition to the regular spatial dimensions. To track the solute concentration in the particle, the amount of solid, represented by m_1 is introduced as a new independent variable. m_1 represents the mass of drug in a single particle, and there is no transport of particle in m_1 axis, which means agglomeration or break-up of particles is neglected. Particle size, represented by its radius R, is the 2nd new dimension. Because no evaporation of the drug (solute) occurs, the minimum radius value is no longer 0, but

$$R_{min} = \left(\frac{3m_1}{4\pi\rho_d}\right)^{\frac{1}{3}} \tag{3.1}$$

which means,

$$\left(\frac{3m_1}{4\pi\rho_d}\right)^{\frac{1}{3}} \leq R < \infty \tag{3.2}$$

Mass of solvent in a single droplet is a derived quantity, and it is not to be directly conserved. Mass of solute and solvent are calculated as follows,

$$\text{Vol}_1 = \frac{w_1}{\rho_{H_2O}} + \frac{m_1}{\rho_d} \tag{3.3}$$

$$m_1 = \frac{3}{4}\pi R^3 * (\text{solute concentration}) \tag{3.4}$$

$$w_1 = \rho_{H_2O}\left(\frac{4}{3}\pi R^3 - \frac{m_1}{\rho_d}\right) \tag{3.5}$$

where w_1 is the mass of solvent.

With the introduction of these two new independent variables, a hyper-space with five dimensions is defined. Any position in a cylindrical domain Ω^* of this new hyper-space is represented by the following vector,

$$\vec{\chi}^* = (x, r, \theta, R, m_1) \tag{3.6}$$

In the same way, velocity is defined as,

$$\vec{V}^* = (U, V, W, \dot{R}, \dot{m}_1) \tag{3.7}$$

Here, $\dot{R}$ is the rate of size change, analogous to a velocity, which drives the particles in a manner similar to convection up or down the R axis, and $\dot{m}_1$ is the rate of change of mass of a given particle. The material derivative for a generic quantity is expressed as,

$$\frac{D\phi}{Dt} = \frac{\partial \phi}{\partial t} + U\frac{\partial \phi}{\partial x} + V\frac{\partial \phi}{\partial r} + \frac{W}{r}\frac{\partial \phi}{\partial \theta} + \dot{R}\frac{\partial \phi}{\partial R} + \dot{m}_1\frac{\partial \phi}{\partial m_1} \tag{3.8}$$

3.2.2 Governing Equations

The problem of deposition of hygroscopic or volatile aerosol in confined flow field (e.g. human lung) is a highly time dependent phenomenon, and a system of coupled differential equations must be solved to obtain its solution (deposition in this case). For pharmaceutical aerosols (between 1 and 10 μm in diameter) the mass fraction is generally smaller that 10^{-6}. In such a condition, particles have very little influence on the flow field of the continuous phase, and it is a reasonable assumption to neglect momentum exchange between particles and carrier gas. Assuming the flow velocity is known, the problem reduces to the solution of four balance equations: number concentration and thermal energy for the particle phase and concentration of evaporated solvent and thermal energy for the continuous phase.

The balance equations for particle and continuous phase are,

$$\int_{\Omega^*} \left[\frac{Dn^*}{Dt} - \frac{\partial}{\partial \chi_i}\left(D_j^* \delta_{ij} \frac{\partial n^*}{\partial \chi_j}\right) + \dot{n}_{de}^*\right] dv = 0 \tag{3.9}$$

$$\int_{\Omega^*} \left[\frac{DH^*}{Dt} - \frac{\partial}{\partial \chi_i}\left(D_j^* \delta_{ij} \frac{\partial H^*}{\partial \chi_j}\right) + \dot{Q}_{ev,\,co,\,de}^*\right] dv = 0 \tag{3.10}$$

$$\int_{\Gamma^*} \left[\frac{DC_\infty^*}{Dt} - \frac{\partial}{\partial X_i}\left(D_{j\,vap}^* \delta_{ij} \frac{\partial C_{infty}^*}{\partial X_j}\right) + \dot{W}_{ev,\,w}^*\right] dv = 0 \tag{3.11}$$

$$\int_{\Gamma^*} \left[\frac{DH^*_\infty}{Dt} - \frac{\partial}{\partial X_i} \left(k^*_{a\,j} \delta_{ij} \frac{\partial T^*_{infty}}{\partial X_j} \right) + \dot{Q}^*_{\infty\, co,\, ev,\, w} \right] dv = 0 \qquad (3.12)$$

where, n^* is the particle number concentration, H^* and H^*_∞ are enthalpy of particle and air/vapor mixture respectively, C^*_∞ vapor concentration of volatile species, T^*_∞ is the temperature of the air/vapor mixture, D^*_j is particle diffusivity and $D^*_{j\,vap}$ is the molecular diffusivity of volatile species. The quantity $\dot{n}^*_{de}$ represents the deposition rate and $\dot{Q}^*_{ev,\, co,\, de}$ is the combined heat loss by evaporation, conduction and deposition. $\dot{W}^*_{ev,\, w}$ is equivalent to the combination of total evaporative mass from the particles in the control volume and any contribution from the walls at the boundary of the domain. $\dot{Q}^*_{\infty\, co,\, ev,\, w}$, in a similar manner, corresponds to the heat transferred to all droplets in the control volume by conduction and evaporation plus the heat exchanged with the boundary walls.

In the conservation equations of the continuous phase (Eq. 3.11 and 3.12), the balance is carried out on a control volume of the regular space Γ^*, where space is defined by the following vector

$$\vec{X}^* = (x, r, \theta) \qquad (3.13)$$

In these two equations (Eq. 3.11 and 3.12), the source terms carry the contributions of all particle sizes and mass of solute.

3.2.3 Cross-Sectional Averaging and Simplifications

In most of the existing deposition models [11, 18, 57, 83], respiratory tract is treated as a one dimensional sequence of air ducts with either constant or time dependent cross-sectional area. All the quantities are averaged over the cross-section. This simplification aids in reducing the dimensions of the problem. For this proposed model, the area averaging results in significant reduction in computational effort by reducing two dimensions.

Cross-sectional averaging of any dependent variable ϕ^* can be performed over the

cross-sectional area $A(x)$, and by doing so the surface integral is substituted by simple product of the area times the averaged variable ϕ,

$$\phi \equiv \bar{\phi^*} = \frac{1}{A}\int_A \phi^* dA \qquad or \qquad \int_A \phi^* dA = \phi A \tag{3.14}$$

And the resulting domains after averaging are as follows,

$$\vec{\chi} = (x, R, m_1) \qquad \text{defined in } \Omega \tag{3.15}$$

$$\vec{X} = (x) \qquad \text{defined in } \Gamma \tag{3.16}$$

In this study, the particles are considered as non-hygroscopic and stable after being discharged into the respiratory tract. As a consequence, no mass transfer will occur between the particle and continuous phase. Because of this, only the conservation equation of particle number concentration needs to be considered.

Further simplifications can be made if it is assumed that the particles consist of pure solute, which results in $\dot{m}_1 =$ constant and $w_1 = 0$. Moreover, according to Delhaye [16] even if $A = A(t, X)$, we can write

$$\int_{A_T} \frac{\delta n^*}{\delta t} dA_T = \frac{\delta}{\delta t}\int_{A_T} n^* dA_T \tag{3.17}$$

as long as there is no flux through the duct walls. Incorporating all these simplifications and applying the Divergence Theorem the balance equation for particle number concentration takes the following form (detailed derivation provided in Appendix A),

$$\int_\Omega \frac{\partial(An)}{\partial t} d\Omega + \int_{S_x} \left(AUn - AD_x \frac{\partial n}{\partial x}\right) . \vec{n_x} dS_x + \int_{S_R} \left(A\dot{R}n\right) . \vec{n_R} dS_R + \int_\Omega A\dot{n}_{de} \Omega = 0 \tag{3.18}$$

To solve the discretized system of equations for the particle number concentration in the grid cell for each time interval, strongly implicit method proposed by Stone [81] was used. The removal of particles by deposition is dealt with the source term $A\dot{n}_{de}$. The main objective of the model is to predict the amount of drug deposited in different locations of the lung (extrathoracic, tracheo-bronchial, and alveolar), which is obtained by integrating the source term over time and airway length.

3.2.4 Total Particle Deposition

Primary deposition mechanisms and the factors affecting those are explained in Chapter 2. How these processes are adopted numerically, how they are being converted to the Eulerian viewpoint, and how they are being combined is described in the following sections.

For completeness, functions used in this model to calculate deposition probability are listed below (Table 3.1),

Table 3.1: Deposition functions used in TechAero.

Formula	Mechanism
$P_{ET} = 100 - \frac{100}{11.5\text{Stk}^{1.912}\text{Re}^{0.707}+1}$	Extrathoracic deposition
$P_i = 1.606\ \text{Stk} + 0.0023$	Impaction
$P_s = \frac{2}{\pi}[2\epsilon\sqrt{(1-\epsilon^{2/3})} - \epsilon^{1/3}\sqrt{(1-\epsilon^{2/3})} + arcsin\epsilon^{1/3}]$	Sedimentation
$P_D = 1 - 0.819e^{-14.63h} - 0.097e^{-89.22h} - 0.0325e^{-228h} - 0.0509e^{-125.9h^{2/3}}$, for $h < 0.05$ $P_D = 6.41h^{2/3} - 4.8h - 1.12h^{4/3}$, for $h > 0.05$	Diffusion

Before summing up these individual deposition probabilities, they are converted to the Eulerian perspective. Depending on the conversion scheme these functions are evaluated in terms of either the dimension of the whole generation or control volume dimension. When probabilities are obtained for each control volume these are then combined according to the following expression,

$$P_{Total-cv} = 1 - (1 - P_{I-cv})(1 - P_{S-cv})(1 - P_{D-cv}) \tag{3.19}$$

It should be noted, however, that the expression for the extrathoracic deposition includes the effect of impaction, sedimentation and diffusion implicitly, and is taken care of separately. The above equation is used only inside the lung.

3.2.5 Lagrangian to Eulerian Conversion

As mentioned earlier, equations used to calculate deposition probabilities are either empirical or derived from the Lagrangian perspective, i.e. steady state in nature. In the literature, there are many models to predict aerosol deposition in human respiratory tract, both Lagrangian deposition models and Eulerian. The Lagrangian deposition models use the above mentioned probability equations directly. But in Eulerian models, the deposition probabilities need to be converted into deposition probability rates.

In most of the models [11, 84] the deposition probability rate is calculated simply by dividing the total deposition probability by the residence time, and is assumed constant over the whole generation.

One of the main reasons to prefer Eulerian model over Lagrangian model is to incorporate the effect of time varying flow rate and aerosol concentration encountered in many types of pharmaceutical inhalers, such as metered dose inhalers and dry powder inhalers. Grgic et al. [34] examined, both experimentally and numerically, that unsteady flow enhances mouth-throat deposition significantly. Mouth-throat deposition directly affects lung deposition. So, in order to simulate transient aerosol deposition, deposition functions based on instantaneous deposition are required, which are presently not available. For this objective to be achieved either experimental data based on time dependent deposition or a new set of equations based on Eulerian frame of reference is needed. An alternative approach is to develop a numerical scheme to obtain Eulerian deposition rates equivalent to the present Lagrangian formulas.

In the next two sections, two different ways of calculating the Eulerian deposition rates will be introduced : one based on control volume residence time, and the other is based on lung generation residence time.

3.2.5.1 Total Deposition Based on Lung Generation Residence Time (GRT)

The general transport theorem :

$$\frac{\partial(\rho n)}{\partial t} + \text{div}(\rho n u) = \text{div}(\Gamma \text{grad}(n)) + S_n \tag{3.20}$$

Under the steady state condition, if no diffusion is considered, the one-dimensional convection equation is obtained as follows,

$$\frac{\partial(nu)}{\partial x} = S_n \tag{3.21}$$

where n is in number of particles per unit volume and S_n is the source term (deposition rate) in units of number of particle per volume per time.

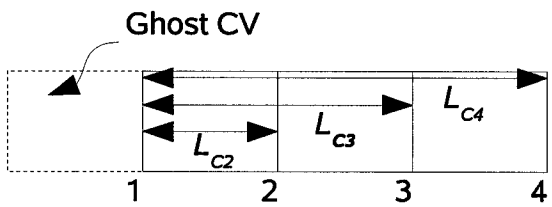

Figure 3.1: Discretization of the domain

Let us consider the figure 3.1 to summarize the discretization concept.

Applying the concept of ghost or auxiliary control volume (CV) for application of boundary condition, the value of the last CV face is shifted to the current CV face, and thus it is assumed that the value at 1 is known. Considering the first CV

$$u\frac{n_1 - n_2}{\Delta x} = \dot{P}_k n_1 \tag{3.22}$$

where, $\dot{P}_k$ is the deposition probability rate per unit time for the whole generation, and Δx is the length of the CV. Therefore,

$$(n_1 - n_2)\frac{u}{L_2} = \dot{P}_k n_1$$

$$\Rightarrow \frac{n_1 - n_2}{\tau_2} = \dot{P}_k n_1$$

$$\Rightarrow n_2 = n_1 - n_1 \dot{P}_k \tau_2 \tag{3.23}$$

Similarly,

$$n_3 = n_2 - n_2 \dot{P}_k (\tau_3 - \tau_2) \tag{3.24}$$

Substituting the value of n_2,

$$\Rightarrow n_3 = n_1 - n_1 \dot{P}_k \tau_3 - n_1 \dot{P}_k^2 \tau_2 \tau_2 + n_1 \dot{P}_k^2 \tau_2 \tau_3 \tag{3.25}$$

and,

$$n_4 = n_3 - n_3 \dot{P}_k (\tau_4 - \tau_3)$$

Neglecting the 3rd and higher order terms,

$$\Rightarrow n_4 = n_1 - n_1 \dot{P}_k \tau_4 - n_1 \dot{P}_k^2 \tau_2 \tau_2 - n_1 \dot{P}_k^2 \tau_3 \tau_3 + n_1 \dot{P}_k^2 \tau_2 \tau_3 + n_1 \dot{P}_k^2 \tau_3 \tau_4 \tag{3.26}$$

and,

$$n_5 = n_1 - n_1 \dot{P}_k \tau_5 - n_1 \dot{P}_k^2 \tau_2 \tau_2 - n_1 \dot{P}_k^2 \tau_3 \tau_3 - n_1 \dot{P}_k^2 \tau_4 \tau_4 + n_1 \dot{P}_k^2 \tau_2 \tau_3 + n_1 \dot{P}_k^2 \tau_3 \tau_4 + n_1 \dot{P}_k^2 \tau_4 \tau_5 \tag{3.27}$$

Once we know the concentration of at all the control volume face we can determine the total deposition as follows,

$$\text{Total Deposition} = (n_1 - n_2) + (n_2 - n_3) + (n_3 - n_4) + (n_4 - n_5)$$

substituting all the individual concentrations,

$$\text{Total Deposition} = n_1 (\dot{P}_k \tau_5 + \dot{P}_k^2 (\tau_2 \tau_2 + \tau_3 \tau_3 + \tau_4 \tau_4) - \dot{P}_k^2 (\tau_3 \tau_4 + \tau_4 \tau_5)) \tag{3.28}$$

In general.

$$\text{Total Deposition} = \dot{P}_k \tau_{N+1} + \dot{P}_k^2 \sum_{2}^{N} \tau_i^2 - \dot{P}_k^2 \sum_{3}^{N} \tau_i \tau_{i+1} \tag{3.29}$$

where, N is the number of control volume, N+1 is the number of control volume faces, and all the indexes represent control volume face.

Edwards [18] used a similar approach for deposition rate calculation.

3.2.5.2 Total Deposition Based on Control Volume Residence Time (CVRT)

This alternative conversion approach was developed during this work and used here for the first time. Similar to the previous approach, under the steady state condition if no diffusion is considered, the one-dimensional convection-diffusion equation takes the following form,

$$\frac{\partial(nu)}{\partial x} = S_n \tag{3.30}$$

where n is the number of particles per unit volume and S_n is the source term (deposition rate) in units of number of particles per volume per time.

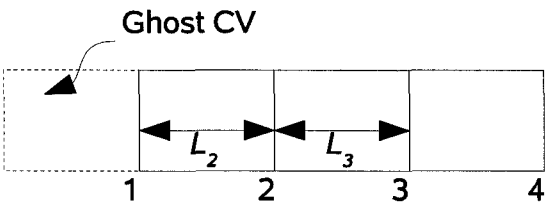

Figure 3.2: Discretization of the domain

Let us consider the figure 3.2 to summarize the discretization concept.

Using the concept of ghost control volume for applying boundary conditions, and considering the first control volume,

$$u\frac{n_1 - n_2}{\Delta x} = \dot{P}_1 n_1 \approx \frac{P_1 n_1}{\Delta t} \tag{3.31}$$

Because in our case Δx is the length of the CV, Δt should also be the residence time in the control volume τ_i. Therefore,

$$\begin{aligned}
(n_1 - n_2)\frac{u}{L_2} &= \frac{P_1 n_1}{\tau_2} \\
\Rightarrow \frac{(n_1 - n_2)}{\tau_1} &= \frac{P_1 n_1}{\tau_1} \\
\Rightarrow n_2 &= n_1(1 - P_1)
\end{aligned} \tag{3.32}$$

Similarly,

$$n_3 = n_1(1 - P_1 - P_2 + P_1P_2)$$

$$\Rightarrow n_3 = n_1(1 - P_1)(1 - P_2) \tag{3.33}$$

and,

$$n_4 = n_1(1 - P_1 - P_2 - P_3 + P_1P_2 + P_2P_3 + P_3P_1 - P_1P_2P_3)$$

$$\Rightarrow n_4 = n_1(1 - P_1)(1 - P_2)(1 - P_3) \tag{3.34}$$

Once we know the concentration of at all the control volume face we can determine the total deposition as follows,

$$\text{Total Deposition} = (n_1 - n_2) + (n_2 - n_3) + (n_3 - n_4)$$

Substituting the individual concentrations at the CV face,

$$\text{Total Deposition} = n_1(1 - (1 - P_1)(1 - P_2)(1 - P_3)) \tag{3.35}$$

In general the total deposition probability becomes

$$\text{Total Deposition Probability} = 1 - (1 - P_1)(1 - P_2)(1 - P_3).....(1 - P_n)$$

$$\Rightarrow \text{Total Deposition Probability} = 1 - \prod_{i=1}^{n}(1 - P_i) \tag{3.36}$$

To the author's knowledge, there is no record of use of this approach in the past.

3.2.6 Lung Model

In TechAero, a symmetrically branching lung model is used (see figure 3.3). The model is based on the morphometric data provided by Phillips et al. [62] for the conducting airways and by Haefeli-Bleuer and Weibel [37] for the alveolar region. The diameter and length of different generations of the lung model are given in Finlay et al. [27]. The volume of an adult lung in this model is 3000 ml.

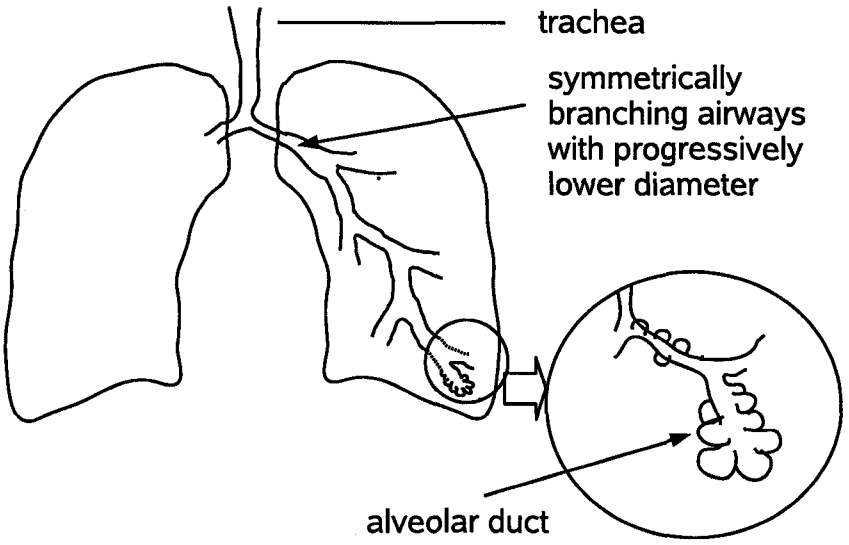

Figure 3.3: Schematic diagram of symmetrically branching lung model.

3.2.7 Boundary Conditions

In TECHAero boundary conditions are specified for both inhalation and exahalation in x, R and m_1 dimensions.

For x dimension: During inhalation

$$\phi = \phi(R, m_1, t), \text{ at the mouth,}$$

and

$$\frac{\partial \phi}{\partial x} = 0, \text{ at the alveoli.}$$

During exhalation,

$$\frac{\partial \phi}{\partial x} = 0, \text{ at the mouth,}$$

and,

$$\phi = \text{constant, at the alveoli.}$$

For R dimension,

$$\phi = \phi(x, m_1, t) = 0, \text{ for all cases.}$$

For m_1 dimension,

$$\phi = \phi(x, R, t) = 0, \text{ for all cases.}$$

3.2.8 TECHAero Usage

TECHAero (Truly Eulerian Code for simulation of Hygroscopic AEROsols) is a Fortran code that implements the theory and methods described above. TECHAero uses the following input and output files:

input.dat contains all the input parameter those can vary depending on the the drug used, ambient conditions, and breathing pattern. Particle properties, parameters to define particle size distribution (MMD, GSD) as well as particle production rate are specified. Input values for grid size in x and R directions along with time step and the convergence tolerance is listed in the input file.

grid.out, locdep.out, gendep.out and *regdep.out* are the TechAero output files. In *grid.out* , the solution grids for x, R and m_1 dimensions are listed, while local specific deposition or dosage in each unit cell and generation are presented in *locdep.out* and *gendep.out* respectively. *redep.out* represents the regional deposition for extrathoracic, tracheo-bronchial and alveolar region as an absolute amount (mg) and as a percentage.

3.3 Scaling Lung Geometry

The effect of microgravity on respiratory anatomy is described in the previous chapter. Significant reduction in functional residual capacity (FRC) has been reported in every experimental studies carried out so far. To examine the effect of change of geometry

on total aerosol deposition, the original lung model was scaled. The length and diameter of the model is scaled by a factor of $(FRC/3l)^{1/3}$ following Finlay [25].

3.3.1 Summary

A description of the deposition model along with the conversion schemes, lung geometry model are presented. Although derived for steady state condition, these two approaches will be used to for conversion for all deposition mechanisms in unsteady situations as well. Validation of the proposed approaches and comparison of total deposition with these methods will be discussed in the following chapters.

Chapter 4

Results and Discussion

4.1 Introduction

This chapter will serve two purposes. The numerical techniques of Lagrangian-to-Eulerian conversion described in the previous chapter will be validated first. Then those techniques will be implemented in the lung simulation code TECHAero (Lange and Finlay [45]) to validate the model with experimental results. Once the validation is done, the model will be used to estimate highly transient deposition, e.g. from DPI's, and to predict deposition from very slow breathing. In the next section TECHAero will be used to predict lung deposition in microgravity, and the result will be compared with both experimental and simulated results from the literature.

4.2 Validation of the Conversion Schemes

Before being implemented into TECHAero the conversion techniques are required to be tested against both theory and experimental results. Heyder and Gebhart [39] described aerosol deposition by sedimentation from constant flow in straight circular tube, which will be used for validation of the conversion techniques.

4.2.1 Different Sedimentation Functions

In the literature there are three different categories of sedimentation functions which were previously described in Chapter 2 (see Table 2.2). Beeckmans [2], Findeisen [24], Landahl [44] used a similar deposition function. In the functional form used by Beeckmans [2],

$$P_s = 1 - \exp(-\frac{gd^2\rho C\tau}{9\pi\mu R}) \tag{4.1}$$

if $v_s = \frac{\rho d^2}{18\mu}$ (particle settling velocity), $a = \frac{\pi d^2}{4}$ (total cross-sectional area of any generation), $Q = AU$ (flow rate) and $\tau = \frac{l}{u}$ (residence time) are substituted, the equation takes the following form

$$P_s = 1 - exp(-\frac{2}{\sqrt{\pi a}} g v_s A \frac{l}{Q}) \tag{4.2}$$

used by Taulbee and Yu [83]. The variable a in this expression represents the cross-sectional area of a single airway in any generation while A is the total cross-sectional area of that particular generation. This formula was derived on the basis of a straight horizontal tube, but the geometry of alveolated airways is significantly different. To accommodate this, Taulbee and Yu [83] added an extra term to the original equation,

$$P_s = (1-\alpha)\frac{cAU}{l}(1 - \exp(-\frac{2}{\sqrt{\pi a}} g v_s A \frac{l}{Q})) + 1.13\frac{c v_s g}{n} N_a^{1/3} V_{aT}^{2/3} \frac{dF}{dz} \tag{4.3}$$

where α represents the fraction of airway surface which is alveolated. This equation is manipulated in such a manner to give the deposition probability rate per unit time per unit length.

Pich [63] developed an analytical method, based on limiting trajectories of particles, to calculate sedimentation probability of colloid particles from laminar flow in circular tubes,

$$P_s = \frac{2}{\pi}[2\epsilon\sqrt{(1-\epsilon^{2/3})} - \epsilon^{1/3}\sqrt{(1-\epsilon^{2/3})} + \arcsin\epsilon^{1/3}] \tag{4.4}$$

where $\epsilon = \frac{3v_s L}{4UD}$ is the sedimentation parameter.

To compare their behavior, these functions were tested for varying particle sizes and flow rates, both in alveolated and non-alveolated airways (Figure 4.1 - 4.4) Difference

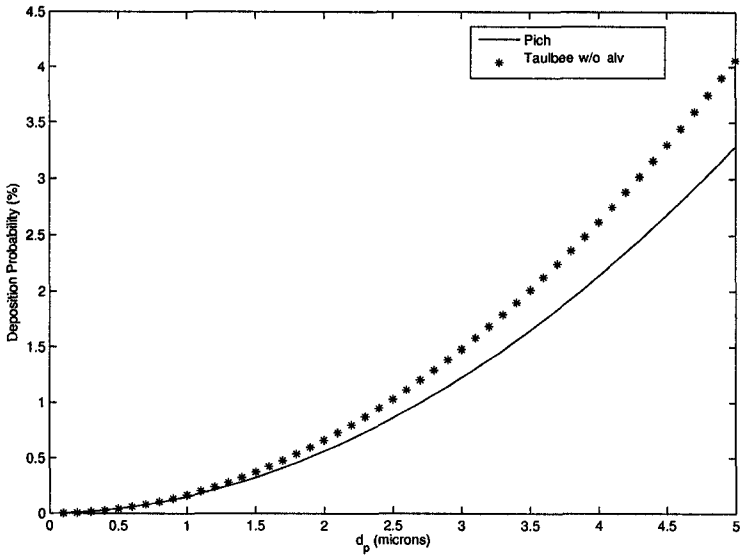

Figure 4.1: Comparison of various sedimentation function in 14th generation for varying particle size.

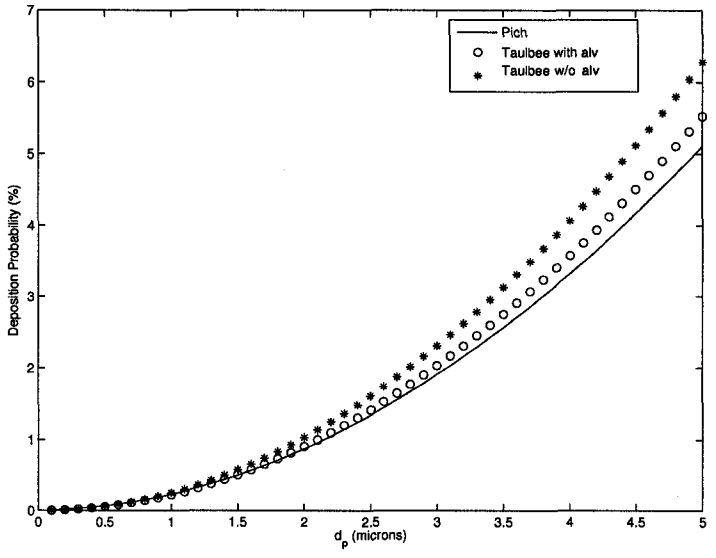

Figure 4.2: Comparison of various sedimentation function in 16th generation for varying particle size.

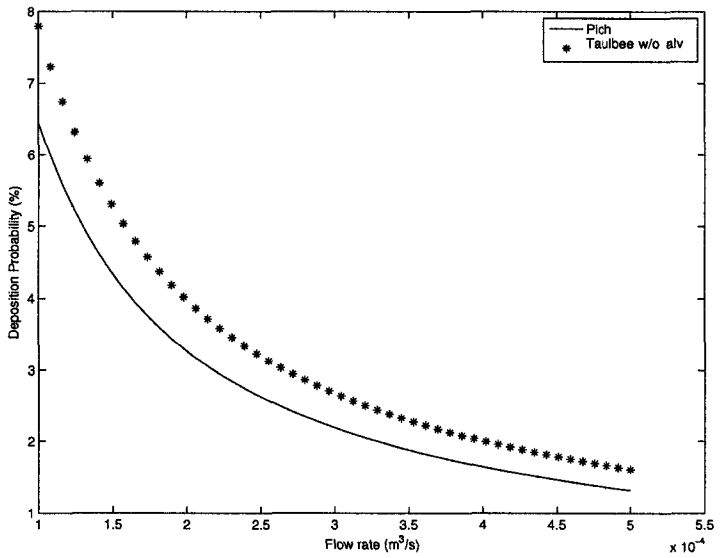

Figure 4.3: Comparison of various sedimentation function in 14th generation for varying flow rate.

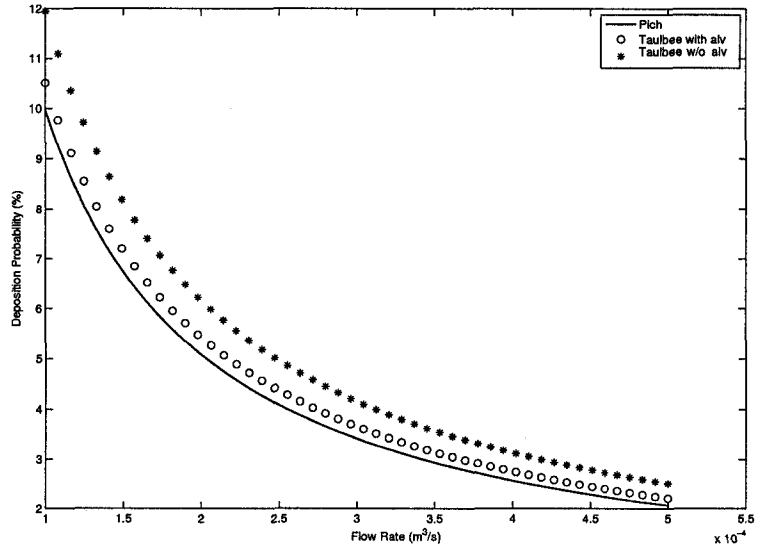

Figure 4.4: Comparison of various sedimentation function in 16th generation for varying flow rate.

was highest between equation 4.4 and 4.2, because equation 4.2 did not take alveolar geometry into consideration. Difference was not very significant between equation 4.4 and 4.3 (the modified function by Taulbee and Yu [83]). The function by Pich [63] (equation 4.4) is recent and has solid mathematical foundation. Moreover, this function had been tested by several researchers for both straight and randomly oriented tubes, suitable for lung simulations purposes. That is why, for the validation purposes, function proposed by Pich [63] (equation 4.4) was used.

4.2.2 Validation: CVRT Approach

For validating the proposed Control Volume Residence Time (CVRT) approach, results from [39] were used. The parameters used in the following calculations were: length of the tube = 100 cm, diameter of the tube = 0.8 cm, diameter of the particle = 3.5 μm, density of droplet particle = 0.91 g/cm^3, volume flow rate = 6 $\sim$ 100 cm^3/s. Here the only variable was flow rate. It is evident from figure 4.5, as the flow rate increases deposition fraction goes down, which is logical because with increasing flow rate particles have less time to settle. The relative error curve is somewhat interesting in nature.

The relative error goes down very sharply with flow rate, but after a certain value it goes up gradually although remaining low (figure 4.6). The reason behind this is that the two curves intersect at a particular flow rate and the numerically predicted value becomes slightly higher than the theoretical prediction. The control volume approach to calculate deposition has one consistent error associated with it, which is the effect of the assumed remixing at the beginning of each control volume face. Because of the remixing this method is not able to follow the limiting trajectory and always estimates less deposition. But from the figure 4.6 it seems likely that at higher velocities the effect of remixing is taken over by some other phenomenon and the numerical prediction starts to give higher deposition than predicted by the theory.

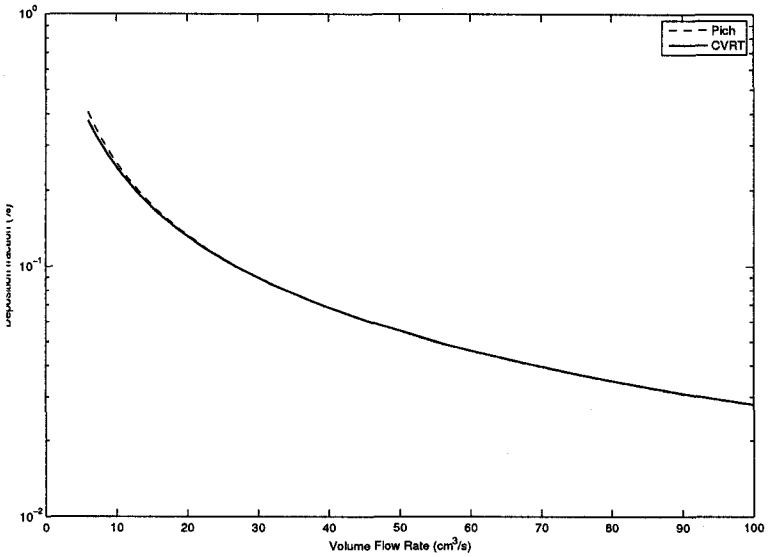

Figure 4.5: Deposition fraction against the volume flow rate.

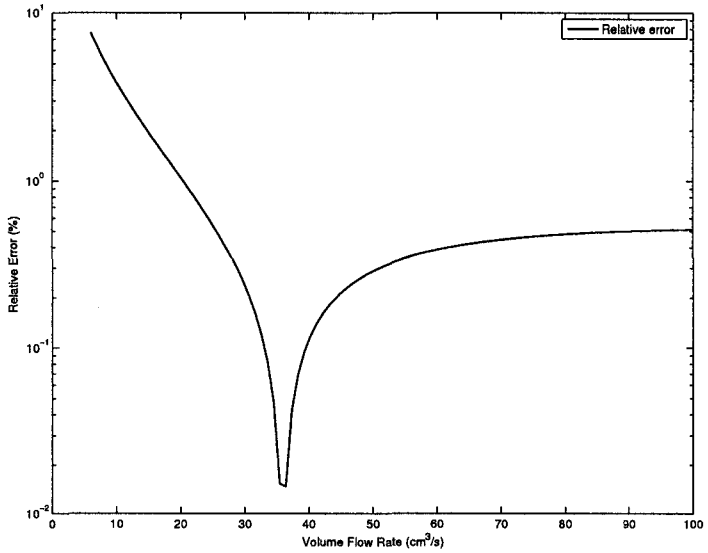

Figure 4.6: Relative error against the volume flow rate.

The theory was validated against the following parameters: number of control volumes, tube length, tube diameter, particle diameter. The parameters studied fall into two categories, one of physical parameters and the other of numerical parameters.

The number of control volumes is a numerical parameter that has nothing to do with the physics or the theory. In the proposed model, if the number of control volumes is

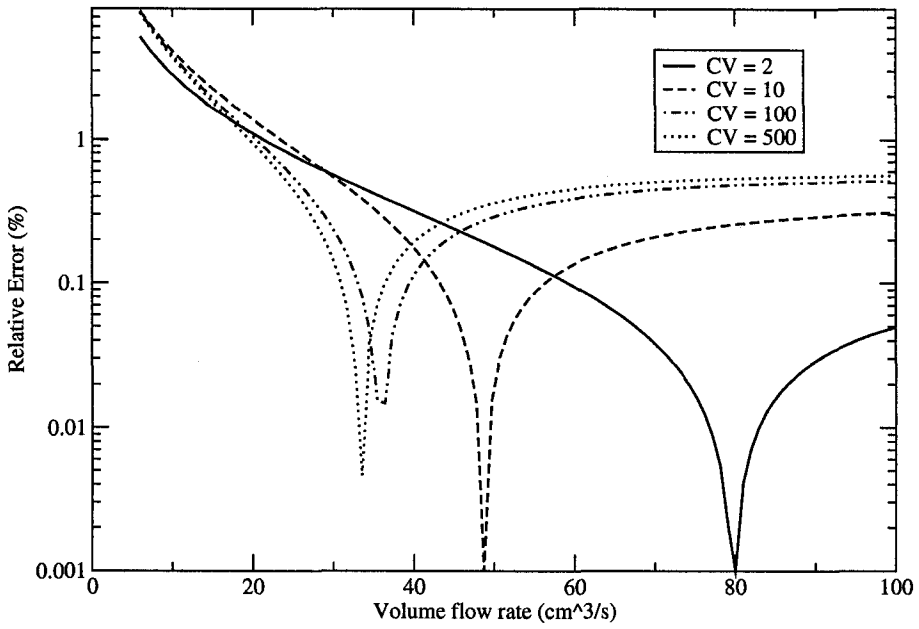

Figure 4.7: Relative error as it changes with the increase of CV number.

equal to 1, the method should give the exact values (no remixing). Indeed, the exact behavior was found (not shown in the plot). When more than one control volume is used, it is obvious that some error will occur as complete remixing takes place in every control volume face. But as the number of control volumes is increased, the error increases slightly but with progressively smaller changes. With the increase of number of control volumes, the deposition in any particular control volume goes to a very small value, and the effect of remixing becomes less significant. From figure 4.7, one can notice a pattern: the error drops sharply up to a certain flow rate and then goes up again, but it remains bounded, and it becomes relatively independent of the flow rate. As flow rate increases the total deposition probability goes down,

and so does the absolute error, even though the relative error remains constant and independent of flow rate. The most interesting aspect is the intersection between the theoretical and numerical curves, from where the error again goes up, and this point shifts towards a lower volume flow rate as the number of control volumes increases.

The effect of various physical parameters was tested at this stage. First parameter to be considered was the total length. When length is considered, one can either vary the size of control volume or the number of control volumes. Keeping the CV size constant causes an uneven number of remixing for different lengths, and keeping the number of CVs constant makes the CV size uneven. Both the approaches were tested. In figure 4.8a the control volume size is fixed while number of control volumes is set to 100 for all cases in figure 4.8b. The trend remains the same, the error decreases with flow rate up to a certain value, then goes up, but stays bound to a lower value at higher flow rates than that at lower flow rates. In both cases the lowest error shifts towards higher flow rate. As in figure 4.7, the intersection point shifts towards lower flow rate as the number of control volumes is increased. For example, for L = 0.5 m, the intersection occurs at 19.4 cm^3/s (number of CV 50 (CV length fixed), figure 4.8a) while intersection is obtained at 18.3 cm^3/s when number of CV is 100 (figure 4.8b) for the same tube length. As the tube length increases, relative error goes up, but at higher velocities the error tends to a similar value. With the increase of tube length more particles are deposited, which makes the error higher. But at higher flow rates, as more particles escape deposition, the relative error is somewhat reduced.

The effect of tube diameter was also checked. Tube diameter is related to the velocity through the pipe. With a slight modification in the equation for sedimentation parameter it is possible to keep only the diameter in the equation.

$$\text{Sedimentation parameter} = \frac{3V_s l}{4UD}$$

$$U = \frac{Q}{A} = \frac{Q}{\frac{\pi}{4}D^2} = \frac{4Q}{\pi D^2}$$

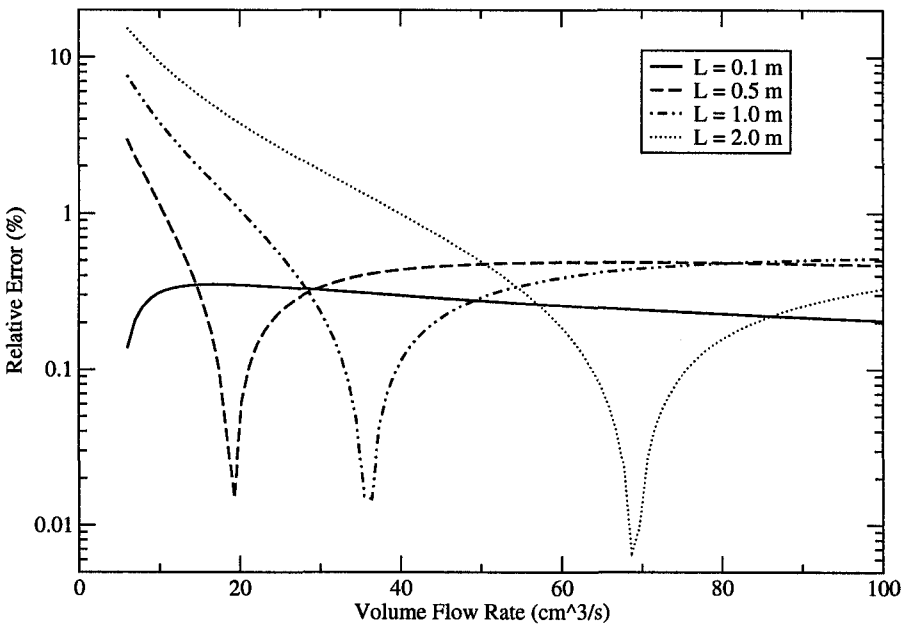

a: Fixed CV length

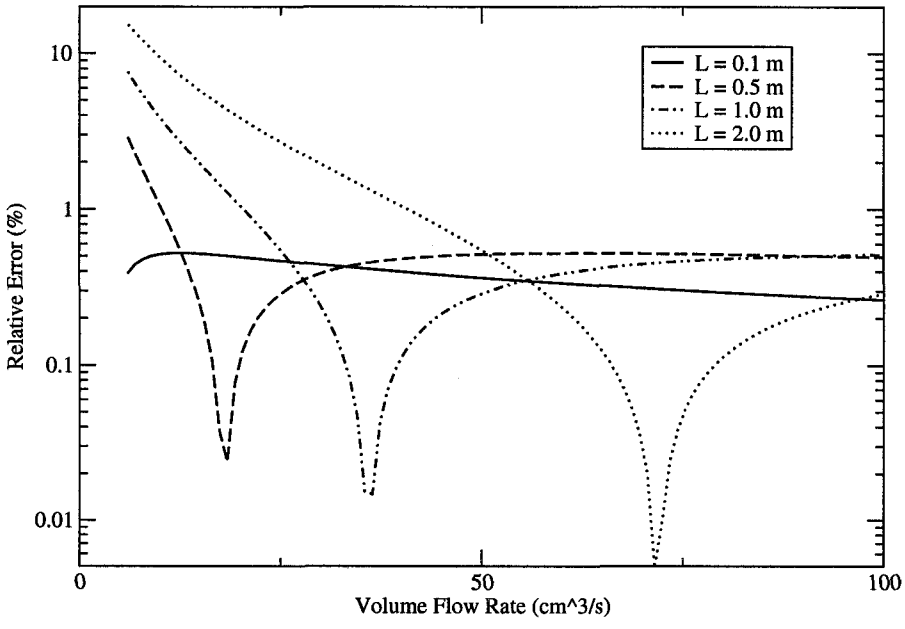

b: Fixed number of CVs

Figure 4.8: Relative error as a function of pipe length.

Combining the two,

$$\text{Sedimentation parameter} = \frac{3V_s l}{4\frac{4Q}{\pi D^2}D} = \frac{3\pi V_s D l}{16Q} \tag{4.5}$$

For the sedimentation parameter to be ≤ 1, i.e. not all particles to be deposited, the

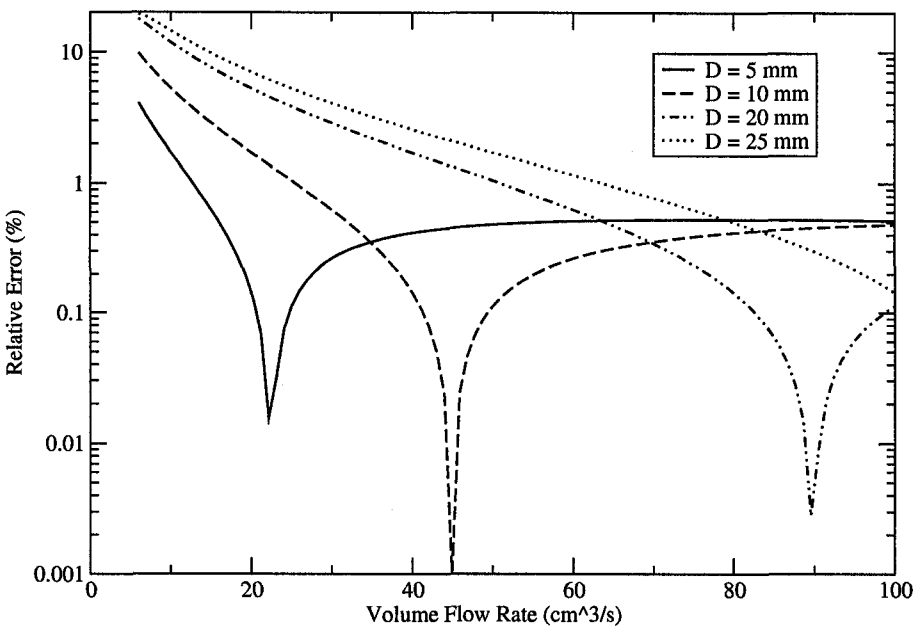

Figure 4.9: Relative error as a function of pipe diameter.

tube diameter cannot exceed 28.5 mm. So, diameter variation for this investigation was maintained within that limit. With the increase of tube diameter, mean fluid velocity goes down, and particles have more time to settle. As a result, deposition is higher and also the corresponding relative error. Error becomes steady at higher flow rates. In this case the intersection point shifts toward the higher flow rate with increasing diameter (figure 4.9).

The last parameter to be tested was the particle size (figure 4.10). Particle size affects the particle settling velocity. Larger particles are more likely to get deposited relative to smaller particles from a flow. A similar trend is observed, relative error goes up with particle size up to a value then starts rising. And the intersection point shifts towards higher flow rate with particle size.

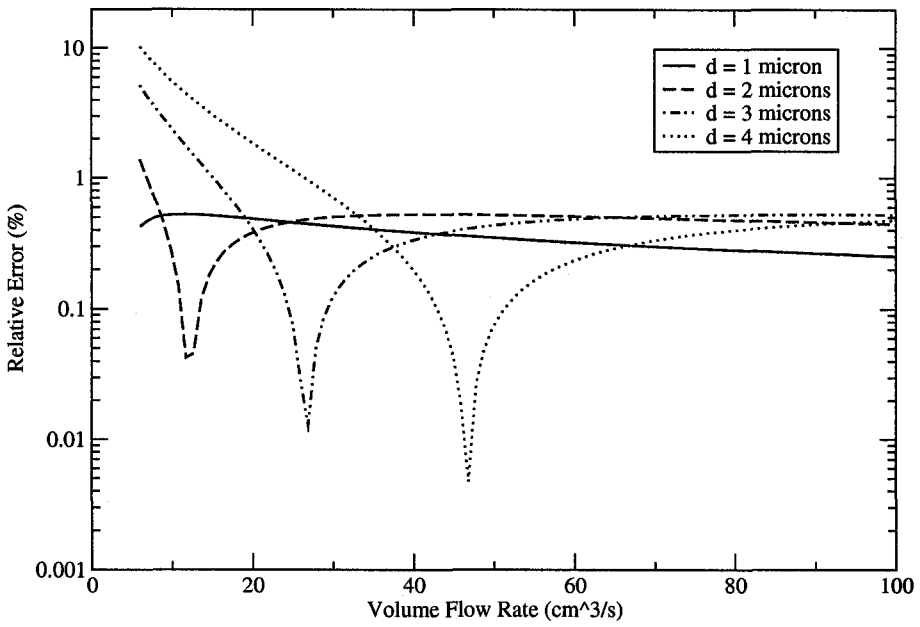

Figure 4.10: Relative error as a function of particle diameter.

In all the cases, the intersection point shows a trend to shift towards higher flow rates. Also as the deposition probability increases the relative error goes up and the location of the intersection between the theoretical and numerical curves shift towards higher flow rates.

4.2.3 Validation: GRT Approach

To validate the Generation Residence Time (GRT) approach, the same parameters as in the validation of the previous proposed theory were used.

Similar to the previous validation, the effect of number of control volumes, tube length, tube diameter and particle size on deposition probability and relative error were investigated.

As in the previous section (CVRT approach), the trends with this method are very similar (figure 4.11 - 4.16). The main difference to be noted is that the numerical

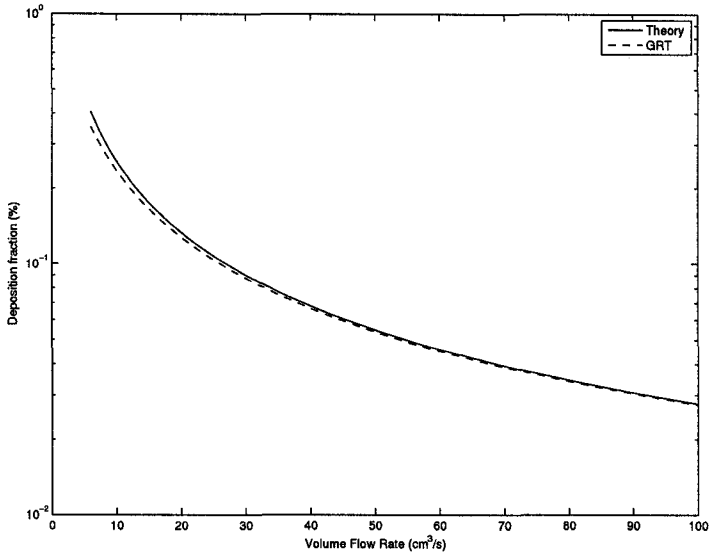

Figure 4.11: Deposition fraction against the volume flow rate.

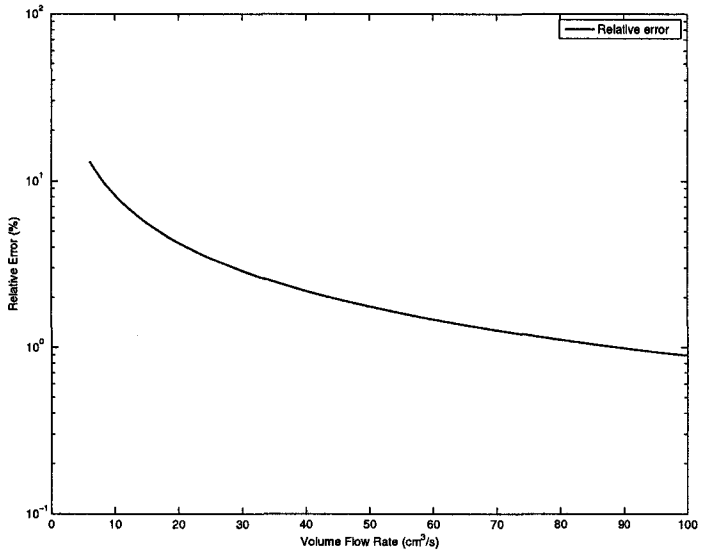

Figure 4.12: Relative error against the volume flow rate.

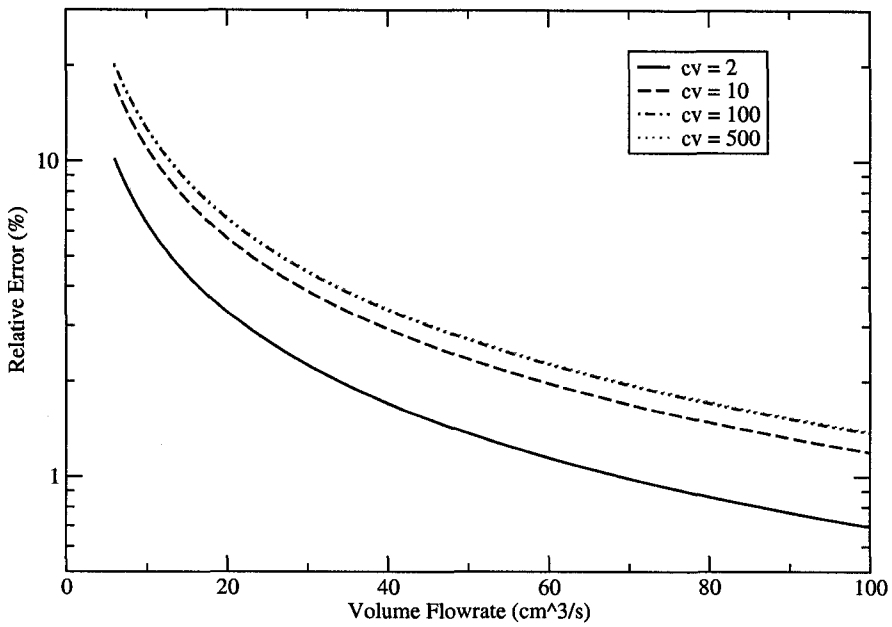

Figure 4.13: Relative error as it changes with the increase of CV number.

estimate never crosses the theoretical deposition curve, i.e. there is no intersection point. In all cases, the higher the magnitude of deposition the higher the relative error, and the relative error goes down with increasing flow rate.

4.2.4 Comparison Of The Two Approaches

In this section the two methods (CVRT and GRT approach) are compared for the same numerical and physical parameters. Through the comparison of the effect of number of control volume (figure 4.17), effect of varying control volume size (figure 4.18), tube diameter (figure 4.19) and particle diameter (figure 4.20), it can be noticed that the new CVRT approach provides much lower relative error than the GRT approach with the variation of number of control volumes, both in high and low flow rates. One reason for this might be that in GRT approach 3rd and higher order terms are being neglected, whereas in CVRT approach nothing is being neglected due to the structure of the formula. In other cases, CVRT results in better agreement with

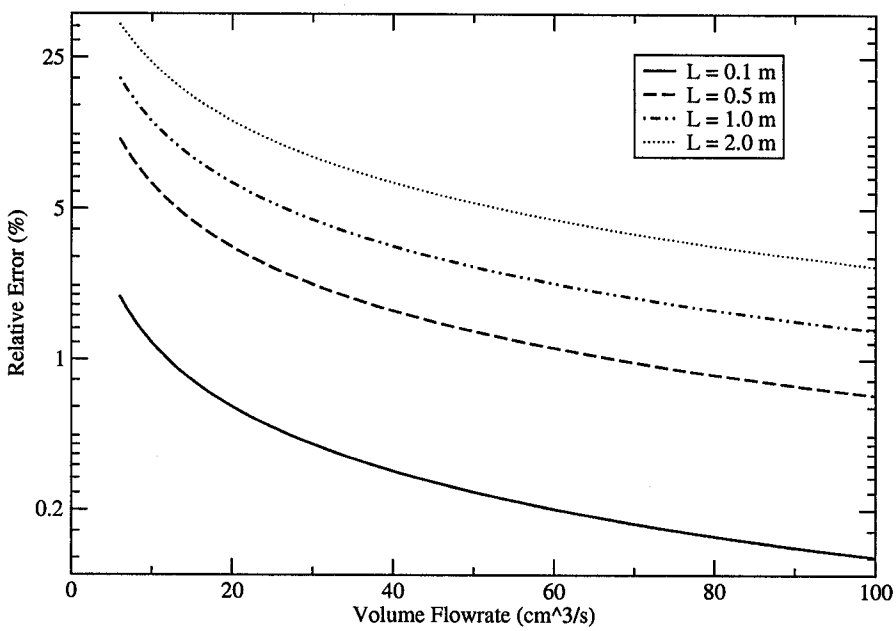

a: Fixed CV length

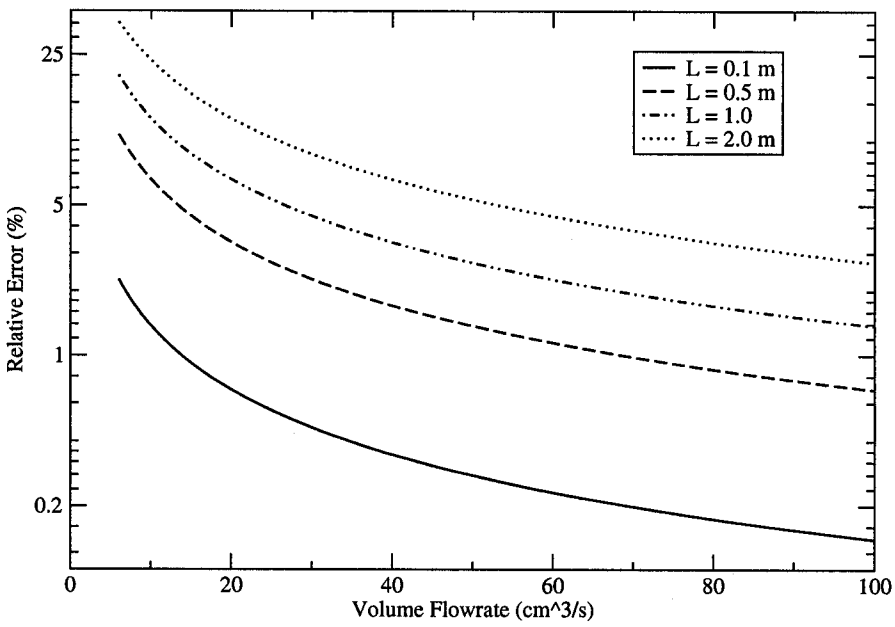

b: Fixed number of CV

Figure 4.14: Relative error as a function of pipe length.

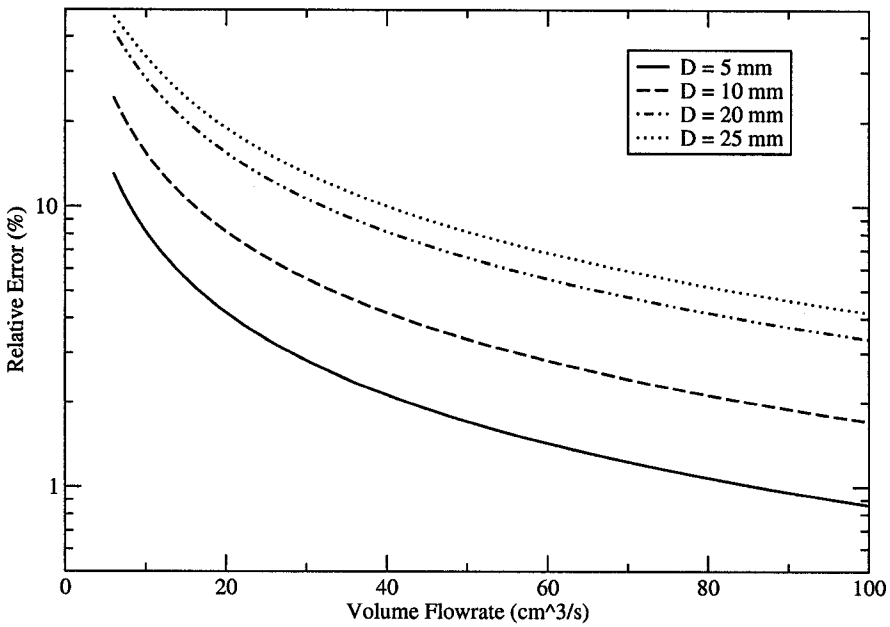

Figure 4.15: Relative error as a function of pipe diameter.

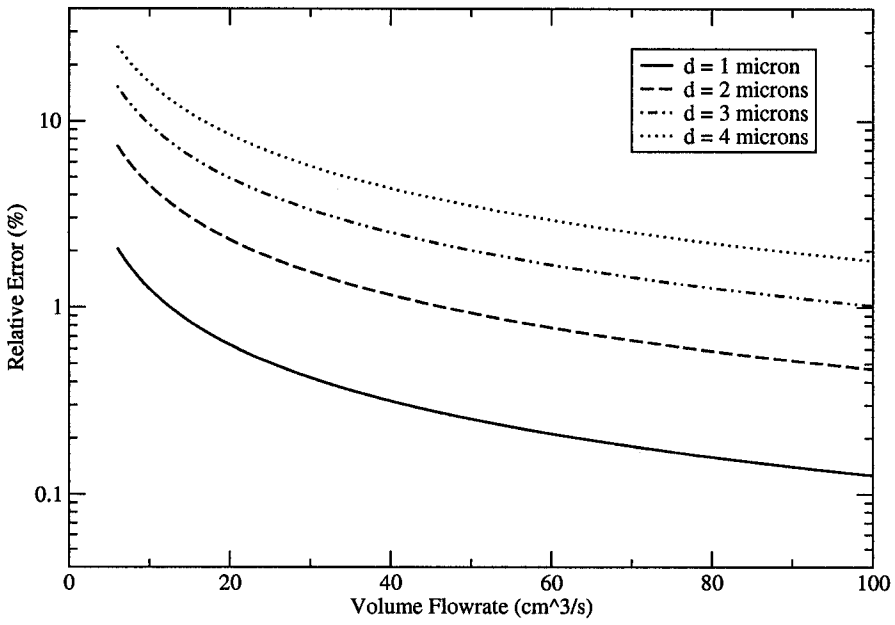

Figure 4.16: Relative error as a function of particle diameter.

the theory in the low flow rate regimes only, where the difference between the two approaches is significant. GRT approach provides better result at relatively higher velocity and smaller tube length and diameter and particle size, i.e. when the deposition parameter is small. However, the difference between the two methods in that regime is not so significant.

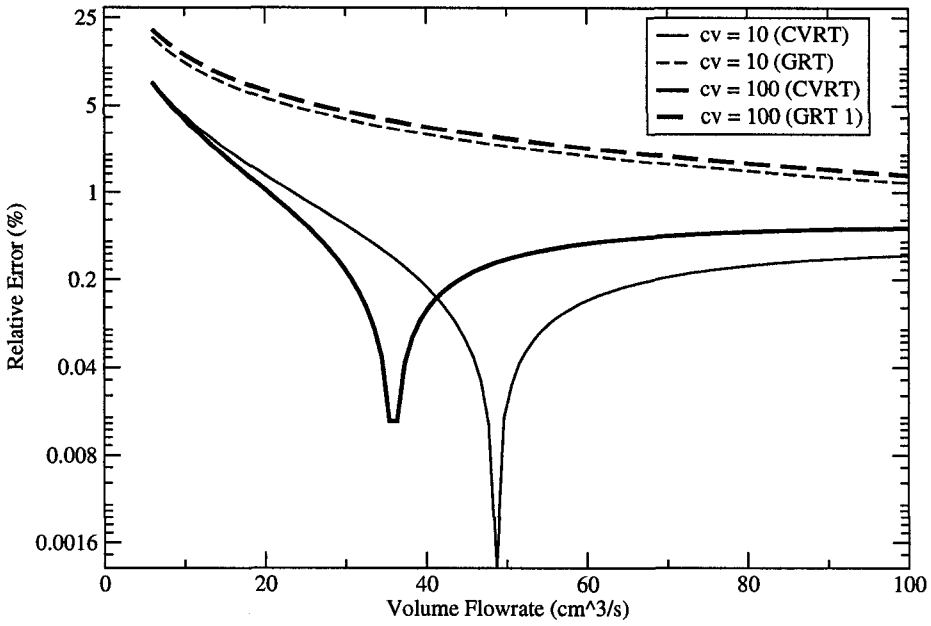

Figure 4.17: Relative error as a function of number of control volumes.

So far the standard case mentioned in Heyder and Gebhart [39] has been considered. When these methods are applied in the human respiratory tract, the airway dimensions are much smaller. Although the flow rates are quite higher than the cases considered here, due to the high number of airways in any particular generation the mean velocity is extremely low in any single airway deep inside the lung. So, a typical flow rate from a dry powder inhaler (between 20 to 100 l/min) would generate velocity between 0.1 to 0.5 m/s in the 13th generation of the lung. Particles inhaled from the inhalers usually are in the range of 0.5 to 5 microns. So, the relative error from the two above-mentioned methods were compared using a particle size of 3.5 microns (figure 4.21). The number of control volumes was set to 5 because of the

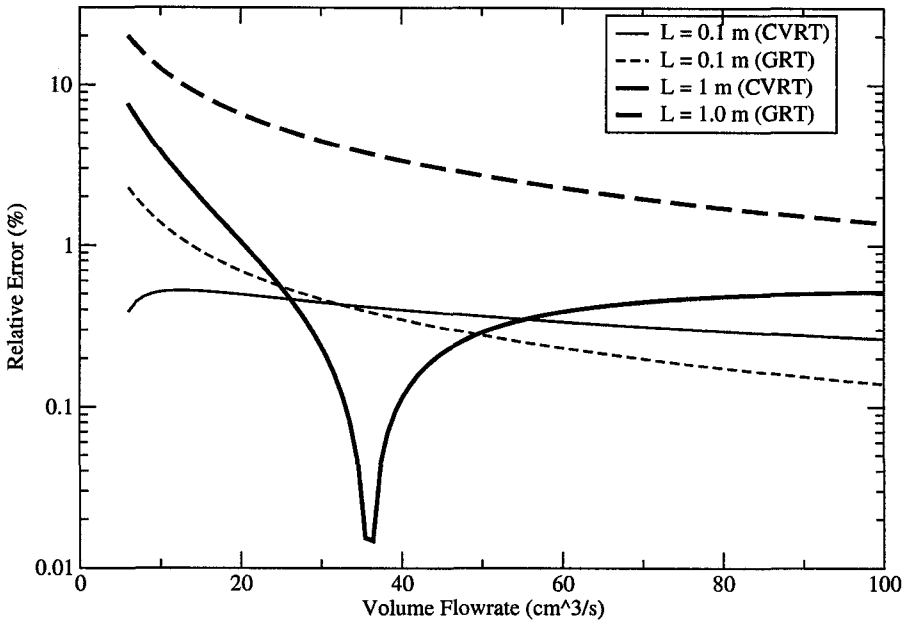

Figure 4.18: Relative error as it changes with the increase tube length with 100 control volumes.

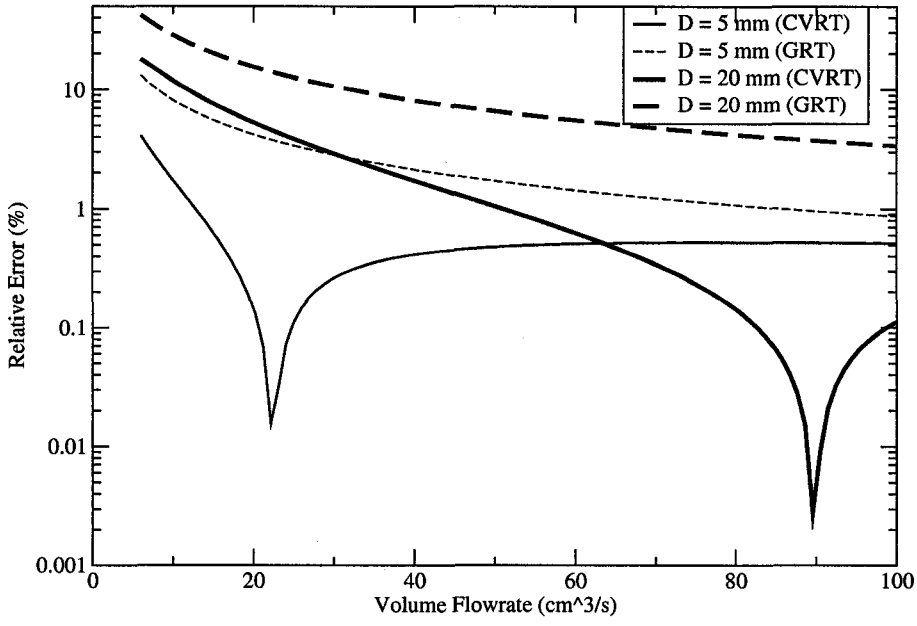

Figure 4.19: Relative error as it changes with the increase tube diameter with 100 control volumes.

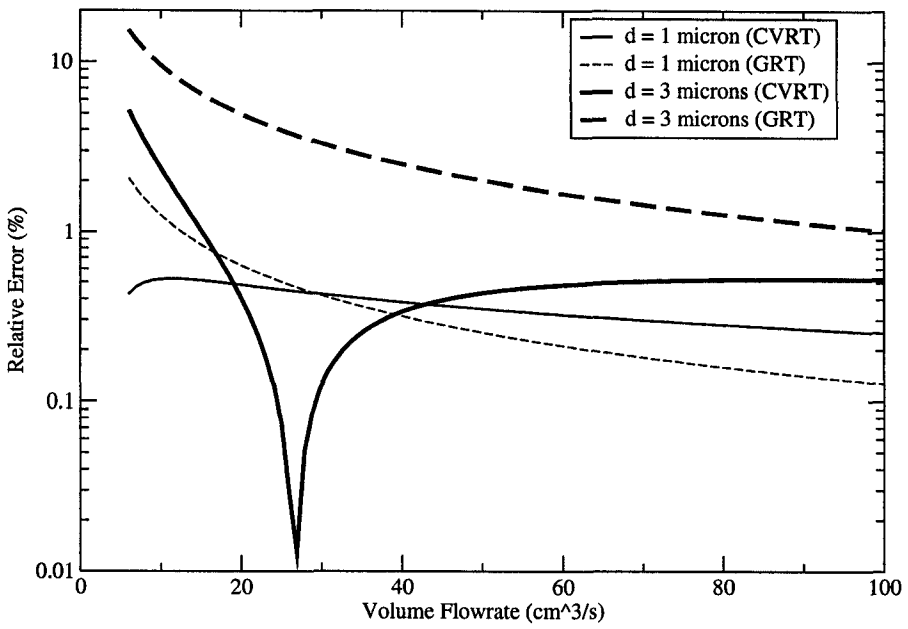

Figure 4.20: Relative error as it changes with the increase tube diameter with 100 control volumes.

small length of the generation. Within the specified range mentioned above, CVRT provides better result in the lower velocities. At a certain velocity GRT starts giving better result, as shown in the figure 4.21 but the difference in both cases remains very small.

4.2.5 Discussion on CVRT Approach

Based on the above comparisons, the point of intersection represents the point of minimum relative error. The location of the intersection point is not fixed, but changes with both numerical and physical parameters. The shift of this intersection was investigated with change of tube length (figure 4.22) and particle diameter (figure 4.23). In both cases the relationship is approximately linear. From these results it seems likely that some dimensionless group or some combination of parameters will bring the curves closer.

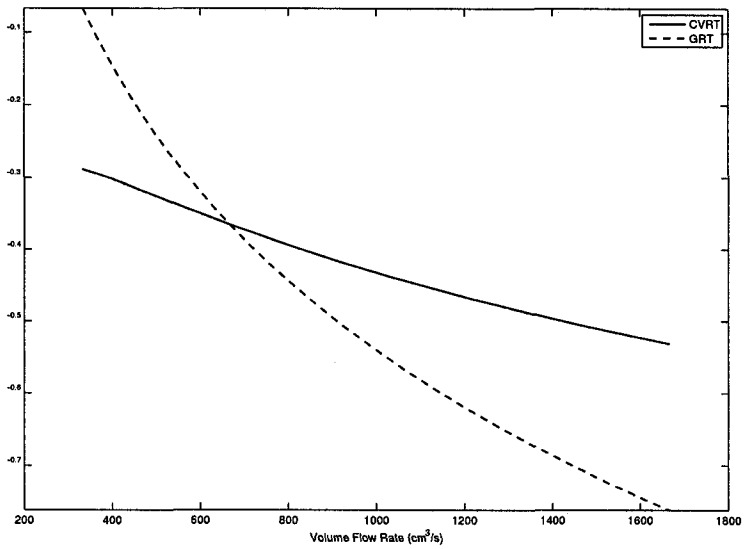

a)

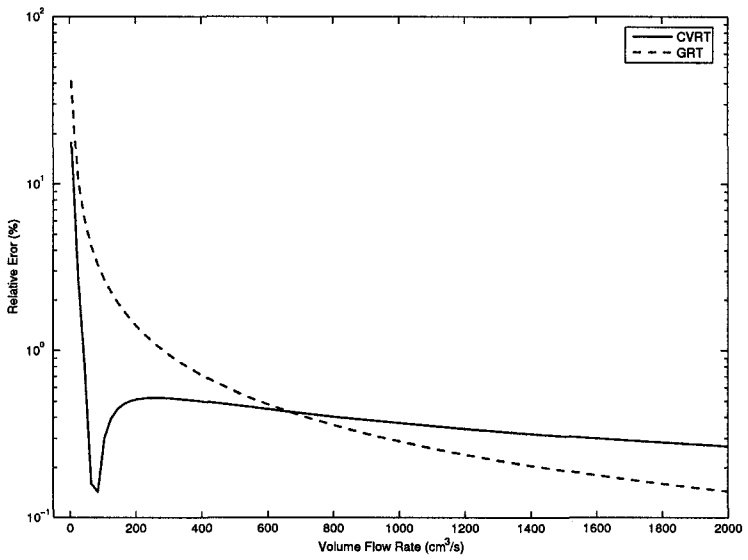

b)

Figure 4.21: Relative error as it changes with the increase of flow rate a) between 20 to 100 l/min, b)wider range

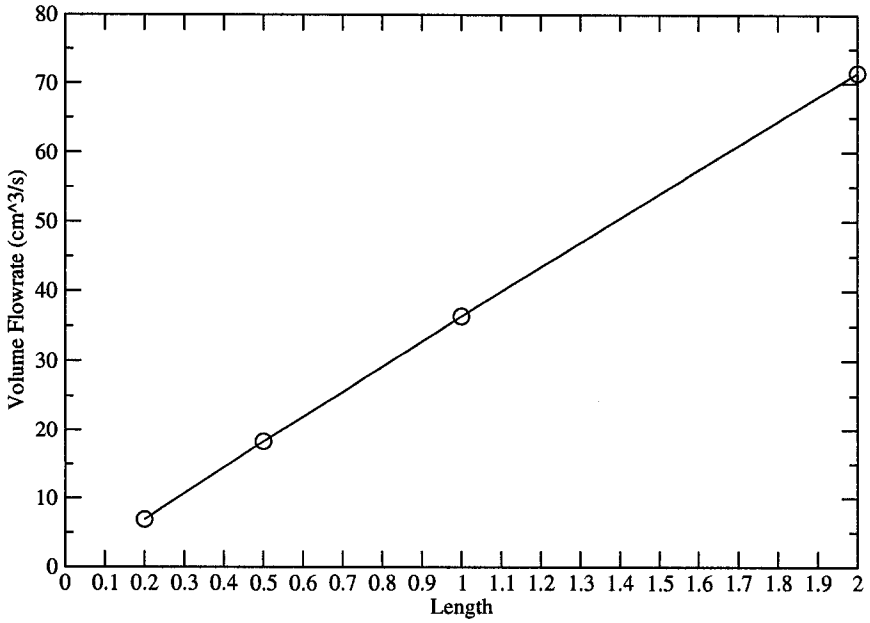

Figure 4.22: Flow rate at minimum relative error (intersection point))as it changes with the increase of tube length with 100 control volumes.

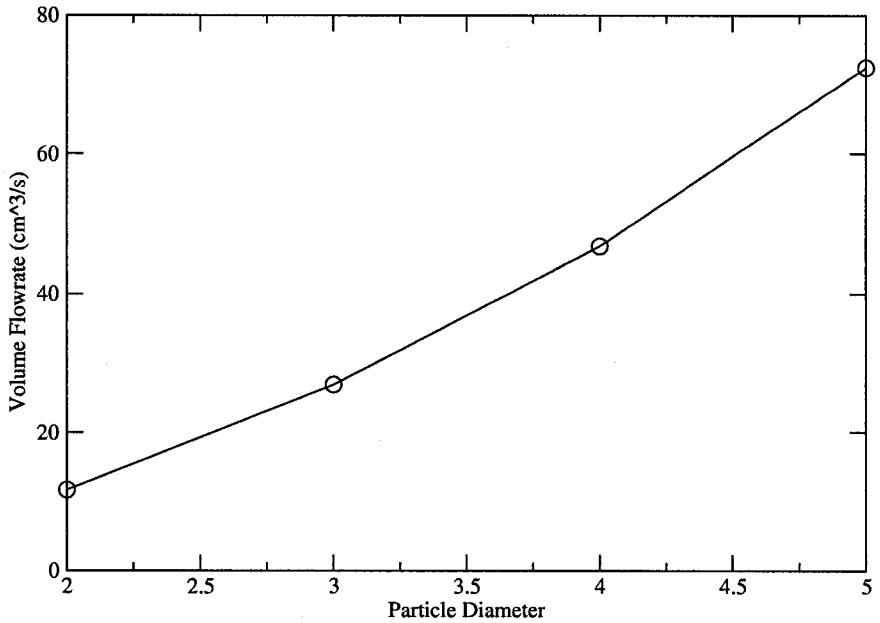

Figure 4.23: Flow rate at minimum relative error (intersection point) as it changes with the increase particle diameter with 100 control volumes.

In order to investigate which parameters affect the total deposition estimate, attempt was made to keep the sedimentation parameters of control volume ϵ_{cv} and of the whole tube ϵ_{tube} constant at their respective value for different combination of parameters. It was found that, it is physically unrealistic. For example, to keep local sedimentation parameter fixed for a reduced control volume length, one option is to lower the flow rate, which in turn will cause the sedimentation parameter of the whole tube to go down, and the situation becomes incomparable.

Another point to be noticed in CVRT approach is that, total deposition probability is calculated by the following formula,

$$\text{Total Deposition Probability} = 1 - \prod_{i=1}^{n}(1 - P_i) \tag{4.6}$$

where n is the number of CVs. By keeping the sedimentation parameter fixed as the number of control volumes is increased the product tends to become progressively smaller, making the total deposition probability larger. So, it can be stated that the deposition probability and the associated relative error when using the control volume approach is not only dependent on the sedimentation parameters of the control volume and of the whole tube, but is also dependent on the number of control volumes.

With the above mentioned insight, it is very likely that some combination of ϵ_{cv}, ϵ_{tube} and n (number of CVs) will form an invariant and will bring the different curves from section 4.2.2 on top of each other. An attempt was made to use $n * \epsilon_{cv} * \epsilon_{tube}$ on the abscissa (figure 4.24), and this approach succeeded reasonably well to bring all the curves closer. Only a few attempts were made towards the unification of all error curves due to time constraints, and a more detailed analysis was beyond the scope of this thesis.

4.3 Lung Deposition Model Validation

Both the Lagrangian-Eulerian conversion schemes, generation residence time and control volume residence time approach, were implemented into TECHAero. TECHAero

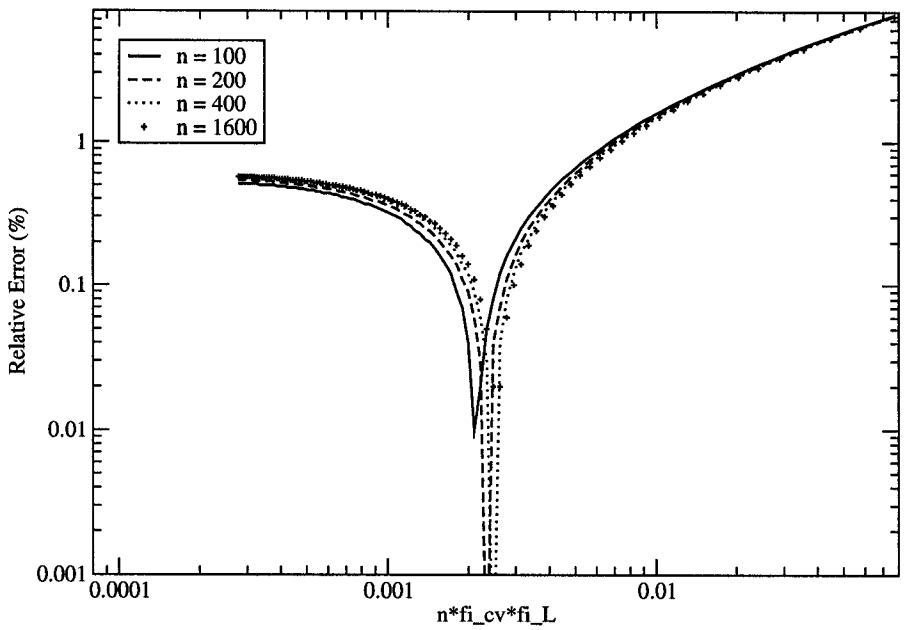

Figure 4.24: An attempt to unify the error curves (L= 100 cm, D = 0.8 cm, d= 3.5 $/mu$m.

was tested for grid independence using CVRT approach. The criterion was successfully satisfied as shown in figure 4.25.

The deposition model was then validated against published *in vivo* results. TECHAero was used to predict total and regional particle deposition in the human respiratory tract for particle sizes ranging from 0.25-8.25 μm, tidal volume 700 cc, inspiratory flow rate 400 cc/s and breath period of 4 s.

From figure 4.26-4.29 it is evident that both the schemes give good agreement with the *in vivo* data given the large scatter of the experimental data. Because of the inclusion of axial diffusion, compared with Lagrangian method, even with a shallow breath the aerosol penetrates deep into the lung. So, TECHAero is able to better represent the penetration and deposition that actually takes place deep inside the lung.

Contribution of different deposition mechanisms were also tested and are shown in

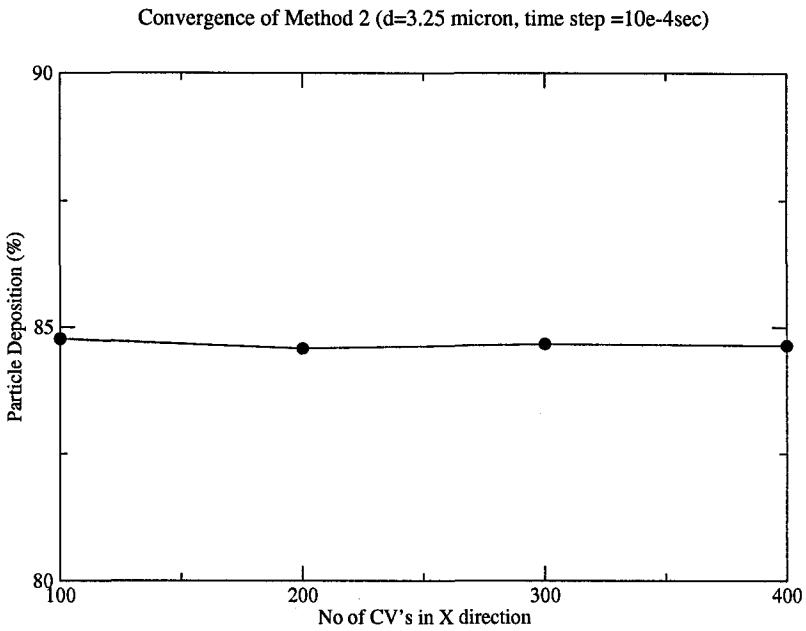

Figure 4.25: Convergence of TECHAero using CVRT approach (d = 3.25 microns, time step = 10e-4 s).

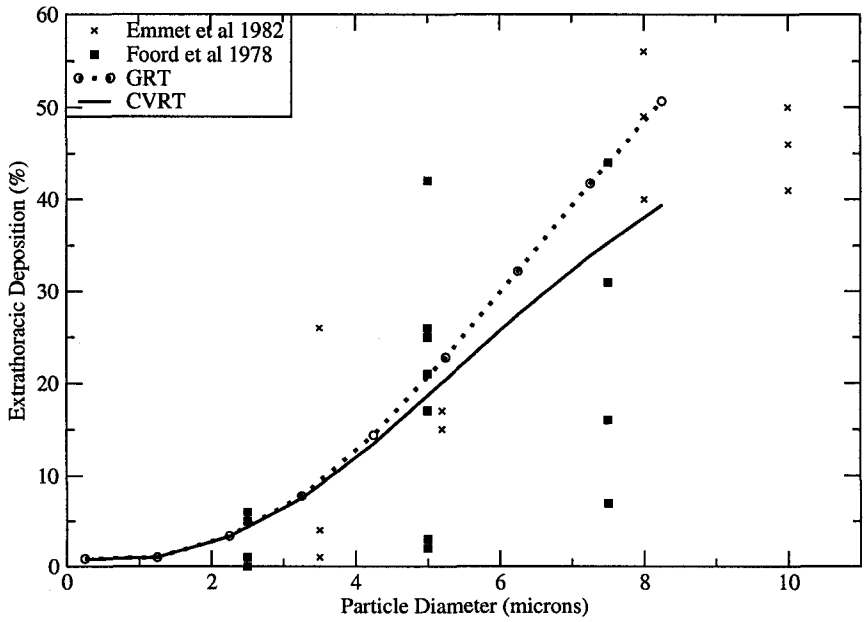

Figure 4.26: Comparison of extra-thoracic (ET) deposition.

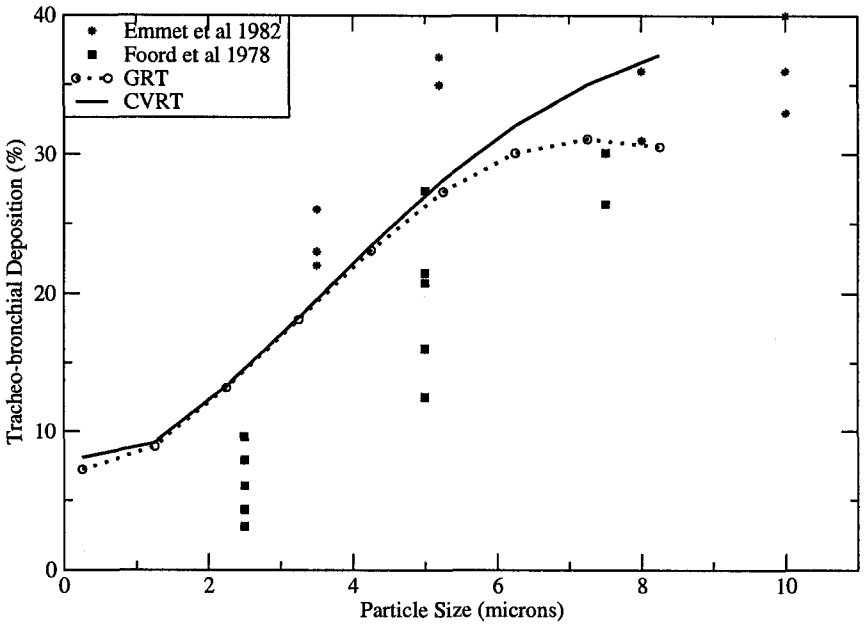

Figure 4.27: Comparison of tracheo-bronchial (TB) deposition.

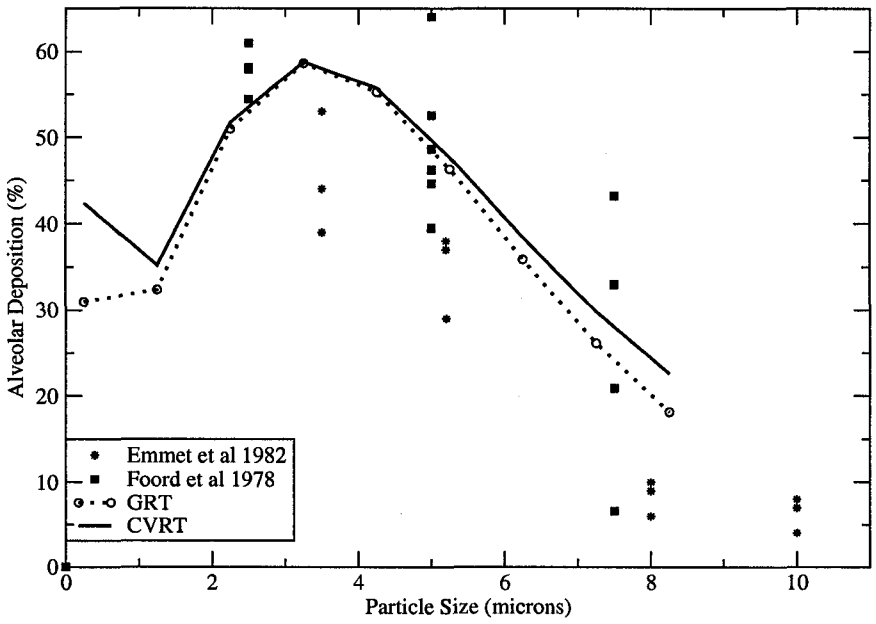

Figure 4.28: Comparison of alveolar deposition.

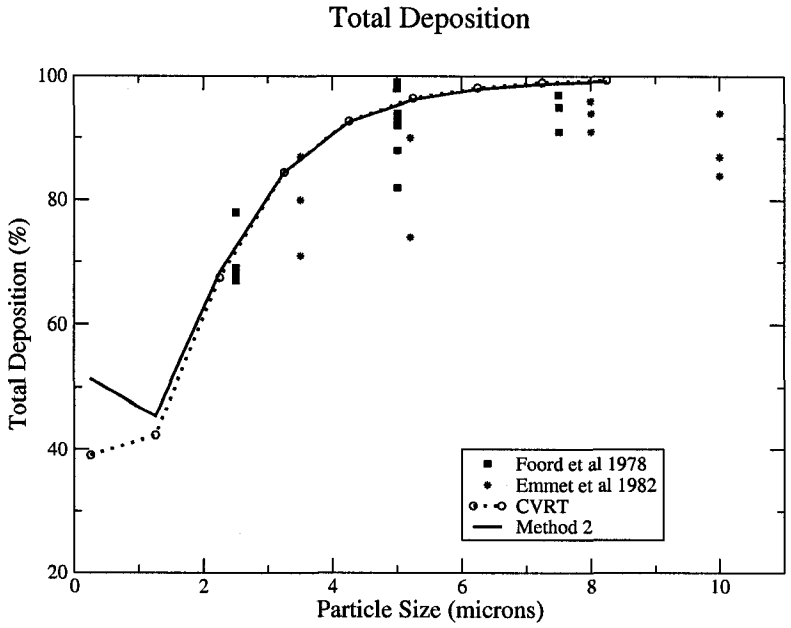

Figure 4.29: Comparison of total lung deposition.

figure 4.30. For particles with diameter less than 0.5 μm diffusion is known to be the dominant deposition mechanism. As the particle size increases, sedimentation and impaction become more significant. For particle sizes 0.5 μm to 2.5 μm sedimentation dominates and for particles with diameter larger than 2.5 μm impaction becomes increasingly dominant. CVRT approach was used in this analysis. The contributions of these deposition mechanisms estimated by TECHAero are in excellent agreement with those typical ranges (Chan and Lippmann [8]).

4.4 Highly Transient Deposition

In cases when the flow rate reaches its maximum value in very short time from begin of inhalation, the deposition associated with it can be treated as highly transient deposition. The time dependent breathing can be simulated as shown in figure 4.31. The test was carried out for three different particle sizes. Breathing period was set to 4 seconds with 50 percent inhalation and no breath hold. Maximum flow rate of

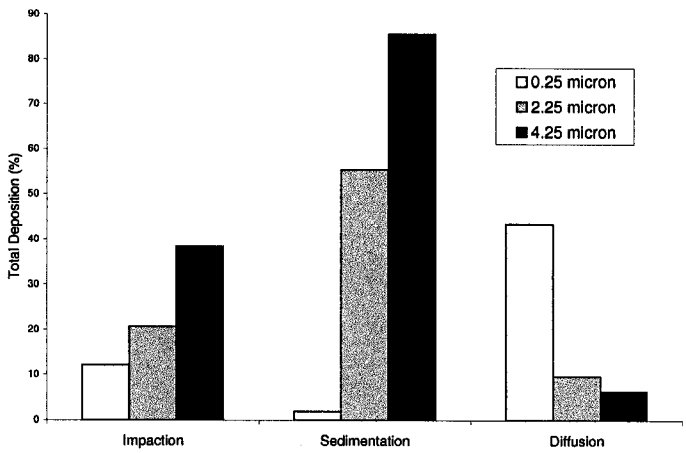

Figure 4.30: Contribution to deposition by different mechanisms.

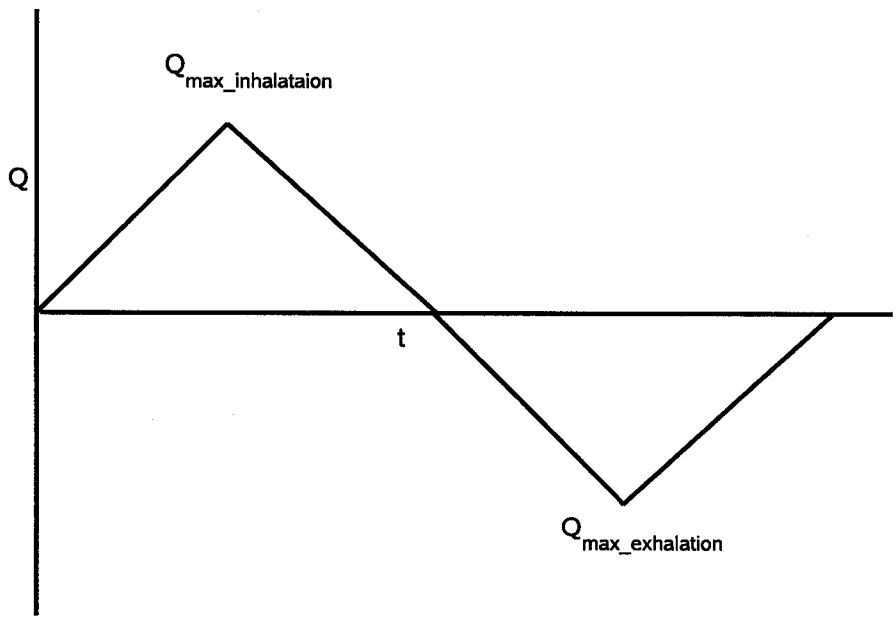

Figure 4.31: Simulating time dependent breathing pattern.

.75 l/s was set to achieve in 1 s.

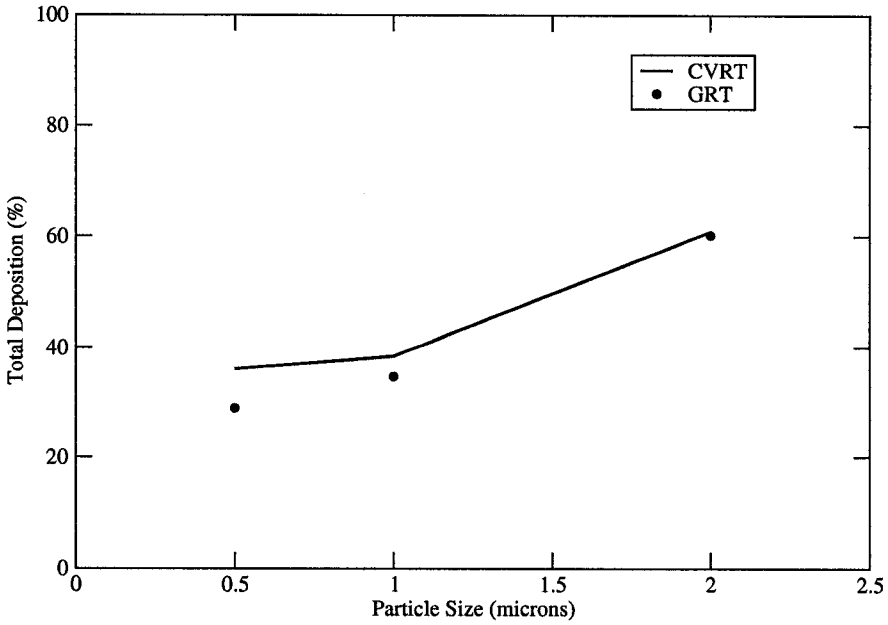

Figure 4.32: Comparison of transient deposition for two different approaches.

From figure 4.32, CVRT approach estimates a higher total deposition (approximately 7 % higher for 0.5 μm, 4% for 1 μm, 1% for 2 μm). This comparison highlights the difference between the two numerical approaches in the case of single breath inhalers. Due to the lack of experimental data under highly time dependent flows, knowledge on this deposition process is very limited, and further research is needed. But, based on the previous analysis, CVRT approach is expected to provide a reasonable prediction.

4.5 Deposition at Very Low Flow Rate

Over the years researchers have found significant intersubject variability in aerosol deposition in human respiratory tract. Brand et al. [5] have shown that this inter-subject variability can be substantially reduced with the aid of controlled breathing pattern. According to this study, at very low inhalation flow rates the variability is low. At the same time bronchial obstruction and extra-thoracic deposition tends to

be negligible. As a result, very low flow rates with controlled breathing is a practical way of delivering drug deep inside the lung.

To simulate a very low flow rate situation, an inhalation flow rate of 0.1 l/s was considered while the tidal volume was fixed as 1 l. Total particle deposition was calculated for particle size of 3 μm. Total deposition predicted using TECHAero was 95 % (1.8% ET, 24% tracheo-bronchial, 69.6% alveolar deposition). The result is in fair agreement with the experiments [5], where total deposition was 79%$\pm$7%. From the simulated ET deposition result it is evident that, with very slow flow rates and controlled breathing it is possible to achieve targeted drug delivery deep inside lung by bypassing the ET region.

Upon investigating closely the reason behind the difference in total deposition, it was found that TECHAero was overestimating the alveolar deposition. Only 48.8% alveolar deposition was estimated by the Lagrangian deposition code RegDep (Finlay et al. [27]).

4.6 Microgravity Deposition

4.6.1 Effect of Geometry

As explained in Chapter 2, there are marked functional differences in lung caused by the effects of microgravity; for example, there is significant differences in regional lung volume, ventilation and gas exchange. Because the lung is extremely compliant and is markedly deformed by its own weight as a consequence of this architecture. In order to determine the accurate deposition prediction in weightlessness, is it very important to determine whether changes in lung geometry play the key role or if an improved and modified diffusion function is needed.

At first the whole lung volume and diameter were scaled down based on the reduction in FRC. Based on the fact that most of the change in FRC is due to abdominal

volume change, it is the alveolar region which contributes to the majority of the volume reduction. Then only the acinus region was scaled, keeping the other regions of the lung intact. For scaling, a reduction of 15% in FRC was used based on the experimental results published by Elliott et al. [21]. The resulting total deposition did not change significantly. So it can be assumed that although the change in geometry is apparent in microgravity, this alone has no significant impact on total deposition. Rather other changes, such as the change in ventilation pattern associated with volume and shape change of the lung, may influence the deposition site and amount.

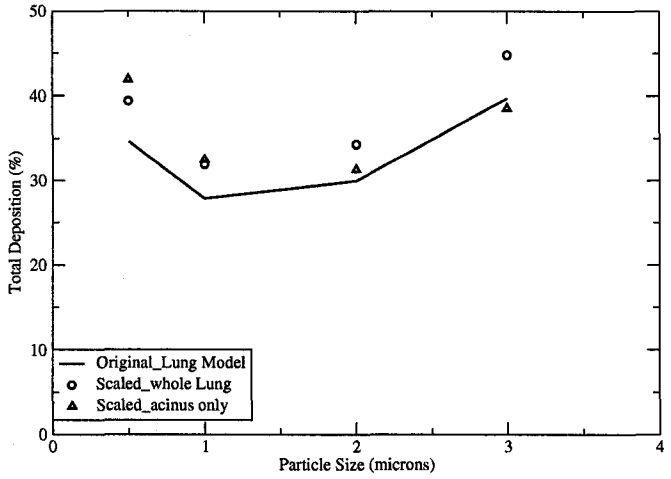

Figure 4.33: Effect of lung geometry on total deposition.

4.6.2 Comparison of Total Deposition

The effect of gravity on the anatomy and physiology of lung have been discussed in detail in chapter 2. In the weightless environment, because of zero sedimentation, more particles penetrate deep into the lung and local deposition distribution is altered. So, inclusion of axial diffusion in TECHAero makes it suitable for predicting microgravity deposition. The simulated results from TECHAero were tested against the experimental results published by Darquenne et al. [12]. For simulation the following

parameters were used:

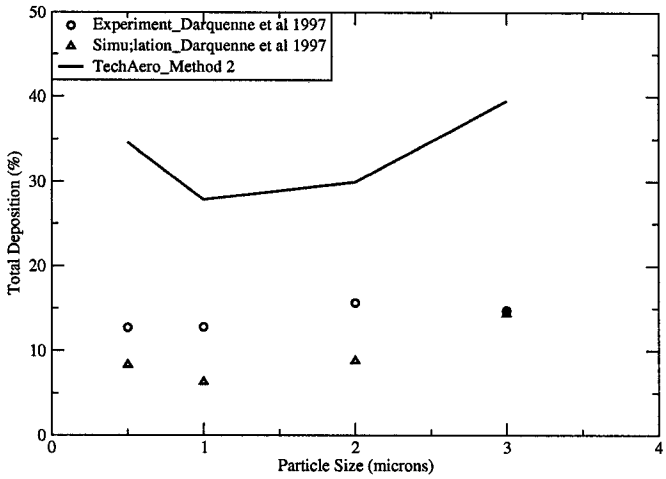

Figure 4.34: Total deposition in microgravity.

- Tidal volume = 0.75 l
- Aerosol flow rate = 0.4 l/s
- Aerosol concentration :
  - 10^4 particles/ml for 0.5 μm and 1 μm particle.
  - 5x10^3 particles/ml for 2 μm particle.
  - 10^3 particles/ml for 3 μm particles.

The result is shown in figure 4.34. Probable reasons behind the large differences between TECHAero and simulated results by Darquenne et al. [12] might be the different impaction function and geometry of the extra-thoracic (ET) region (represented by a single cylinder of 2.9 cm^2 and 17.0 cm length in [12]). Moreover, Darquenne et al. [12] used the same deposition functions in the ET region as in the rest of the lung.

To test the effect of the different deposition function, the impaction function in TECHAero was replaced by the function used in [12] and a drastic reduction was

observed (figure 4.35). But this change in the impaction function is not well justified, because the function used in TECHAero is based on more recent *in vivo* data. The

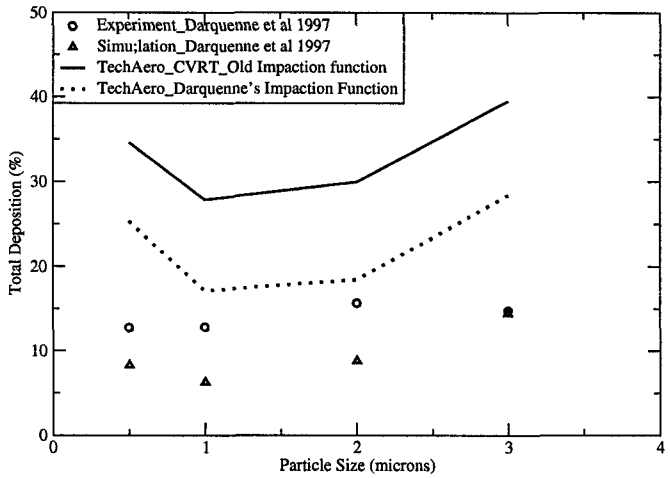

Figure 4.35: Comparison of Impaction functions in calculating Total Deposition in Microgravity

other scope for improvement was changing the deposition function used in the ET region. Using the same functions both in the lung and the ET region is not justified, because the ET region is significantly different in geometry from the lung airways. The fluid dynamics is also quite different there. Grgic et al. [33] has proposed a new ET deposition function based on the most recent geometric model and *in vivo* data. Incorporation of this function is expected to give better results. The new ET function was added into TECHAero and contributed some improvements in the deposition prediction (figure 4.36), but it did not reduce the large overestimation in TECHAero.

Because of the absence of regional deposition data in microgravity, it is difficult to say in which region of the lung TECHAero is overpredicting deposition. There is a possibility of over-estimating alveolar deposition, as encountered in the case of low inhalation flow rate. Because in both cases more particles travel deep inside the lung: in microgravity, due to the absence of gravity, and in low flow rate because of very low ET deposition.

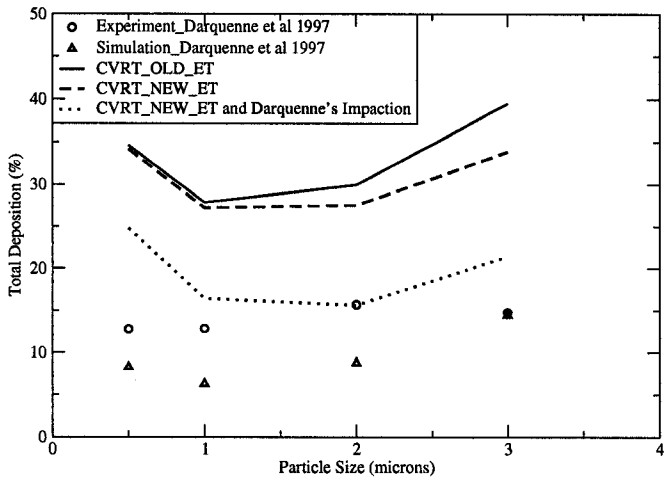

Figure 4.36: Comparison of ET functions in calculating Total Deposition in Microgravity.

Although the present work focused on the Lagrangian-Eulerian conversion of sedimentation deposition, it seems that a similar analysis regarding deposition by diffusion will be necessary to improve TECHAero's prediction of lung deposition in microgravity and with low flow rates.

Chapter 5

Conclusions

In this study, two numerical schemes to calculate deposition probability rate using the current Lagrangian deposition functions were introduced, validated and implemented in the Eulerian lung deposition code TECHAero. TECHAero was then used to estimate aerosol deposition in human respiratory tract under different clinically relevant situations, such as normal steady state, highly transient and very low flow rates. Finally, TECHAero was used to predict microgravity deposition.

Two numerical techniques were used, one based on lung generation residence time and the other, developed and used for the first time, based on control volume residence time. Both the techniques were derived from general transport equation under the assumption of steady state condition with no diffusion.

Deposition by sedimentation was selected for validation purposes, because the function has solid mathematical background and was validated experimentally by several researchers.

Neither of the schemes showed the well known limiting trajectory, because of the effect of remixing at the entry of each control volume. Both methods showed dependency on the number of control volumes, length and diameter of the whole tube, particle size and flow rate. The generational residence time approach showed higher relative

error as compared with the control volume residence time approach in most of the cases. The control volume approach showed higher error in some cases at higher flow rate, but in those cases the relative error itself was very small.

An attempt was made to find a dimensionless parameter or combination of different parameters that would bring all the curves closer and would form a basis from where suitable control volume parameter could be determined. The simple product of the number of control volumes, control volume and generation sedimentation parameters used in the abscissa produced a reasonably good result in that direction.

Total and regional aerosol deposition results from TECHAero showed good agreement with the experimental results. Alveolar deposition was always in the higher end of the experimental data. During controlled breathing at a very low flow rate and in microgravity, TECHAero overpredicted total deposition. It was assumed that the over-estimation was in the alveolar region, because for the extra-thoracic region the most recently developed deposition function was used. Diffusion dominates in the alveolar region, and in the case of microgravity (because of no sedimentation) and low flow rate condition (because of low extrathoracic deposition) more particles were drawn into the alveolar region. In both cases TECHAero overpredicts alveolar deposition and hence the total deposition.

In this study, both the proposed schemes were validated for sedimentation and showed good agreement. It was assumed that the schemes would also work for diffusion and impaction. But in practice the methods did not work well for diffusion, maybe because of the non-linearity involved in the function. So, further research is required to find a suitable conversion scheme for the deposition probability by diffusion. Future research is also required in the direction of a single dimensional or dimensionless group that will govern the parameter selection during lung simulation to keep the error to a minimum.

Bibliography

[1] I. Balásházy, W. Hofmann, and T. Martonen. Inspiratory particle deposition in airway bifurcation models. *J. Aerosol Sci.*, 22(1):287–301, 1991.

[2] J. M. Beeckmans. The deposition of aerosols in the respiratory tract 1. mathematical analysis and comparison with experimental data. *Can. J. Physiology and Pharmacology*, 43:157–172, 1965.

[3] J. M. Beeckmans. Alveolar deposition of aerosols on the moon and in the outer space. *Nature*, 211:208, 1966.

[4] S. M. Bowes-III and D. L. Swift. Deposition of inhaled particles in the oral airway during oronasal breathing. *Aerosol Science and Technology*, 11:157–167, 1989.

[5] P. Brand, I. Friemel, T. MMeyer, H. Schulz, J. Heyder, and K. Haubinger. Total deposition of theraputic particles during spontaneous and controlled inhalation. *J. Pharmaceutical Sci.*, 89(6):724–731, 2000.

[6] H. Brenner. Macrotransport processed: brownian tracers as stochastic averages in effective-medium theories of heterogeneous media. *J. Statistical Physics*, 62 (5/6):1095–1119, 1991.

[7] F. S. Cai and C. P. Yu. Inertial and interceptional deposition of spherical particles and fibers in a bifurcating airway. *J. Aerosol Sci.*, 19:679–688, 1988.

[8] T. L. Chan and M. Lippmann. Experimental measurements and empirical modelling of the regional deposition of inhaled particles in humans. *Am. Ind. Hyg. Assoc. J.*, 41:399–409, 1980.

[9] S. Chandrasekhar. Stochastic problems in physics and astronomy. *Rev. Mod. Phys.*, 15:846–853, 1943.

[10] Y.-S. Cheng, Y. Yamada, H.-C. Yeh, and D. L. Swift. Diffusional deposition of ultrafine aerosols in a human nasal cast. *J. Aerosol Sci.*, 6:741–751, 1988.

[11] C. Darquenne and M. Paiva. One-dimensional simulation of aerosol transport and deposition in the human lung. *J. Appl. Physiol.*, 77(6):2889–2898, 1994.

[12] C. Darquenne, M. Paiva, J. B. West, and G. K. Prisk. Effect of microgravity and hypergravity on deposition of 0.5- to 3-m-diameter aerosol in the human lung. *J. Appl. Physiol.*, 83(6):2029–2036, 1997.

[13] C. N. Davies. Deposition of particles in the human lungs as a function of particle size and breathing pattern: an empirical model. *Ann. Occup. Hyg.*, 26:119–135, 1982.

[14] W. H. DeHaan. Mouth-throat deposition with non-balastic pharmaceutical aerosol inhalation devices. Ph.D., University of Alberta, Edmonton, Alberta, Canada, 2002.

[15] W. H. DeHaan and W. H. Finlay. Predicting estrathoracic deposition from dry powder inhalers. *J. Aerosol Sci.*, 35(3):309–331, 2004.

[16] J. M. Delhaye. *Thermohydraulics of Two-phase Systems for Industrial Design and Nuclear Engineering.* McGraw Hill, New York, 1981.

[17] D. A. Edwards. A general theory of the macrotransport of nondepositing particles in the lung by convective dispersion. *J. Aerosol Sci.*, 25(3):543–565, 1994.

[18] D. A. Edwards. The macrotransport of aerosol particles in the lung: aerosol deposition phenomena. *J. Aerosol Sci.*, 26(2):293–317, 1995.

[19] J. Edyvean, M. Estenne, M. Paiva, and L. A. Engel. Lung and chest wall mechanics in microgravity. *J. Appl. Physiol.*, 71:1956–1966, 1991.

[20] M. J. Egan and W. Nixon. A model of aerosol deposition in the lung for use in inhalation dose assessments. *Radiation Protection Dosimetry*, 11(1):5–17, 1985.

[21] A. R. Elliott, G. K. Prisk, H. J. B. Guy, and J. B. West. Lung volumes in sustained microgravity on spacelab sls-1. *J. Appl. Physiol.*, 77:2005–2014, 1994.

[22] G. A. Ferron. The size of soluble aerosol particles as a function of the humidity of the air. Aplication to the human respiratory tract. *J. Aerosol Sci.*, 8:251–267, 1977.

[23] G. A. Ferron, W. G. Kreyling, and B. Haider. Inhalation of salt aerosol particles – II. Growth and deposition in the respiratory tract. *J. Aerosol Sci.*, 19(5): 611–631, 1988.

[24] W. Findeisen. Über das absetzen kleiner, in der luft suspendierter teilchen in der menschlichen lunge. *Pflüger Arch. F. d. ges. Physiol.*, 236:367–379, 1935.

[25] W. H. Finlay. *The Mechanics of Inhaled Pharmaceutical Aerosols: An Introduction.* Academic Press, London, 2001.

[26] W. H. Finlay and K. W. Stapleton. The effect on regional lung deposition of coupled heat and mass transfer between hygroscopic droplets and their surrounding phase. *J. Aerosol Sci.*, 26(4):655–670, 1995.

[27] W. H. Finlay, C. F. Lange, M. King, and D. P. Speert. Lung delivery of aerosolized dextran. *Am. J. Respir. Crit. Care Med.*, 161:91–97, 2000.

[28] N. Foord, A. Black, and M. Walsh. Regional deposition of 2.5-7.5 μm diameter inhaled particles in healthy male non-smokers. *J. Aerosol Sci.*, 9:343–357, 1978.

[29] N. A. Fuchs. *The Mechanics of Aerosols.* Dover Publications, Inc., New York, 1964.

[30] R. Gawronski and K. W. Szewczyk. Inertial deposition of particles in the human branching airways. *J. Aerosol Sci.*, 17(5):795–801, 1986.

[31] T. R. Gerrity, P. S. Lee, F. J. Hass, A. Marinelli, P. Werner, and R. V. Lourenço. Calculated deposition of inhaled particles in the airway generations of normal subjects. *J. Appl. Physiol.*, 47(4):867–873, 1979.

[32] P. G. Gormley and K. Kennedy. Diffusion from a stream flowing through a cylindrical tube. *Proc. Roy. Irish Soc.*, 52A:163, 1949.

[33] B. Grgic, W. H. Finlay, P. K. P. Burnell, and A. F. Heenan. In vitro intersubject and intrasubject deposition measurements in realistic mouth- throat geometries. *J. Aerosol Sci.*, 35:1025–1040, 2004.

[34] B. Grgic, A. R. Martin, and W. H. Finlay. Effect of unsteady flow rate increase on in vitro mouth throat deposition of inhaled bolus. *J. Aerosol Sci.*, 37:1222–1233, 2006.

[35] J. L. Gurman, M. Lippmann, and R. B. Schlesinger. Particle deposition in replicate cast of the human upper tracheobronchial tree under constant and cyclic inspiratory flow. *J. Aerosol Sci. and Tech.*, 3:245–252, 1984.

[36] H. J. B. Guy, G. K. Prisk, A. R. Elliott, R. A. Deutscgman-III, and J. B. West. Inhomogeneity of pulmonary ventilation during sustained microgravity as determined by single breathe washouts. *J. Appl. Physiol.*, 76:1719–1729, 1994.

[37] B. Haefeli-Bleuer and E. R. Weibel. Morphometry of the human pulmonary acinus. *Anat. Rec.*, 220:401–414, 1988.

[38] J. E. Hansen and E. P. Ampaya. Human air spaces, sizes, areas, and volumes. *J. Appl. Physiol.*, 38(6):990–995, 1975.

[39] J. Heyder and J. Gebhart. Gravitational deposition of particles from laminar aerosol flow through inclined circular tubes. *J. Aerosol sci.*, 8:289–295, 1977.

[40] R. A. Hoffman and J. Billingham. Effect of altered g levels on deposition of particulates in the human respiratory tract. *J. Appl. Physiol*, 38:955–960, 1975.

[41] D. B. Ingham. Diffusion of aerosols from a stream flowing through a cylindrical tube. *J. Aerosol Sci.*, 6:125–132, 1975.

[42] J. R. Johnston, K. D. Isles, and D. C. F. Muir. Inhaled particles. volume IV. Pergamon Press, Oxford, 1977.

[43] C. S. Kim, D. M. Fischer, D. J. Lutz, and T. R. Gerrity. Particle deposition in bifurcating airway models with varying airway geometry. *J. Aerosol Sci.*, 25: 567–581, 1994.

[44] H. D. Landahl. On the removal of air-borne droplets by the human respiratory tract. *Bull. Math. Biophys*, 12:43–56, 1950.

[45] C. F. Lange and W. H. Finlay. A fully Eulerian approach to the simulation of volatile/hygroscopic aerosols. In N. Chigier, editor, *Proceedings of the Eighth International Conference on Liquid Atomization and Spray Systems*, pages 1443–1444, Pasadena, 2000.

[46] C. F. Lange and W. H. Finlay. A fully Eulerian approach to the simulation of volatile/hygroscopic aerosols. In G. E. Schneider, editor, *Proceedings of the Ninth Annual Conference of the CFD Society of Canada*, pages 279–283, Waterloo, ON, 2001. CFD Society of Canada.

[47] C. F. Lange and W. H. Finlay. Liquid atomising nebulizing and other methods of producing aerosols. *J. Aerosol Med.*, 19(1):28–35, 2006.

[48] I. Langmuir. Evaporation of small sphere. *Phys. Rev.*, 12:368–370, 1918.

[49] M. Lippmann. The effect of particle size on the regional deposition of inhaled aerosols in the human respiratory tract. *Am. Ind. Hyg. Assoc. J.*, pages 257–275, 1969.

[50] M. Lippmann. *Regional deposition of particles in the human respiratory tract*, chapter 14, pages 213–232. Handbook of Physiology Section 9: Reactions to Environmental Agents. American Physiological Society, Bethesda, MD, 1977.

[51] T. B. Martonen. Deposition of inhaled particulate matter in the upper respiratory tract, larynx and bronchial airways: a mathematical description. *Journal of Toxicology and Environmental Health*, 12:787–800, 1983.

[52] T. B. Martonen and Z. Zhang. Comments on recent data for particle deposition in human nasal passages. *J. Aerosol Sci.*, 23(6):667–674, 1992.

[53] B. J. Mason. *The Physics of Clouds.* Clarendon Press, 1971.

[54] F. J. Miller, T. B. Martonen, M. G. Ménache, R. C. Graham, D. M. Spektor, and M. Lippmann. Influence of breathing mode and activity level on the regional deposition of inhaled particles and implications for regulatory standards. *Ann. Occup. Hyg.*, 32(Suppl. 1):3–10, 1988. Inhaled Particles VI.

[55] P. E. Morrow. Aerosol characterization and deposition. *Am. Rev. Respir. Dis.*, 110(6 Pt. 2):88–99, 1974.

[56] D. C. F. Muir. Influence of gravitational changes on the deposition of aerosols in the lung of a man. *Aerosp. Med.*, pages 159–161, 1967.

[57] W. Nixon and M. J. Egan. Modelling study of regional deposition of inhaled aerosols with special reference to effects of ventilation asymmetry. *J. Aerosol Sci.*, 15(5):563–579, 1987.

[58] D. E. Olsen, G. A. Dart, and G. F. Filley. Pressure drop and fluid flow regime of air inspired into the human lung. *J. Appl. Physiol*, 28(4):482–494, 1970.

[59] A. Pack, M. B. Hooper, W. Nixon, and J. C. Taylor. A computational model of pulmonary gas transport incorporating effective diffusion. *Respir. Physiol*, 29: 101–124, 1977.

[60] M. Paiva, M. Estenne, and L. A. Engel. Lung volumes, chest wall configuration, and pattern of breathing in microgravity. *J. Appl. Physiol.*, 67:1542–1550, 1989.

[61] D. D. Persons, G. D. Hess, W. J. Muller, and P. W. Scherer. Airway deposition of hygroscopic heterodispersed aerosols: results of a computer calculation. *J. Appl. Physiol.*, 63(3):1195–1204, 1987.

[62] C. G. Phillips, S. R. Kaye, and R. C. Schroter. A diameter-based reconstruction of the branching pattern of the human bronchial tree. Part I: Description and application. *Respir. Physiol.*, 98:193–217, 1994.

[63] J. Pich. Theory of gravitational deposition of particles from laminar flows in channels. *j. Aerosol Sci.*, 3:351–361, 1972.

[64] G. K. Prisk, H. J. B. Guy, A. R. Elliott, and J. B. West. Inhomogeneity of pulmonary perfusion during sustained microgravity on sls-1. *J. Appl. Physiol.*, 76:1730–1738, 1994.

[65] A. P. Roth. The effect of breathing pattern on nebulizer drug delivery. M.Sc., University of Alberta, Edmonton, Alberta, Canada, 2001.

[66] A. P. Roth, C. F. Lange, and W. H. Finlay. The effect of breathing pattern on nebulizer drug delivery. *J. Aerosol Med.*, 16(3):325–339, 2003.

[67] G. Rudolf, J. Gebhart, J. Heyder, C. F. Schiller, and W. Stahlhofen. An empirical formula describing aerosol deposition in man for any particle size. *J. Aerosol Sci.*, 17(3):350–355, 1986.

[68] G. Rudolf, R. Köbrich, and W. Stahlhofen. Modelling and algebraic formulation of regional deposition in man. *J. Aerosol Sci.*, 21(Suppl. 1):S403–S406, 1990.

[69] R. Sarangapani and A. S. Wexler. Modeling aerosol bolus dispersion in human airways. *J. Aerosol Sci.*, 30(10):1345–1362, 1999.

[70] C. F. Sawin, A. E. Nicogossian, J. A. Rummel, and E. L. Michel. Pulmonary function evaluation during the skylab and appollo-soyuz missions washout. *Aviat. Space Environ. Med.*, 47:168–172, 1976.

[71] P. W. Scherer, L. H. Schendalman, and N. M. Greene. Simultaneous diffusion and convection in single breath lung washout. *Bull. Math. Biophysics*, 34:393–412, 1972.

[72] P. W. Scherer, L. H. Schendalman, N. M. Greene, and A. Bouhuys. Measurement of axial diffusivities in a model of the bronchial airways. *J. Appl. Physiol.*, 38 (4):719–723, 1975.

[73] R. B. Schlesinger, D. E. Bohning, T. L. Chan, and M. Lippmann. Paricle deposition in a hollow cast of human tracheobronchial tree. *J. Aerosol Sci.*, 8:429–445, 1977.

[74] G. C. Smaldone. Smart nebulizers. *Respir. Care*, 47:1434–1441, 2002.

[75] H. Smith, editor. *Human respiratory tract model for radiological protection*, volume ICRP publication 66 of *Annals of the ICRP*. Pergamon, Oxford, 1994.

[76] W. Stahlhofen, J. Gebhart, and J. Heyder. Experimental determination of the regional deposition of aerosol particles in the human respiratory tract. *Am. Ind. Hyg. Assoc. J.*, 41(6):385–398a, 1980.

[77] W. Stahlhofen, G. Rudolf, and A. C. James. Intercomparison of experimental regional aerosol deposition data. *J. Aerosol Med.*, 2(3):285–308, 1989.

[78] K. Stapleton and W. Finlay. Deposition of medical aerosols in the respiratory tract. Report MA-1, Department of Mechanical Engineering, University of Alberta, Edmonton, Alberta, 1997.

[79] K. W. Stapleton and W. H. Finlay. Determining solution concentration within aerosol droplets output by jet nebulizers. *J. Aerosol Sci.*, 26(1):137–145, 1995.

[80] K. W. Stapleton, W. H. Finlay, and P. Zuberbuhler. An in vitro method for determining regional dosages delivered by jet nebulizers. *J. Aerosol Med.*, 7(4): 325–344, 1994.

[81] H. L. Stone. Iterative solutions of implicit approximations of multi-dimensional partial differential equaitons. *SIAM J. Num. anal.*, 5:530–558, 1968.

[82] D. L. Swift, N. Montassier, P. K. Hopke, K. Karpen-Hayes, Y.-S. Cheng, Y. F. Su, H. C. Yeh, and J. C. Strong. Inspiratory deposition of ultrafine particles in human nasal replicate cast. *J. Aerosol Sci.*, 23(1):65–72, 1992.

[83] D. B. Taulbee and C. P. Yu. A theory of aerosol deposition in the human respiratory tract. *J. Appl. Physiol.*, 38(1):77–85, 1975.

[84] D. B. Taulbee, C. P. Yu, and J. Heyder. Aerosol transport in the human lung from analysis of single breath. *J. Appl. Physiol.: Respirat. Environ. Exercise Physiol*, 44(5):803–812, 1978.

[85] G. Taylor. Dispersion of soluble matter in solvent flowing slowly through a tube. *Proc. Roy. Soc. London, Ser. A*, 219:186–203, 1953.

[86] J. W. Thomas. Gravity setting of particles in horizontal tube. *J. Air Pollut. Contr. Ass.*, 8:32–34, 1958.

[87] A. Voss and W. H. Finlay. Deagglomeration of dry powder pharmaceutical aerosols. *Int. J. Pharm.*, 248:39–50, 2002.

[88] P. E. Wagner. *Aerosol Microphysics, Vol. II*, page 127. Springer, Berlin, 1982.

[89] C. Wang. Gravitational deposition of particle from laminar flows in inclined channels. *J. Aerosol Sci.*, 6:191–204, 1975.

[90] K. Wark and C. F. Warner. *Air Pollution: Its Origin and Control.* Herper Collins, New York, 1981.

[91] E. R. Weibel. *Morphology of the human lung.* Acedemic Publishers, New York, 1963.

[92] H.-C. Yeh and G. M. Schum. Models of human lung airways and their application to inhaled particle deposition. *Bull. Math. Biology*, 42:461–480, 1980.

[93] H.-C. Yeh, R. G. Cuddihy, R. F. Phalen, and I.-Y. Chang. Comparisons of calculated respiratory tract deposition of particles based on the proposed NCRP model and the new ICRP66 model. *Aerosol Sci. Technol.*, 25:134–140, 1996.

[94] C. P. Yu and C. K. Diu. A comprehensive study of aerosol deposition in different lung models. *American Industrial Hygiene Association Journal*, 43(1):54–65, 1982.

[95] C. P. Yu, C. K. Diu, and T. T. Soong. Statistical analysis of aerosol deposition in the nose and mouth. *American Industrial Hygiene Association Journal*, 42 (10):726–733, 1981.

[96] C. P. Yu, L. Zhang, M. H. Becquemin, M. Roy, and A. Bouchikhi. Algebraic modeling of total and regional deposition of inhaled particles in the human lung of various ages. *J. Aerosol Sci.*, 23(1):73–79, 1992.

Appendix A

Derivation

Position and velocity vector in the cylindrical domain Ω of the 5 dimensional hyperspace,

$$\vec{\chi} = (x, r, \theta, R, m) \tag{A.1}$$

$$\vec{V} = (u, v, w, \dot{R}, \dot{m}) \tag{A.2}$$

The particle concentration transport equation,

$$\int_{\Omega^*} \left[\frac{\partial n^*}{\partial t} + \frac{\partial (V_i^* n^*)}{\partial X_i} + \frac{\partial}{\partial X_i}(-D_j^* \delta_{ij} \frac{\partial n^*}{\partial X_j}) + \dot{\eta}_{dep}^* \right] \mathrm{d}\Omega^* = 0 \tag{A.3}$$

.

Here * stands for original, non-averaged variables. Simplification can be dnme based on several factors. For fully developed flow V=0 and W=0. For axisymmetric geometry $\frac{\partial}{\partial \theta} = 0$. If there is no coagulation or breakup $\vec{m} = 0$. $D_R = D_m = 0$ because of no diffusion in R and m direction, and $D_\theta = D_r = \infty$ for instanteneous cross-sectional diffusion.

Based on these simplifications the above equation reduces to,

$$\int_{\Omega^*} \left[\frac{\partial n^*}{\partial t} + \frac{\partial (U^* n^*)}{\partial X} + \frac{\partial (\dot{R}^* n^*)}{\partial R} - \frac{\partial}{\partial X}(D^* \frac{\partial n^*}{\partial X}) + \dot{\eta}_{dep}^* \right] \mathrm{d}\Omega^* = 0 \tag{A.4}$$

.

Now with $\mathrm{d}A = (r\mathrm{d}\theta)\mathrm{d}r$ and $\mathrm{d}\Omega = \mathrm{d}x\mathrm{d}R\mathrm{d}m$ and area averaging of any arbitrary

propoerty $\phi = \bar{\phi^*} = \frac{1}{A}\int_A \phi^* \mathrm{d}A$,

$$\int_\Omega \int_A \left[\frac{\partial n^*}{\partial t} + \frac{\partial (U^* n^*)}{\partial X} + \frac{\partial (\dot{R}^* n^*)}{\partial R} - \frac{\partial}{\partial X}(D^* \frac{\partial n^*}{\partial X}) + \dot{\eta}^*_{dep} \right] \mathrm{d}\Omega dA = 0 \qquad \text{(A.5)}$$

.

Now according to Delhaye (1981) even if $A = A(t, X)$, because there is no flux through the duct walls,

$$\int_{A_T} \frac{\delta n^*}{\delta t} \mathrm{d}A_T = \frac{\delta}{\delta t} \int_{A_T} n^* \mathrm{d}A_T \qquad \text{(A.6)}$$

Total cross sectional area is a combination of the airway lumen and alveolar part, so $A_T = A_d + A_a$, and further simplification of defferent terms is possible, which are as follows,

$$\int_{A_T} \frac{\partial}{\partial X}(U^* n^* - D^* \frac{\delta n^*}{\delta X}) \mathrm{d}A_T = \frac{\partial}{\partial X} \int_{A_d + A_a} (U^* n^* - D^* \frac{\delta n^*}{\delta X}) \mathrm{d}(A_d + A_a) \qquad \text{(A.7)}$$

. Because $U^* = 0$ and $D^* = 0$ in A_a,

$$\int_{A_T} \frac{\partial}{\partial X}(U^* n^* - D^* \frac{\delta n^*}{\delta X}) \mathrm{d}A_T = \frac{\partial}{\partial X} \int_{A_d} (U^* n^* - D^* \frac{\delta n^*}{\delta X}) \mathrm{d}A_d \qquad \text{(A.8)}$$

which then becomes

$$\int_{A_T} \frac{\partial}{\partial X}(U^* n^* - D^* \frac{\delta n^*}{\delta X}) \mathrm{d}A_T = \frac{\partial}{\partial X}(A_d U n - A_d D \frac{\delta n}{\delta X}) \qquad \text{(A.9)}$$

and,

$$\int_{A_T} \frac{\partial}{\partial R}(\dot{R}^* n^*) \mathrm{d}A_T = \frac{\delta}{\delta R}(A_T \dot{R} n) \qquad \text{(A.10)}$$

and,

$$\int_{A_T} \dot{\eta}^*_{dep} \mathrm{d}A_T = A_T \dot{\eta}_{dep} \qquad \text{(A.11)}$$

Now subsituting these in equation (3),

$$\int_\Omega \left[\frac{\partial (n A_T)}{\partial t} + \frac{\partial}{\partial X}(A_d U n - A_d D \frac{\delta n}{\delta X}) + \frac{\delta}{\delta R}(A_T \dot{R} n) + A_T \dot{\eta}_{dep} \right] \mathrm{d}\Omega = 0 \qquad \text{(A.12)}$$

Now applying Green's theorem,

$$\int_\Omega \frac{\partial (n A_T)}{\partial t} d\Omega + \int_{S_X} \frac{\partial}{\partial X}(A_d U n - A_d D \frac{\delta n}{\delta X}).\vec{n}_X dS_x + \int_{S_R} (A_T \dot{R} n).\vec{n}_R \mathrm{d}S_R + \int_\Omega A_T \dot{\eta_{dep}} \mathrm{d}\Omega d\Omega = 0 \qquad \text{(A.13)}$$

Appendix B

TECHAero Subroutine

B.1 Original *deposprob.f*

```
      subroutine DeposProb(Breath,Compute,CountDistr,deltat,DepositProb,
     &                     DiffBrown,FlowRate,FreePath,Generation,
     &                     GenStartIndx,hygro,jmin,Lunggen,LungModel,
     &                     maxcell,maxclassl,maxclcl,maxclgl,maxdiml,
     &                     maxgenl,maxgradl,Mouth_Breath,MouthGen,MS,Ni,
     &                     Nj,Nl,numvarl,R,rhoeffSolu,TracheaGen,
     &                     TrachOrigDim,U,W,x,xs)
*************************************************************************
*  This subroutine calculates the deposition rate coefficient of the    *
*  particles by the mechanisms of impaction, sedimentation and          *
*  diffusion. In the case of breath hold, only sedimentation and        *
*  diffusion are considered.                                            *
*   NOTE: The probability values for all balance equations must be      *
*         the same. (compute the probabilities once for every outer     *
*         iteration)                                                   *
*************************************************************************
* LIST OF VARIABLES:
*  INPUT
*   Breath(:),Compute(:),CountDistr(:),deltat,DiffBrown(:),FlowRate,
*   FreePath(:),Generation(:),GenStartIndx(:),hygro,jmin(:),Lunggen,
*   LungModel(:,:),maxcell,maxclassl,maxclcl,maxclgl,maxdiml,maxgenl,
*   maxgradl,Mouth_Breath,MouthGen,MS(:),Ni,Nj,Nl,numvarl,R(:),rhoeffSolu,
*   TracheaGen,TrachOrigDim(:),U(:),W(:),x(:),xs(:)
*
*  OUTPUT
*   DepositProb(:)
*
*  LOCAL
*   AerodynD - droplets' aerodynamic diameter in [microns].
*   Cc1,Cc2,Cc3 - coefficients for the Cunningham slip correction factor.
*   Ccunn - Cunningham slip correction factor.
*   DBr_cgs - Brownian diffusivity converted to [cm2/s].
*   DiffPar - diffusion parameter used for deposition by diffusion.
*   DropVolume - volume of a droplet of a given size bin [m3].
*   ETLength - length of extrathoracic region [m].
*   Flowcc - absolute value of total flow rate converted to [cc/s].
*   fracLength - fraction of the generation length used in the pseudo-Eulerian
*    deposition functions.
*   GenDiameter - airway diameter [m].
*   GenLength - airway length [m].
*   genProbDiffus - generational probability of deposition by diffusion.
*   genProbImp - generational probability of deposition by inertial impaction.
*   genProbSedim - generational probability of deposition by sedimentation.
*   grav - gravity acceleration [m/s2].
*   iend,istart - auxiliary variables used to set loop limits.
*   Inhalcc - inhalation volume converted to [cc].
*   InhalVol - inhalation volume [m3].
*   jstart - starting index for loops on R, based on jmin().
*   k - lung generation.
*   Knudsen - Knudsen number.
```

```
*   ProbDiffus - probability of deposition by diffusion in the lung.
*   ProbDmouth - probability of deposition by diffusion in the mouth.
*   ProbDnose - probability of deposition by diffusion in the nose.
*   ProbImpact - probability of deposition by inertial impaction in the lung.
*   ProbISmouth - probability of deposition by impaction and sedimentation in the mouth.
*   ProbISnose - probability of deposition by impaction and sedimentation in the nose.
*   Probmouth - total deposition probability in the mouth and larynx.
*   Probnose - total deposition probability in the nose.
*   ProbSedim - probability of deposition by sedimentation in the lung.
*   ProbET - total deposition probability in the extra-thoracic region.
*   ProbTotal - total deposition probability in the lung.
*   ResidTime - residence time of particles in a given generation [s].
*   rhoCarrier - density of the carrier gas (air)[kg/m3].
*   rhoDroplet - effective density of the solution [kg/m3].
*   rhoSolvt - density of the solvent (water - the only substance that
*    evaporates!)[kg/m3].
*   ScalefactTr - scaling factor based on the tracheal diamenter.
*   SedimPar - sedimentation parameter.
*   SettlVel - particle settling velocity [m/s].
*   Stokes - Stokes number.
*   Sutherland - Sutherland constant [K].
*   viscos - carrier (air) dynamic viscosity [N s/m2].
*
**********************************************************************
      implicit none
      include 'param.inc'    ! pointing and fixed parameters
*-- global variables --
      integer Generation(*),GenStartIndx(*),jmin(*),
     &        Lunggen,maxcell,maxclassl,maxclcl,maxclgl,maxdiml,maxgenl,
     &        maxgradl,MouthGen,Ni,Nj,Nl,numvarl,TracheaGen
      real*8 Breath(6),CountDistr(*),deltat,DepositProb(*),
     &       DiffBrown(*),FlowRate,FreePath(*),
     &       LungModel(7,*),Mouth_Breath,MS(*),
     &       R(*),rhoeffSolu,TrachOrigDim(2),U(*),
     &       W(*),x(*),xs(*)
      logical Compute(*),hygro
*-- local variables --
      integer i,iend,ij,ijl,istart,j,jstart,jl,k,l
      real*8 AerodynD,aux_cos38,aux_DiffPar,aux_ProbDmouth,
     &       aux_ProbDnose,aux_ProbISmouth,aux_ProbISnose,aux_SedimPar,
     &       aux_SettlVel,aux_Stokes,Cc1,Cc2,Cc3,Ccunn,DBr_cgs,DiffPar,
     &       DropVolume,ETLength,Flowcc,fracLength,GenDiameter,
     &       GenLength,genProbDiffus,genProbImp,genProbSedim,grav,
     &       Inhalcc,InhalVol,Knudsen,Pi,ProbDiffus,ProbDmouth,
     &       ProbDnose,ProbET,ProbImpact,ProbISmouth,ProbISnose,
     &       Probmouth,Probnose,ProbSedim,ProbTotal,ResidTime,
     &       rhoCarrier,rhoDroplet,rhoSolvt,Rj,ScalefactTr,
     &       SedimPar,SettlVel,Stokes,Ui,viscos

*     -- initializations --
      Pi=dacos(-1.d0)
      viscos=1.9d-5          ! air at 37oC
      rhoCarrier=1.1387d0    ! air at 37oC
      rhoSolvt=1.0d3         ! water
      grav=9.81d0
      ScalefactTr=LungModel(2,TracheaGen)/(TrachOrigDim(2)+small)
      InhalVol=Breath(1)
      Flowcc=abs(FlowRate)*1.d6      ! converts m3/s to cc/s and positive
      Inhalcc=InhalVol*1.d6          ! converts m3 to cc
      if (Compute(icount) .and. .not.hygro) then         ! TODO: use a better conditional test!!!
        Cc1=1.142d0          ! for solid particles
        Cc2=0.558d0          ! (from Allen and Raabe 1985,
        Cc3=0.999d0          !  in Aerosol Measurement, Willeke & Baron)
      else
        Cc1=1.207d0          ! for oil droplets
        Cc2=0.440d0          ! (from Rader 1989,
        Cc3=0.596d0          !  in Aerosol Measurement, Willeke & Baron)
      end if

*     -- auxiliary variables --
      aux_ProbISmouth=(Flowcc*ScalefactTr**3.d0)**.6d0*
     &                (Inhalcc*ScalefactTr**2.d0+small)**(-.2d0)
      aux_ProbDmouth=-9.d0*(Mouth_Breath*Flowcc*ScalefactTr+small)**
     &                     (-1.d0/8.d0)
      aux_ProbISnose=(1.d0-Mouth_Breath)*Flowcc*ScalefactTr**3.d0
      aux_ProbDnose=-18.d0*((1.d0-Mouth_Breath)*Flowcc*ScalefactTr
     &                     +small)**(-1.d0/8.d0)
      aux_SettlVel=grav/(4.5d0*viscos)
      aux_cos38=cos(38.25d0*Pi/180.d0)



*----- calculate deposition probabilities in the mouthpiece -----
      if (MouthGen .ne. 1) then
        GenLength=LungModel(1,1)
        GenDiameter=LungModel(2,1)
        if (FlowRate .ne. 0.d0) then
```

```
          ResidTime=GenLength/abs(U(GenStartIndx(i)))
        else
          ResidTime=deltat                        ! TODO: check!!!
        end if
        aux_SedimPar=3.d0*ResidTime/(4.d0*GenDiameter)
        istart=2
        iend=GenStartIndx(MouthGen)-1
        do i=istart,iend   ! loop on x (mouthpiece)
          fracLength=(x(i)-xs(istart-1)) / GenLength
          do l=2,Nl-1         ! loop on MS
            jstart=max(2,jmin(l))
            do j=jstart,Nj-1     ! loop on R
              jl=j+(l-1)*Nj
              ijl=i+(j-1)*Ni+(l-1)*Ni*Nj
              Rj=R(j)

              if (Lunggen .ne. 1) then  !--------- case of full lung -------------

                DepositProb(ijl)=0.d0          ! no deposition in normal mouthpiece

              else                       !----- test-case of pure "mouthpiece" ----

*              -- effective density of the solution --
                DropVolume=4.d0*Pi*(Rj*Rj*Rj)/3.d0
                rhoDroplet=(MS(l)+W(jl))/(DropVolume+small)         ! equiv. grid discret.

*              -- Cunningham slip correction --
                Knudsen=FreePath(i)/Rj
                Ccunn=1.d0+Knudsen*(Cc1+Cc2*exp(-Cc3/Knudsen))

*              -- probability of deposition by sedimentation in the whole gen.(from Pich,1972) --
                SettlVel=aux_SettlVel*(rhoDroplet-rhoCarrier)*
     &                                Ccunn*Rj*Rj
                SedimPar=aux_SedimPar*SettlVel
                if (SedimPar .lt. 1.d0) then
                  ProbSedim=2.d0*(sqrt(1.d0-SedimPar**(2.d0/3.d0))*
     &                            (2.d0*SedimPar-SedimPar**(1.d0/3.d0))
     &                           +asin(SedimPar**(1.d0/3.d0)))/Pi
                else
                  ProbSedim=1.d0        ! all particles within limiting trajectory
                end if

*              -- deposition rate coefficient --
                DepositProb(ijl)=ProbSedim/
     &                           (ResidTime*(1.d0-ProbSedim*fracLength))

              end if
            end do
          end do
        end do
      end if


*----- calculate deposition probabilities in the mouth/nose+pharynx+larynx -----
*      (model from Rudolf et al.,1994 and ICRP, 1994, p. 243-253)
*     -- all ET generations are treated together as one, because
*         the deposition model does not distinguish among them --

      if (FlowRate .ne. 0.d0) then

*       -- calculate residence time for all ET generations --
        ETLength=0.d0
        ResidTime=0.d0
        do k=MouthGen,TracheaGen-1
          GenLength=LungModel(1,k)
          ETLength=ETLength+GenLength
          i=GenStartIndx(k)                       ! first cell is used to obtain
          ResidTime=ResidTime+GenLength/abs(U(i)) !  the generational velocity
        end do    !...k

        istart=GenStartIndx(MouthGen)
        iend=GenStartIndx(TracheaGen)-1
        do i=istart,iend        ! loop on x (extra-thoracic region)
          fracLength=(x(i)-xs(istart-1)) / ETLength
          do l=2,Nl-1        ! loop on MS
            jstart=max(2,jmin(l))
            do j=jstart,Nj-1      ! loop on R
              ij=i+(j-1)*Ni
              jl=j+(l-1)*Nj
              ijl=i+(j-1)*Ni+(l-1)*Ni*Nj
              Rj=R(j)
              DBr_cgs=DiffBrown(ij)*1.d4     ! convert to cm2/s

*             -- effective density and aerodynamic diameter --
              DropVolume=4.d0*Pi*(Rj*Rj*Rj)/3.d0
              rhoDroplet=(MS(l)+W(jl))/(DropVolume+small)         ! equiv. grid discret.
              AerodynD=rhoDroplet*(2.d0*Rj*1.d6)/1.d3     ! in [microns] (1.d3=water dens.)
```

```
*           -- deposition on oropharynx and larynx --
*             __impaction+sedimentation__ (ICRP eq. D.30)
              ProbISmouth=1.d0 - 1.d0/
     &                        (1.1d-4*(AerodynD*AerodynD*
     &                                 aux_ProbISmouth)**1.4d0+1.d0)
*             __diffusion__ (ICRP eq. D.31)
              ProbDmouth=1.d0 - exp(sqrt(DBr_cgs)*aux_ProbDmouth)
*             __composition__
              Probmouth=1.d0 - (1.d0-ProbISmouth)*(1.d0-ProbDmouth)

*           -- nose deposition --
              Probnose=0.d0
              if (Mouth_Breath .lt. 1.d0) then
*               __impaction+sedimentation__ (ICRP eq. D.23)
                ProbISnose=1.d0 - 1.d0/(3.d-4*(AerodynD*AerodynD*
     &                                   aux_ProbISnose)+1.d0)
*               __diffusion__ (ICRP eq. D.28)
                ProbDnose=1.d0 - exp(sqrt(DBr_cgs)*aux_ProbDnose)
*               __composition__
                Probnose=1.d0 - (1.d0-ProbISnose)*(1.d0-ProbDnose)
              end if

*           -- total deposition probability --
              ProbET=Probmouth + (1.d0-Mouth_Breath)*Probnose

*           -- deposition rate coefficient --
              DepositProb(ijl)=ProbET/
     &                         (ResidTime*(1.d0-ProbET*fracLength))

            end do    !...j
          end do    !...i
        end do    !...i

       else
*       -- no models for breath hold deposition in ET region! --
       end if


*------ calculate deposition probabilities in the lung ------------
       istart=GenStartIndx(TracheaGen)
       iend=Ni-1
       do i=istart,iend        ! loop on x (TB and Alveolar regions)
         k=Generation(i)
         GenLength=LungModel(1,k)
         GenDiameter=LungModel(2,k)
         Ui=U(i)                        ! NOTE: Ui is negative at exhalation!!
         if (Ui .ne. 0.d0) then
           ResidTime=GenLength/abs(Ui)
         else
           if (.false.) then         !!!TO DO ! case of breath hold
             ResidTime=Breath(6)*60.d0/Breath(2)       ! time of breath hold (Ui=0)
           else
             ResidTime=1.d10          ! case of zero flow crossing (provisional)
           end if
         end if
         fracLength=(x(i)-xs(GenStartIndx(k)-1)) / GenLength

*        -- auxiliary variables --
         aux_Stokes=abs(Ui)/(4.5d0*viscos*GenDiameter)
         aux_SedimPar=3.d0*ResidTime*aux_cos38/(4.d0*GenDiameter)     ! valid only in the lung
         aux_DiffPar=ResidTime/(GenDiameter**2.d0)

         do l=2,Nl-1        ! loop on MS
           jstart=max(2,jmin(l))
           do j=jstart,Nj-1      ! loop on R
             ij=i+(j-1)*Ni
             jl=j+(l-1)*Nj
             ijl=i+(j-1)*Ni+(l-1)*Ni*Nj
             Rj=R(j)

*            -- effective density of the solution --
             DropVolume=4.d0*Pi*(Rj*Rj*Rj)/3.d0
             rhoDroplet=(MS(l)+W(jl))/(DropVolume+small)         ! equiv. grid discret.

*            -- Cunningham slip correction --
             Knudsen=FreePath(i)/Rj
             Ccunn=1.d0+Knudsen*(Cc1+Cc2*exp(-Cc3/Knudsen))

*            -- probability of deposition by inertial impaction --
*               (from Chan&Lippmann,1980)
             if (Ui .ne. 0.d0) then
               Stokes=aux_Stokes*rhoDroplet*Rj*Rj*Ccunn    ! (see Raabe,1982)
               genProbImp=1.606d0*Stokes+.0023d0           !generational probability
               ProbImpact=genProbImp*deltat/
     &                    (ResidTime*(1.d0-genProbImp*fracLength))
```

```
          else
            ProbImpact=0.d0
          end if

*         -- probability of deposition by sedimentation --
*           (from Pich,1972 + angle correction from Heyder&Gebhart,1977)
          if (k .ne. TracheaGen) then
            SettlVel=aux_SettlVel*(rhoDroplet-rhoCarrier)*Ccunn*Rj*Rj
            SedimPar=aux_SedimPar*SettlVel
            if (SedimPar .lt. 1.d0) then
              genProbSedim=2.d0*(sqrt(1.d0-SedimPar**(2.d0/3.d0))
     &                    *(2.d0*SedimPar-SedimPar**(1.d0/3.d0))
     &                    +asin(SedimPar**(1.d0/3.d0)))/Pi
            else
              genProbSedim=1.d0    ! all particles within limiting trajectory
            end if
          else
            genProbSedim=0.d0      ! no deposition by sedimentation in the trachea
          end if
*           -- pseudo-Eulerian implementation --
          ProbSedim=genProbSedim*deltat/
     &              (ResidTime*(1.d0-genProbSedim*fracLength))

*         -- probability of deposition by diffusion --
          DiffPar=aux_DiffPar*DiffBrown(ij)
          if (DiffPar .gt. 5.d-2) then             ! value at which the 2 functions cross

*           -- (from Ingham,1975, for large DiffPar) --
            genProbDiffus=1.d0 -.819d0*exp(-14.63d0*DiffPar)
     &                  -.097d0*exp(-89.22d0*DiffPar)
     &                  -.0325d0*exp(-228.d0*DiffPar)
     &                  -.0509d0*exp(-125.9d0*DiffPar**(2.d0/3.d0))
          else

*           -- (from Gormley & Kennedy,1949, for small DiffPar) --
*                (Added by AR 2001/03/28)
            genProbDiffus= 6.41d0*DiffPar**(2.d0/3.d0)
     &                  - 4.8d0*DiffPar
     &                  - 1.123d0*DiffPar**(4.d0/3.d0)
          end if

*           -- pseudo-Eulerian implementation --
          ProbDiffus=genProbDiffus*deltat/
     &               (ResidTime*(1.d0-genProbDiffus*fracLength))

*         -- total deposition probability --
          ProbTotal=1.d0 - (1.d0-ProbImpact)*(1.d0-ProbSedim)     ! for independent depos. mechanisms
     &                   *(1.d0-ProbDiffus)

*         -- limits for deposition probability --
          if (ProbTotal .gt. 1.d0) then
            print *,"Warning: ProbTotal>1 in generation ",k
            ProbTotal=1.d0
          else if (ProbTotal .lt. 0.d0) then
            print *,"Warning: ProbTotal<0 in generation ",k
            ProbTotal=0.d0
          end if

*         -- deposition rate coefficient --
          DepositProb(ijl)=ProbTotal/deltat

        end do   !...j
      end do   !...l
    end do    !...i


    return
    end
*-----------------------------------------------------------------------
```

B.2 Modified *deposprob.f*

```
      subroutine DeposProb(Breath,Compute,CountDistr,deltat,DepositProb,
     &                     DiffBrown,FlowRate,FreePath,Generation,
     &                     GenStartIndx,hygro,jmin,Lunggen,LungModel,
     &                     maxcell,maxclassl,maxclcl,maxclgl,maxdiml,
     &                     maxgenl,maxgradl,Mouth_Breath,MouthGen,MS,Ni,
     &                     Nj,Nl,numvarl,R,rhoeffSolu,TracheaGen,
     &                     TrachOrigDim,U,W,x,xs,deltaxs)

************************************************************************
*New variables
c cvResT = residence time in each control volume
c V_ET = volume of CV in ideal mouth throat
c L_ET = center line length of ideal mouth throat
c Dm_ET = mean diameter of ideal mouth throat
c Um_ET = mean velocity of ideal mouth throat
c Rem_ET = flow Reynolds number in ideal ET

************************************************************************
      implicit none
      include 'param.inc'    ! pointing and fixed parameters
*-- global variables --
      integer Generation(*),GenStartIndx(*),jmin(*),
     &        Lunggen,maxcell,maxclassl,maxclcl,maxclgl,maxdiml,maxgenl,
     &        maxgradl,MouthGen,Ni,Nj,Nl,numvarl,TracheaGen
      real*8 Breath(6),CountDistr(*),deltat,DepositProb(*),
     &       DiffBrown(*),FlowRate,FreePath(*),
     &       LungModel(7,*),Mouth_Breath,MS(*),
     &       R(*),rhoeffSolu,TrachOrigDim(2),U(*),
     &       W(*),x(*),xs(*),deltaxs(*)
      logical Compute(*),hygro
*-- local variables --
      integer i,iend,ij,ijl,istart,j,jstart,jl,k,l
      real*8 AerodynD,aux_cos38,aux_DiffPar,aux_ProbDmouth,
     &       aux_ProbDnose,aux_ProbISmouth,aux_ProbISnose,aux_SedimPar,
     &       aux_SettlVel,aux_Stokes,Cc1,Cc2,Cc3,Ccunn,DBr_cgs,DiffPar,
     &       DropVolume,ETLength,Flowcc,fracLength,GenDiameter,
     &       GenLength,genProbDiffus,genProbImp,genProbSedim,grav,
     &       Inhalcc,InhalVol,Knudsen,Pi,ProbDiffus,ProbDmouth,
     &       ProbDnose,ProbET,ProbImpact,ProbISmouth,ProbISnose,
     &       Probmouth,Probnose,ProbSedim,ProbTotal,ResidTime,
     &       rhoCarrier,rhoDroplet,rhoSolvt,Rj,ScalefactTr,
     &       SedimPar,SettlVel,Stokes,Ui,viscos, cvResT,V_ET,L_ET,
     &     Dm_ET,Um_ET,Re_m_ET,Stk_m_ET,aux_stk_m_ET

*     -- initializations --
      Pi=dacos(-1.d0)
      viscos=1.9d-5          ! air at 37oC
      rhoCarrier=1.1387d0    ! air at 37oC
      rhoSolvt=1.0d3         ! water
      grav=9.81d0
      ScalefactTr=LungModel(2,TracheaGen)/(TrachOrigDim(2)+small)
      InhalVol=Breath(1)
      Flowcc=abs(FlowRate)*1.d6      ! converts m3/s to cc/s and positive
      Inhalcc=InhalVol*1.d6          ! converts m3 to cc
      if (Compute(icount) .and. .not.hygro) then         ! TODO: use a better conditional test!!!
        Cc1=1.142d0          ! for solid particles
        Cc2=0.558d0          ! (from Allen and Raabe 1985,
        Cc3=0.999d0          !  in Aerosol Measurement, Willeke & Baron)
      else
        Cc1=1.207d0          ! for oil droplets
        Cc2=0.440d0          ! (from Rader 1989,
        Cc3=0.596d0          !  in Aerosol Measurement, Willeke & Baron)
      end if

*     -- auxiliary variables --
      aux_ProbISmouth=(Flowcc*ScalefactTr**3.d0)**.6d0*
     &                (Inhalcc*ScalefactTr**2.d0+small)**(-.2d0)
      aux_ProbDmouth=-9.d0*(Mouth_Breath*Flowcc*ScalefactTr+small)**
     &                (-1.d0/8.d0)
      aux_ProbISnose=(1.d0-Mouth_Breath)*Flowcc*ScalefactTr**3.d0
      aux_ProbDnose=-18.d0*((1.d0-Mouth_Breath)*Flowcc*ScalefactTr
     &                 +small)**(-1.d0/8.d0)
      aux_SettlVel=grav/(4.5d0*viscos)
      aux_cos38=cos(38.25d0*Pi/180.d0)



*----- calculate deposition probabilities in the mouthpiece -----
      if (MouthGen .ne. 1) then
        GenLength=LungModel(1,1)
        GenDiameter=LungModel(2,1)
        if (FlowRate .ne. 0.d0) then
```

```
          ResidTime=GenLength/abs(U(GenStartIndx(1)))
        else
          ResidTime=deltat                        ! TODO: check!!!
        end if
        aux_SedimPar=3.d0*ResidTime/(4.d0*GenDiameter)
        istart=2
        iend=GenStartIndx(MouthGen)-1
        do i=istart,iend   ! loop on x (mouthpiece)
          fracLength=(x(i)-xs(istart-1)) / GenLength
          do l=2,Nl-1        ! loop on MS
            jstart=max(2,jmin(l))
            do j=jstart,Nj-1     ! loop on R
              jl=j+(l-1)*Nj
              ijl=i+(j-1)*Ni+(l-1)*Ni*Nj
              Rj=R(j)

              if (Lunggen .ne. 1) then  !--------- case of full lung -------------

                DepositProb(ijl)=0.d0          ! no deposition in normal mouthpiece

              else                       !----- test-case of pure "mouthpiece" ----

*              -- effective density of the solution --
                DropVolume=4.d0*Pi*(Rj*Rj*Rj)/3.d0
                rhoDroplet=(MS(l)+W(jl))/(DropVolume+small)         ! equiv. grid discret.

*              -- Cunningham slip correction --
                Knudsen=FreePath(i)/Rj
                Ccunn=1.d0+Knudsen*(Cc1+Cc2*exp(-Cc3/Knudsen))

*              -- probability of deposition by sedimentation in the whole gen.(from Pich,1972) --
                SettlVel=aux_SettlVel*(rhoDroplet-rhoCarrier)*
     &                              Ccunn*Rj*Rj
                SedimPar=aux_SedimPar*SettlVel
                if (SedimPar .lt. 1.d0) then
                  ProbSedim=2.d0*(sqrt(1.d0-SedimPar**(2.d0/3.d0))*
     &                         (2.d0*SedimPar-SedimPar**(1.d0/3.d0))
     &                       +asin(SedimPar**(1.d0/3.d0)))/Pi
                else
                  ProbSedim=1.d0        ! all particles within limiting trajectory
                end if

*              -- deposition rate coefficient --
                DepositProb(ijl)=0.0d0

              end if
            end do
          end do
        end do
      end if


*----- calculate deposition probabilities in the mouth/nose+pharynx+larynx -----
*      (model from Rudolf et al.,1994 and ICRP, 1994, p. 243-253)
*     -- all ET generations are treated together as one, because
*         the deposition model does not distinguish among them --

      if (FlowRate .ne. 0.d0) then

*       -- calculate residence time for all ET generations --
        ETLength=0.d0
        ResidTime=0.d0
        do k=MouthGen,TracheaGen-1
          GenLength=LungModel(1,k)
          ETLength=ETLength+GenLength
          i=GenStartIndx(k)                    ! first cell is used to obtain
          ResidTime=ResidTime+GenLength/abs(U(i)) !  the generational velocity
        end do    !...k



*********************************
c new ET funciton proposed by grgic et al 2004
*********************************
V_ET = 76.8d-6 ! (m^3) provided my Grgic et al 2004 as average ET volume
L_ET = 18.8d-2 ! (m) provided my Grgic et al 2004 as average ET length

Dm_ET = 2.0*(sqrt(V_ET/(pi*L_ET))) ! mean diameter
Um_ET = abs(FlowRate)*L_ET/V_ET ! mean flow velocity

Re_m_ET = rhoCarrier*Um_ET*Dm_ET/viscos
aux_stk_m_ET = Um_ET/(18.0d0*viscos*Dm_ET)

* Pen_mouth_throat = 1.0d0
***********************************
```

```
        istart=GenStartIndx(MouthGen)
        iend=GenStartIndx(TracheaGen)-1
        do i=istart,iend        ! loop on x (extra-thoracic region)
c          fracLength=(x(i)-xs(istart-1)) / ETLength
  cvResT = deltaxs(i)/abs(U(i))


          do l=2,Nl-1        ! loop on MS
            jstart=max(2,jmin(l))
            do j=jstart,Nj-1      ! loop on R
              ij=i+(j-1)*Ni
              jl=j+(l-1)*Nj
              ijl=i+(j-1)*Ni+(l-1)*Ni*Nj
              Rj=R(j)
              DBr_cgs=DiffBrown(ij)*1.d4     ! convert to cm2/s

*             -- effective density and aerodynamic diameter --
              DropVolume=4.d0*Pi*(Rj*Rj*Rj)/3.d0
              rhoDroplet=(MS(l)+W(jl))/(DropVolume+small)         ! equiv. grid discret.
              AerodynD=rhoDroplet*(2.d0*Rj*1.d6)/1.d3     ! in [microns] (1.d3=water dens.)

****************************************

      Stk_m_ET = aux_stk_m_ET*rhoDroplet*Rj*Rj


              Probmouth=1.0d0 - 1.0d0/(1i.5d0*((Stk_m_ET)*
     & (Re_m_ET**0.37d0))**1.912+1.0d0)

*********************************

*             -- nose deposition --
              Probnose=0.d0

*             -- total deposition probability --
              ProbET=Probmouth + (1.d0-Mouth_Breath)*Probnose

*             -- deposition rate coefficient --
* because there is no time scale present in the above formula, deposition probability is same in same in all cv, so
* i decided to divide it by CV_residence time to get the rate
              DepositProb(ijl)=ProbET*cvResT/
     &                         (cvResT*ResidTime)

            end do    !...j
          end do    !...l
        end do    !...i

      else
*      -- no models for breath hold deposition in ET region! --
      end if



*------ calculate deposition probabilities in the lung ------------
      istart=GenStartIndx(TracheaGen)
      iend=Ni-1
      do i=istart,iend        ! loop on x (TB and Alveolar regions)
        k=Generation(i)
        GenLength=LungModel(1,k)
        GenDiameter=LungModel(2,k)
        Ui=U(i)                          ! NOTE: Ui is negative at exhalation!!
        if (Ui .ne. 0.d0) then
          ResidTime=GenLength/abs(Ui)
        else
          if (.false.) then         !!!TO DO ! case of breath hold
            ResidTime=Breath(6)*60.d0/Breath(2)       ! time of breath hold (Ui=0)
          else
            ResidTime=1.d10          ! case of zero flow crossing (provisional)
          end if
        end if
        fracLength=(x(i)-xs(GenStartIndx(k)-1)) / GenLength
cvResT = deltaxs(i)/abs(U(i))


*       -- auxiliary variables --
        aux_Stokes=abs(Ui)/(4.5d0*viscos*GenDiameter)
        aux_SedimPar=3.d0*cvResT*aux_cos38/(4.d0*GenDiameter)     ! valid only in the lung
        aux_DiffPar=cvResT/(GenDiameter**2.d0)

        do l=2,Nl-1        ! loop on MS
          jstart=max(2,jmin(l))
          do j=jstart,Nj-1      ! loop on R
            ij=i+(j-1)*Ni
            jl=j+(l-1)*Nj
            ijl=i+(j-1)*Ni+(l-1)*Ni*Nj
            Rj=R(j)
```

```
*          -- effective density of the solution --
           DropVolume=4.d0*Pi*(Rj*Rj*Rj)/3.d0
           rhoDroplet=(MS(l)+W(jl))/(DropVolume+small)         ! equiv. grid discret.

*          -- Cunningham slip correction --
           Knudsen=FreePath(i)/Rj
           Ccunn=1.d0+Knudsen*(Cc1+Cc2*exp(-Cc3/Knudsen))

*          -- probability of deposition by inertial impaction --
*             (from Chan&Lippmann,1980)
           if (Ui .ne. 0.d0) then
             Stokes=aux_Stokes*rhoDroplet*Rj*Rj*Ccunn     ! (see Raabe,1982)
             genProbImp=1.606d0*Stokes+.0023d0            !generational probability
c because there is no time scale in the impaction fuction, the following factorization is dione
c to estimate probability for the cv
 ProbImpact=genProbImp*cvResT/
     &                 (ResidTime)
           else
             ProbImpact=0.d0
           end if

*          -- probability of deposition by sedimentation --
*             (from Pich,1972 + angle correction from Heyder&Gebhart,1977)
           if (k .ne. TracheaGen) then
             SettlVel=aux_SettlVel*(rhoDroplet-rhoCarrier)*Ccunn*Rj*Rj
             SedimPar=aux_SedimPar*SettlVel
             if (SedimPar .lt. 1.d0) then
               genProbSedim=2.d0*(sqrt(1.d0-SedimPar**(2.d0/3.d0))
     &                          *(2.d0*SedimPar-SedimPar**(1.d0/3.d0))
     &                          +asin(SedimPar**(1.d0/3.d0)))/Pi
             else
               genProbSedim=1.d0    ! all particles within limiting trajectory
             end if
           else
             genProbSedim=0.d0      ! no deposition by sedimentation in the trachea
           end if
*           -- pseudo-Eulerian implementation --
           ProbSedim=genProbSedim

*          -- probability of deposition by diffusion --
           DiffPar=aux_DiffPar*DiffBrown(ij)
           if (DiffPar .gt. 5.d-2) then             ! value at which the 2 functions cross

*            -- (from Ingham,1975, for large DiffPar) --
             genProbDiffus=1.d0 -.819d0*exp(-14.63d0*DiffPar)
     &                    -.097d0*exp(-89.22d0*DiffPar)
     &                    -.0325d0*exp(-228.d0*DiffPar)
     &                    -.0509d0*exp(-125.9d0*DiffPar**(2.d0/3.d0))
           else

*            -- (from Gormley & Kennedy,1949, for small DiffPar) --
*                 (Added by AR 2001/03/28)
             genProbDiffus= 6.41d0*DiffPar**(2.d0/3.d0)
     &                    - 4.8d0*DiffPar
     &                    - 1.123d0*DiffPar**(4.d0/3.d0)
           end if

*            -- pseudo-Eulerian implementation --
           ProbDiffus=genProbDiffus

*          -- total deposition probability --
           ProbTotal=1.d0 - (1.d0-ProbImpact)*(1.d0-ProbSedim)     ! for independent depos. mechanisms
     &                     *(1.d0-ProbDiffus)

*          -- limits for deposition probability --
           if (ProbTotal .gt. 1.d0) then
             print *,"Warning: ProbTotal>1 in generation ",k
             ProbTotal=1.d0
           else if (ProbTotal .lt. 0.d0) then
             print *,"Warning: ProbTotal<0 in generation ",k
             ProbTotal=0.d0
           end if

*          -- deposition rate coefficient --
c total deposition probability is devided by the cv residence time to obtain the deposition probability rate
           DepositProb(ijl)=ProbTotal/cvResT

         end do   !...j
       end do   !...l
     end do    !...i


     return
     end
*-----------------------------------------------------------------------
```

Appendix C

TECHAero Data Files

C.1 Input file: *input.dat*

```
#  INPUT DATA FILE FOR TECHAERO (don't delete comment lines!)
#  (next line is the Problem Title [max. 80 chars.])
all function are original except the impaction of Darquenne et al
0.93            # program version
# ---- Discretization Parameters ----
t f f f         # logical flags for variables to compute (Count,T,Cinf,Tinf)
f               # logical flag for hygroscopicity
100    20        # number of grid points in x and R directions
1.d-2           # time step [s]
15              # max. no. of iterations per time step
1.0d0           # time between plot outputs [s]
1.0d0           # time discretization factor (expl=0;Cr-Nic=0.5;impl=1)
0.0d0           # convective discretization blending factor (UDS=0;CDS=1)
1.d0 .8d0 1.d0 1.d0    # under-relaxation factors for Count,T,Cinf,Tinf
1.d-4           # convergence tolerance
# ---- Ambient and Physiological Data ----
/home/mirahman/TechAero/philhaef.dat    # path and file name for the lung model [max. 80 chars.]
 0.d0  0.d0     # mouthpiece dimensions (length, equiv. diam.) [cm]
20.  50.        # ambient temp [oC], ambient RH [%]
16.0d0          # breaths/min
1               # number of breath cycles to compute
24.0d0          # max. inhalation flow rate [l/min]
50.d0  0.d0     # % time inhaling, % time holding
1.              # mouth breathing fraction
0. 2. 18. 1.70  # scaling of lung geometry (flag [scale=1],sex[f=1;m=2],age[yrs],height[m])
0   f           # pediatric lung: age [mo. or 0=adult], flag for stand. ped. brthng. (overrides input data)
f   f           # log. flags for: reading breath input file, scaling input breath function
# ---- Aerosol Data ----
NaCl            # name of solute compound 1 [max. 12 chars.]
x               # name of solute compound 2 [max. 12 chars.]
x               # name of solute compound 3 [max. 12 chars.]
x               # name of solute compound 4 [max. 12 chars.]
0.  0. 0. 0.  # initial conc. for each compound(4) [mg/ml=kg/m3] (use density if solid particle)
0.  0. 0. 0. # density of each compound(4) [kg/m3]
0.  0. 0. 0. # specific heat of each compound(4) [J/(kg K)]
0.  0. 0. 0.  # solubility of each compound(4) [%w/w]
0. 0. 0. 0.  # mol. weight of each compound(4) [g/mol=kg/kmol] (set to 0 for non-ideal chem.)
0.  0. 0. 0.   # van't Hoff factor for each compound(4) (set to 0 for non-ideal chem.)
0.4d0  0.6d00     # lower and upper cuttoff diameters [microns]
f  t  t         # logical flags for: initially lognormal, initially monodisperse, pure solvent(no solute)
f  f            # logical flags for time dependence of: particle production rate, size distrib. parameters
0.5d0 1.0id0      # initial MMD or monodisperse diameter [microns], initial GSD
4.0d6           # max. particle production rate at inhalation [1/s]
20.d0           # droplets' temperature at inhalation [oC]
```

C.2 Grid File: *grid.out*

#	x	cell size ; no. of points= 100
1	0.00000E+00	1.00000E-90
2	5.00000E-03	1.00000E-02
3	1.50000E-02	1.00000E-02
4	2.50000E-02	1.00000E-02
5	3.45909E-02	9.18182E-03
6	4.37727E-02	9.18182E-03
7	5.29545E-02	9.18182E-03
8	6.21364E-02	9.18182E-03
9	7.13182E-02	9.18182E-03
10	8.05000E-02	9.18182E-03
11	8.96818E-02	9.18182E-03
12	9.88636E-02	9.18182E-03
13	1.08045E-01	9.18182E-03
14	1.17227E-01	9.18182E-03
15	1.26409E-01	9.18182E-03
16	1.36000E-01	1.00000E-02
17	1.46000E-01	1.00000E-02
18	1.56000E-01	1.00000E-02
19	1.66000E-01	1.00000E-02
20	1.76000E-01	1.00000E-02
21	1.86000E-01	1.00000E-02
22	1.96000E-01	1.00000E-02
23	2.06000E-01	1.00000E-02
24	2.19897E-01	1.77943E-02
25	2.37691E-01	1.77943E-02
26	2.55486E-01	1.77943E-02
27	2.73280E-01	1.77943E-02
28	2.91074E-01	1.77943E-02
29	3.08869E-01	1.77943E-02
30	3.26663E-01	1.77943E-02
31	3.41583E-01	1.20467E-02
32	3.53630E-01	1.20467E-02
33	3.65677E-01	1.20467E-02
34	3.76964E-01	1.05272E-02
35	3.86981E-01	9.50705E-03
36	3.96027E-01	8.58575E-03
37	4.04526E-01	8.41228E-03
38	4.12520E-01	7.57559E-03
39	4.19719E-01	6.82212E-03
40	4.26539E-01	6.81729E-03
41	4.32893E-01	5.89142E-03
42	4.38384E-01	5.09130E-03
43	4.43080E-01	4.29914E-03
44	4.47093E-01	3.72805E-03
45	4.50574E-01	3.23281E-03
46	4.53792E-01	3.20453E-03
47	4.56887E-01	2.98499E-03
48	4.59770E-01	2.78048E-03
49	4.62602E-01	2.88304E-03
50	4.65422E-01	2.75820E-03
51	4.68121E-01	2.63877E-03
52	4.70752E-01	2.62323E-03
53	4.73304E-01	2.48075E-03
54	4.75717E-01	2.34602E-03
55	4.78053E-01	2.32670E-03
56	4.80303E-01	2.17330E-03
57	4.82405E-01	2.03001E-03
58	4.84422E-01	2.00485E-03
59	4.86348E-01	1.84579E-03
60	4.88120E-01	1.69936E-03
61	4.89802E-01	1.66419E-03
62	4.91388E-01	1.50848E-03
63	4.92826E-01	1.36733E-03
64	4.94171E-01	1.32109E-03
65	4.95424E-01	1.18535E-03
66	4.96548E-01	1.06356E-03
67	4.97592E-01	1.02407E-03
68	4.98564E-01	9.19794E-04
69	4.99437E-01	8.26138E-04
70	5.00271E-01	8.41272E-04
71	5.01054E-01	7.24607E-04
72	5.01728E-01	6.24121E-04
73	5.02296E-01	5.12580E-04
74	5.02774E-01	4.43570E-04
75	5.03188E-01	3.83850E-04
76	5.03578E-01	3.95526E-04
77	5.03957E-01	3.62409E-04
78	5.04304E-01	3.32065E-04
79	5.04632E-01	3.24405E-04
80	5.04946E-01	3.02856E-04
81	5.05239E-01	2.82739E-04

82	5.05524E-01	2.88430E-04
83	5.05803E-01	2.69590E-04
84	5.06064E-01	2.51980E-04
85	5.06308E-01	2.36210E-04
86	5.06539E-01	2.26535E-04
87	5.06761E-01	2.17255E-04
88	5.06983E-01	2.26667E-04
89	5.07210E-01	2.26667E-04
90	5.07437E-01	2.26667E-04
91	5.07665E-01	2.29199E-04
92	5.07893E-01	2.26657E-04
93	5.08118E-01	2.24143E-04
94	5.08336E-01	2.12767E-04
95	5.08551E-01	2.16643E-04
96	5.08770E-01	2.20590E-04
97	5.09002E-01	2.43333E-04
98	5.09245E-01	2.43333E-04
99	5.09488E-01	2.43333E-04
100	5.09610E-01	1.00000E-90

#	R	bin width	; no. of points=	10
1	1.45000E-06	1.00000E-90		
2	1.45625E-06	1.25000E-08		
3	1.46875E-06	1.25000E-08		
4	1.48125E-06	1.25000E-08		
5	1.49375E-06	1.25000E-08		
6	1.50625E-06	1.25000E-08		
7	1.51875E-06	1.25000E-08		
8	1.53125E-06	1.25000E-08		
9	1.54375E-06	1.25000E-08		
10	1.55000E-06	1.00000E-90		

#	MS	grade width	; no. of points=	3
1	0.00000E+00	1.00000E-90		
2	0.00000E+00	1.00000E+00		
3	0.00000E+00	1.00000E-90		

C.3 Local Deposition : *locdep.out*

#gen.	x[cm]	specif.dos.[mg/cm]	specif.solv.[mg/cm]	- manual calculation test (pure inhalation, U=0.001 m/s)
1	5.00000E-01	0.00000E+00	0.00000E+00	
1	1.50000E+00	0.00000E+00	0.00000E+00	
1	2.50000E+00	0.00000E+00	0.00000E+00	
2	3.45909E+00	0.00000E+00	0.00000E+00	
2	4.37727E+00	0.00000E+00	0.00000E+00	
2	5.29545E+00	0.00000E+00	0.00000E+00	
2	6.21364E+00	0.00000E+00	0.00000E+00	
2	7.13182E+00	0.00000E+00	0.00000E+00	
2	8.05000E+00	0.00000E+00	0.00000E+00	
2	8.96818E+00	0.00000E+00	0.00000E+00	
2	9.88636E+00	0.00000E+00	0.00000E+00	
2	1.08045E+01	0.00000E+00	0.00000E+00	
2	1.17227E+01	0.00000E+00	0.00000E+00	
2	1.26409E+01	0.00000E+00	0.00000E+00	
3	1.36000E+01	0.00000E+00	0.00000E+00	
3	1.46000E+01	0.00000E+00	0.00000E+00	
3	1.56000E+01	0.00000E+00	0.00000E+00	
3	1.66000E+01	0.00000E+00	0.00000E+00	
3	1.76000E+01	0.00000E+00	0.00000E+00	
3	1.86000E+01	0.00000E+00	0.00000E+00	
3	1.96000E+01	0.00000E+00	0.00000E+00	
3	2.06000E+01	0.00000E+00	0.00000E+00	
4	2.19897E+01	0.00000E+00	2.70912E-06	
4	2.37691E+01	0.00000E+00	8.03766E-06	
4	2.55486E+01	0.00000E+00	1.31047E-05	
4	2.73280E+01	0.00000E+00	1.79218E-05	
4	2.91074E+01	0.00000E+00	2.25002E-05	
4	3.08869E+01	0.00000E+00	2.68505E-05	
4	3.26663E+01	0.00000E+00	3.09833E-05	
5	3.41583E+01	0.00000E+00	3.39735E-06	
5	3.53630E+01	0.00000E+00	1.00749E-05	
5	3.65677E+01	0.00000E+00	1.64160E-05	
6	3.76964E+01	0.00000E+00	4.27565E-06	
6	3.86981E+01	0.00000E+00	1.26763E-05	
6	3.96027E+01	0.00000E+00	2.06489E-05	
7	4.04526E+01	0.00000E+00	5.38491E-06	
7	4.12520E+01	0.00000E+00	1.59642E-05	
7	4.19719E+01	0.00000E+00	2.60035E-05	
8	4.26539E+01	0.00000E+00	6.78627E-06	
8	4.32893E+01	0.00000E+00	2.01205E-05	
8	4.38384E+01	0.00000E+00	3.27793E-05	
9	4.43080E+01	0.00000E+00	8.55468E-06	
9	4.47093E+01	0.00000E+00	2.53699E-05	
9	4.50574E+01	0.00000E+00	4.13453E-05	
10	4.53792E+01	0.00000E+00	1.07948E-05	
10	4.56887E+01	0.00000E+00	3.20222E-05	
10	4.59770E+01	0.00000E+00	5.22083E-05	
11	4.62602E+01	0.00000E+00	1.36248E-05	
11	4.65422E+01	0.00000E+00	4.04213E-05	
11	4.68121E+01	0.00000E+00	6.59171E-05	
12	4.70752E+01	0.00000E+00	1.71352E-05	
12	4.73304E+01	0.00000E+00	5.08090E-05	
12	4.75717E+01	0.00000E+00	8.28054E-05	
13	4.78053E+01	0.00000E+00	2.14735E-05	
13	4.80303E+01	0.00000E+00	6.35737E-05	
13	4.82405E+01	0.00000E+00	1.03402E-04	
14	4.84422E+01	0.00000E+00	2.70002E-05	
14	4.86348E+01	0.00000E+00	7.96983E-05	
14	4.88120E+01	0.00000E+00	1.29155E-04	
15	4.89802E+01	0.00000E+00	3.41991E-05	
15	4.91388E+01	0.00000E+00	1.00586E-04	
15	4.92826E+01	0.00000E+00	1.62334E-04	
16	4.94171E+01	0.00000E+00	4.34243E-05	
16	4.95424E+01	0.00000E+00	1.27309E-04	
16	4.96548E+01	0.00000E+00	2.04736E-04	
17	4.97592E+01	0.00000E+00	5.47977E-05	
17	4.98564E+01	0.00000E+00	1.60555E-04	
17	4.99437E+01	0.00000E+00	2.58062E-04	
18	5.00271E+01	0.00000E+00	6.88480E-05	
18	5.01054E+01	0.00000E+00	2.02123E-04	
18	5.01728E+01	0.00000E+00	3.25698E-04	
19	5.02296E+01	0.00000E+00	2.27863E-04	
19	5.02774E+01	0.00000E+00	6.66505E-04	
19	5.03188E+01	0.00000E+00	1.07025E-03	
20	5.03578E+01	0.00000E+00	3.03856E-04	
20	5.03957E+01	0.00000E+00	8.89924E-04	
20	5.04304E+01	0.00000E+00	1.43444E-03	
21	5.04632E+01	0.00000E+00	4.39529E-04	
21	5.04946E+01	0.00000E+00	1.27832E-03	
21	5.05239E+01	0.00000E+00	2.04705E-03	

22	5.05524E+01	0.00000E+00	6.48325E-04
22	5.05803E+01	0.00000E+00	1.85162E-03
22	5.06064E+01	0.00000E+00	2.91665E-03
23	5.06308E+01	0.00000E+00	9.85645E-04
23	5.06539E+01	0.00000E+00	2.69848E-03
23	5.06761E+01	0.00000E+00	4.06433E-03
24	5.06983E+01	0.00000E+00	1.42722E-03
24	5.07210E+01	0.00000E+00	3.45542E-03
24	5.07437E+01	0.00000E+00	4.47705E-03
25	5.07665E+01	0.00000E+00	1.32159E-03
25	5.07893E+01	0.00000E+00	2.21929E-03
25	5.08118E+01	0.00000E+00	1.87732E-03
26	5.08336E+01	0.00000E+00	3.76934E-04
26	5.08551E+01	0.00000E+00	3.15168E-04
26	5.08770E+01	0.00000E+00	1.29242E-04
27	5.09002E+01	0.00000E+00	1.32239E-05
27	5.09245E+01	0.00000E+00	5.40358E-06
27	5.09488E+01	0.00000E+00	1.93146E-06

C.4 Generation Deposition : *gendep.out*

#gen.	dosage[mg]	dosage[%]	solv.dose[mg]	solv.dose[%]	- manual calculation test (pure inhalation, U=0.001 m/s)
1	0.00000E+00	0.000	0.00000E+00	0.000	
2	0.00000E+00	0.000	0.00000E+00	0.000	
3	0.00000E+00	0.000	0.00000E+00	0.000	
4	0.00000E+00	0.000	2.17281E-04	2.075	
5	0.00000E+00	0.000	3.60054E-05	0.344	
6	0.00000E+00	0.000	3.42811E-05	0.327	
7	0.00000E+00	0.000	3.43636E-05	0.328	
8	0.00000E+00	0.000	3.31692E-05	0.317	
9	0.00000E+00	0.000	2.65019E-05	0.253	
10	0.00000E+00	0.000	2.75343E-05	0.263	
11	0.00000E+00	0.000	3.24710E-05	0.310	
12	0.00000E+00	0.000	3.65257E-05	0.349	
13	0.00000E+00	0.000	3.98033E-05	0.380	
14	0.00000E+00	0.000	4.20719E-05	0.402	
15	0.00000E+00	0.000	4.30611E-05	0.411	
16	0.00000E+00	0.000	4.26022E-05	0.407	
17	0.00000E+00	0.000	4.16988E-05	0.398	
18	0.00000E+00	0.000	4.07655E-05	0.389	
19	0.00000E+00	0.000	8.23255E-05	0.786	
20	0.00000E+00	0.000	9.19026E-05	0.878	
21	0.00000E+00	0.000	1.10851E-04	1.059	
22	0.00000E+00	0.000	1.42111E-04	1.357	
23	0.00000E+00	0.000	1.72711E-04	1.649	
24	0.00000E+00	0.000	2.12153E-04	2.026	
25	0.00000E+00	0.000	1.22671E-04	1.171	
26	0.00000E+00	0.000	1.76988E-05	0.169	
27	0.00000E+00	0.000	5.00269E-07	0.005	

C.5 Regional Deposition : *regdep.out*

```
                        TechAero
   Truly Eulerian Code for simulation of Hygroscopic AEROsols.
                      Version  0.93
 Copyright 1999,2000 Aerosol Research Laboratory of Alberta, U. of A.

 Title of the run:
 manual calculation test (pure inhalation, U=0.001 m/s)


 Computation Parameters:
  Computed: count_distr.
  Number of grid points:    100 in X,     10 in R and      3 in MS.
  Time step [s]:   6.209E-03
  Time discret. factor:  1.00
  Convection discret. factor:  0.00

 Ambient and Physiological Data:
  Lung geometry model: Phillips&al.+Haefeli-Bleuer&Weibel/3.05 litres
  Mouthpiece dimensions (L,D)[cm]:   3.000  2.000
  Ambient temperature [oC]:  20.000
  Ambient humidity [%]:  50.000
  Lung corresponds to an adult at 50% TLC.
  Inhalation volume [l]:   0.748
  Breaths per minute:   16.000
  Number of breath cycles:   1
  Inhal., breath hold, exhal. [%]:  50.00,   0.00,  50.00
  Mouth breathing fraction [%]:   1.00

 Aerosol Data:
  Particles of pure: water
  Total amount inhaled [ml]:   1.047E-02
  Initially monodisperse aerosol.
  Initial diameter [microns]:   3.000E+00

 Regional dosages [mg | %]:
(percentages of total inhaled =  1.047E-02 mg)
  Extra-thoracic:      0.000E+00 |   0.00
  Tracheo-bronchial:   7.281E-04 |   6.95
  Alveolar:            9.529E-04 |   9.10
  Total dosage:        1.681E-03 |  16.05
```